

## Supplementary Information

### **Molecular Sn(II) Precursors for Room Temperature Deposition of Crystalline Elemental Tin**

Janelle Bykowski,<sup>a,‡</sup> Jocelyn Sinclair,<sup>a,‡</sup> Jonathan Trach,<sup>a</sup> Michael J. Ferguson,<sup>a</sup> and Eric Rivard<sup>\*,a</sup>

<sup>a</sup> Department of Chemistry, University of Alberta, 11227 Saskatchewan Dr., Edmonton, Alberta, Canada T6G 2G2. E-mail: [erivard@ualberta.ca](mailto:erivard@ualberta.ca)

<sup>‡</sup> These authors contributed equally.

## Contents

1. Experimental procedures .....	S2
1.1 General.....	S2
1.2 Characterization of solid materials .....	S2
1.3 Synthetic procedures and reactivity .....	S3
2. NMR spectra .....	S6
3. X-ray crystallographic data.....	S27
4. SEM and EDX images of deposited Sn .....	S30
5. X-ray photoelectron spectroscopy and powder X-ray diffraction .....	S37
6. Raman spectra of deposited Sn.....	S39
7. Computational data .....	S40
8. References.....	S55

# 1. Experimental procedures

## 1.1 General

All reactions were performed using standard Schlenk techniques under an atmosphere of nitrogen or in a nitrogen-filled glove box (Innovative Technology, Inc.). Solvents were dried using a Grubbs-type solvent purification system manufactured by Innovative Technology, Inc., degassed (freeze-pump-thaw method), and stored under an atmosphere of nitrogen prior to use; the exception is  $\text{Me}_3\text{SiOSiMe}_3$  which was degassed (freeze-pump-thaw) and stored over 4 Å molecular sieves prior to use.  $\text{SnCl}_2$ , potassium *tert*-butoxide, and *tert*-butanol were purchased from Sigma-Aldrich and used as received. Potassium hydride was purchased from Sigma-Aldrich and was washed with hexanes and pentane prior to use to remove the mineral oil. 4,4,5,5-Tetramethyl-1,2-dioxaborolane (HBpin) was purchased from Oakwood Chemicals and used as received. **PB** (1,2- $^i\text{Pr}_2\text{P}(\text{C}_6\text{H}_4)\text{BCy}_2$  (Cy = cyclohexyl) and N-N-dimethylimidazolium iodide were prepared according to literature procedures.<sup>S1,S2</sup>  $^1\text{H}$ ,  $^{11}\text{B}/^{11}\text{B}\{^1\text{H}\}$ ,  $^{13}\text{C}\{^1\text{H}\}$ , and  $^{119}\text{Sn}$  NMR spectra were recorded on a Varian Inova 400 or 500 MHz spectrometer and referenced externally to  $\text{Me}_4\text{Si}$  ( $^1\text{H}$ ,  $^{13}\text{C}\{^1\text{H}\}$ ),  $\text{F}_3\text{B}\cdot\text{OEt}_2$  ( $^{11}\text{B}/^{11}\text{B}\{^1\text{H}\}$ ) and  $\text{SnMe}_4$  ( $^{119}\text{Sn}$ ). Elemental analyses were performed by the Analytical and Instrumentation Laboratory at the University of Alberta. Melting points were obtained in sealed glass capillaries under nitrogen using a MelTemp melting point apparatus and are uncorrected.

## 1.2 Characterization of solid materials

Powder XRD patterns were collected on a Rigaku Ultima IV powder diffractometer equipped with a  $\text{Co K}\alpha$  radiation source ( $\text{K}\alpha_1 = 1.78900 \text{ \AA}$ ,  $\text{K}\alpha_2 = 1.79283 \text{ \AA}$ ) operating at 40 kV and 40 mA. A D/Tex Ultra detector was used, with an iron filter to eliminate the  $\text{K}\beta$  radiation at 1.62083 Å. Approximately 5 mg of sample was placed on zero-background silicon holders and mounted in the instrument. Diffraction data were collected in continuous scan mode between 5 and 90° in 2θ with a step size of 0.0200°.

Raman spectra were acquired using a Reinshaw's inVia Raman Confocal Spectrometer (532 nm, 50 mW, 120 s exposure time).

X-ray photoelectron spectroscopy (XPS) was conducted on a PHI VersaProbe III at the nanoFAB facility at the University of Alberta operating in energy spectrum mode at 50 W. The base and operating chamber pressure were maintained at  $10^{-8}$  Pa. A monochromatic Al  $\text{K}\alpha$  source (1486.6 eV) was used to irradiate the samples, and the spectra were obtained with an electron take-off angle of 45°. Survey spectra were collected using a circular spot (250 μm), and 280 eV pass energy with a step of 0.1 eV. The data were processed using CasaXPS software (VAMAS), and spectra were internally referenced to adventitious carbon (C 1s emission at 284.8 eV).

Scanning electron microscopy (SEM) was performed using a Zeiss Sigma 300 VP-FESEM instrument, equipped with both secondary and backscattered electron detectors and a Bruker energy dispersive X-ray spectroscopy (EDS) system. An acceleration voltage of 10 kV was employed for all samples measured. Samples of Sn deposited on either <100> oriented *n*-type silicon wafers (obtained from University Wafer, 4'' size, 500 μm thickness) or copper foil (Sigma-Aldrich, 0.25 mm thickness) were prepared by exposing the substrates to the Sn molecular precursor dissolved in toluene (0.010 M to 0.30 M) followed by the addition of the appropriate equivalent(s) of HBpin to induce tin metal deposition (see Fig. S45). After 2 or

3.5 hours of reaction time, the volatiles were removed under vacuum and the wafers/plates were washed with dry toluene (2 × 2 mL) and then dried by vacuum; the substrates were then fastened to aluminum stubs using carbon tape and submitted for further analysis.

### 1.3 Synthetic procedures and reactivity

**Preparation of K[Sn(O<sup>t</sup>Bu)<sub>3</sub>]:** To SnCl<sub>2</sub> (4.416 g, 23.29 mmol) in 50 mL of THF at –78 °C was added a solution of K[O<sup>t</sup>Bu] (7.840 g, 69.87 mmol) in 50 mL of THF at the same temperature. The reaction mixture was stirred and warmed gradually to room temperature for 10 hours and the volatiles were then removed by vacuum. Et<sub>2</sub>O (2 × 100 mL) was added to the flask, and the suspension was filtered through a pad of Celite to collect the supernatant. Removal of the volatiles from the filtrate *in vacuo* afforded K[Sn(O<sup>t</sup>Bu)<sub>3</sub>] (5.156 g, 59 %) as a white solid. Crystals of K<sub>2</sub>[Sn(O<sup>t</sup>Bu)<sub>3</sub>]<sub>2</sub>•2 THF suitable for X-ray crystallography were obtained by cooling a saturated THF solution of K[Sn(O<sup>t</sup>Bu)<sub>3</sub>] to –35 °C for 3 days. Data for K[Sn(O<sup>t</sup>Bu)<sub>3</sub>]: <sup>1</sup>H NMR (C<sub>6</sub>D<sub>6</sub>): δ 1.39 (s, 27H, OC(CH<sub>3</sub>)<sub>3</sub>). <sup>53b</sup> <sup>13</sup>C {<sup>1</sup>H} NMR (C<sub>6</sub>D<sub>6</sub>): δ 35.9 (OC(CH<sub>3</sub>)<sub>3</sub>), 69.9 (OC(CH<sub>3</sub>)<sub>3</sub>). <sup>119</sup>Sn {<sup>1</sup>H} NMR (C<sub>6</sub>D<sub>6</sub>, 500 MHz): δ –250.0. Anal. Calc. for KC<sub>12</sub>H<sub>27</sub>SnO<sub>3</sub>: C, 38.22; H, 7.22. Found: C, 38.09; H, 6.96%.

**Preparation of [Sn(O<sup>t</sup>Bu)<sub>2</sub>]<sub>2</sub> (1):** A solution of SnCl<sub>2</sub> (0.128 g, 0.675 mmol) in 5 mL of THF at –35 °C was added dropwise to a stirring slurry of K[Sn(O<sup>t</sup>Bu)<sub>3</sub>] (0.521 g, 1.38 mmol) in 10 mL of cold toluene at the same temperature. The reaction mixture was stirred and warmed to room temperature for 2 hours, after which the volatiles were removed. The solid was extracted with 2 × 10 mL of pentane, and the combined extracts were filtered through Celite. The volatiles were removed from the filtrate by vacuum to give **1** as a white solid (0.403 g, 75 %). Crystals suitable for X-ray crystallography were obtained by cooling a concentrated solution of **1** in pentane to –35 °C for 1 day. <sup>1</sup>H NMR (C<sub>6</sub>D<sub>6</sub>): δ 1.45 (broad s, 36H, OC(CH<sub>3</sub>)<sub>3</sub>). <sup>53a</sup> <sup>13</sup>C {<sup>1</sup>H} NMR (C<sub>6</sub>D<sub>6</sub>): δ 31.9 (OC(CH<sub>3</sub>)<sub>3</sub>), 73.3 (OC(CH<sub>3</sub>)<sub>3</sub>). <sup>119</sup>Sn {<sup>1</sup>H} NMR (C<sub>6</sub>D<sub>6</sub>, 400 MHz): δ –91.6. Anal. Calc. for C<sub>16</sub>H<sub>36</sub>Sn<sub>2</sub>O<sub>4</sub>: C, 36.27; H, 6.85. Found: C, 35.44; H, 6.64%.

**Preparation of ImMe<sub>2</sub>•SnCl<sub>2</sub> (2):** In a variation of a literature procedure,<sup>S2</sup> N,N-dimethylimidazolium iodide (0.206 g, 0.919 mmol) and KH (0.176 g, 4.39 mmol) were suspended in 10 mL of THF and stirred for 4 hours. The precipitate was allowed to settle, and the orange solution containing free ImMe<sub>2</sub> (ImMe<sub>2</sub> = (HCNMe)<sub>2</sub>C:) was filtered into a vial containing SnCl<sub>2</sub> (0.174 g, 0.918 mmol) suspended in 4 mL of THF. The reaction mixture was stirred for 15 minutes, and the volatiles were then removed from the reaction mixture to give **2** as a white solid (0.261 g, 99 %). Crystals suitable for X-ray crystallography were obtained by cooling a concentrated solution of **2** in THF to –35 °C for one day. <sup>1</sup>H NMR (CDCl<sub>3</sub>): δ 4.09 (s, 6H, NCH<sub>3</sub>), 6.97 (s, 2H, N(CH)<sub>2</sub>N). <sup>13</sup>C {<sup>1</sup>H} NMR (CDCl<sub>3</sub>): δ 37.8 (NCH<sub>3</sub>), 123.1 (N(CH)<sub>2</sub>N), 179.8 (NCN). <sup>119</sup>Sn NMR (CDCl<sub>3</sub>, 500 MHz): δ –600.4. Mp: 165 °C (decomp.). Anal. Calc. for C<sub>5</sub>H<sub>8</sub>N<sub>2</sub>SnCl<sub>2</sub>: C, 21.02; H, 2.82; N, 9.80. Found: C, 21.19; H, 2.83; N, 9.42%.

**Preparation of ImMe<sub>2</sub>•Sn(O<sup>t</sup>Bu)<sub>2</sub> (3) from ImMe<sub>2</sub>•SnCl<sub>2</sub> (2):** A suspension of K[O<sup>t</sup>Bu] (0.095 g, 0.85 mmol) in 3 mL of Et<sub>2</sub>O was added dropwise to a stirring solution of **2** (0.121 g, 0.423 mol) in 5 mL of Et<sub>2</sub>O. The reaction mixture was stirred for 2 hours, after which the precipitate was allowed to settle, and the mother liquor was filtered through Celite. The remaining solid was re-suspended in toluene (10 mL) and stirred for 10 minutes to extract additional product. The extract was filtered through Celite, added to the first extraction, and the volatiles were removed under vacuum to give **3** as a yellow solid (0.088 g, 58 %). Crystals suitable for X-ray crystallography were obtained by cooling a concentrated solution of **3** in Me<sub>3</sub>SiOSiMe<sub>3</sub>/hexanes to –35 °C for 3 days. <sup>1</sup>H NMR (C<sub>6</sub>D<sub>6</sub>): δ 1.62 (s, 18H, C(CH<sub>3</sub>)<sub>3</sub>), 3.49 (s, 6H, NCH<sub>3</sub>), 5.64 (s, 2H, N(CH)<sub>2</sub>N). <sup>13</sup>C {<sup>1</sup>H} NMR (C<sub>6</sub>D<sub>6</sub>): δ 35.4 (OC(CH<sub>3</sub>)<sub>3</sub>), 36.3 (NCH<sub>3</sub>), 70.2 (OC(CH<sub>3</sub>)<sub>3</sub>), 121.0 (N(CH)<sub>2</sub>N), 206.2 (NCN). <sup>119</sup>Sn {<sup>1</sup>H} NMR (C<sub>6</sub>D<sub>6</sub>, 400 MHz): δ –101.3. Mp: 123 °C. Anal. Calc. for C<sub>13</sub>H<sub>26</sub>N<sub>2</sub>SnO<sub>2</sub>: C, 43.24; H, 7.26; N, 7.76. Found: C, 42.87; H, 7.14; N, 7.61%.

**Alternative preparation of ImMe<sub>2</sub>•Sn(O<sup>t</sup>Bu)<sub>2</sub> (3):** In a variation of a literature procedure,<sup>S2</sup> N,N-dimethylimidazolium iodide (0.107 g, 0.478 mmol) and KH (0.057 g, 1.4 mmol) were suspended in 10 mL of THF and stirred for 4 hours. The precipitate was allowed to settle, and the orange solution containing free ImMe<sub>2</sub> was filtered into a vial containing a solution of [Sn(O<sup>t</sup>Bu)<sub>2</sub>]<sub>2</sub> (1) (0.125 g, 0.236 mmol) in 4 mL of THF. The reaction mixture was stirred for 15 minutes, and the volatiles were then removed from the reaction mixture to afford a yellow solid. The solid was dissolved in 3 mL hexanes and filtered through Celite. The volatiles were removed to give ImMe<sub>2</sub>•Sn(O<sup>t</sup>Bu)<sub>2</sub> (3) as a yellow solid (0.118 g, 69 %). NMR data matched those reported above.

**General procedure for the NMR-scale deposition of Sn from precursors [Sn(O<sup>t</sup>Bu)<sub>2</sub>]<sub>2</sub> (1), ImMe<sub>2</sub>•Sn(O<sup>t</sup>Bu)<sub>2</sub> (3), and Sn[N(SiMe<sub>3</sub>)<sub>2</sub>]<sub>2</sub> (4):** Solutions of each precursor in C<sub>6</sub>D<sub>6</sub> (~10 mg in 500 μL) were prepared and loaded into J-Young NMR tubes. The appropriate equivalent(s) of HBpin (4 equiv for 1, 2 equiv for 3, and 1 or 2 equiv for 4) were added by micropipette, and NMR spectra were collected immediately.

**Larger-scale elemental Sn deposition reactions:**

**(a) [Sn(O<sup>t</sup>Bu)<sub>2</sub>]<sub>2</sub> (1) and HBpin:** HBpin (113.0 μL, 0.7788 mmol) was added dropwise at room temperature to a toluene solution (0.010 M) containing [Sn(O<sup>t</sup>Bu)<sub>2</sub>]<sub>2</sub> (1) (0.103 g, 0.195 mmol). A dark brown precipitate formed immediately, and the reaction mixture was stirred for 1 hour to afford Sn metal as a lustrous grey solid. The volatiles were removed under vacuum, and the solid was washed twice with 2 mL of toluene and dried (0.046 g, quantitative yield of Sn metal).

**(b) ImMe<sub>2</sub>•Sn(O<sup>t</sup>Bu)<sub>2</sub> (3) and HBpin:** HBpin (26.8 μL, 0.185 mmol) was added dropwise at room temperature to a toluene solution (0.010 M) containing ImMe<sub>2</sub>•Sn(O<sup>t</sup>Bu)<sub>2</sub> (3) (0.033 g, 0.093 mmol). A dark grey suspension formed immediately, and the reaction mixture was allowed to stir for 1 hour to afford Sn metal as a grey solid. Removing the volatiles under vacuum revealed the presence of an off-white residue, postulated to be an adduct of ImMe<sub>2</sub> and <sup>t</sup>BuOBpin. The grey solid was washed sequentially with toluene and THF (3 mL of each) to remove the white residue, although trace amounts continued to adhere to the Sn surface (final mass of Sn metal, 0.012 g, was 1 mg higher than expected for a quantitative yield).

**(c) Sn[N(SiMe<sub>3</sub>)<sub>2</sub>]<sub>2</sub> (4) and HBpin:** HBpin (100.4 μL, 0.6919 mmol) was added dropwise at room temperature to a toluene solution (0.010 M) containing Sn[N(SiMe<sub>3</sub>)<sub>2</sub>]<sub>2</sub> (4) (0.152 g, 0.346 mmol). A dark brown precipitate formed immediately, and the reaction mixture was allowed to stir for 1 hour to afford Sn metal as a lustrous grey solid. The volatiles were removed under vacuum, and the solid was washed with toluene and dried again (0.041 g, quantitative yield of Sn metal). Data for (Me<sub>3</sub>Si)<sub>2</sub>NBpin: <sup>1</sup>H NMR (C<sub>6</sub>D<sub>6</sub>): δ 0.36 (s, 18H, Si(CH<sub>3</sub>)<sub>3</sub>), 1.03 (s, 12H, [C(CH<sub>3</sub>)<sub>2</sub>]<sub>2</sub>).<sup>S4</sup> <sup>13</sup>C {<sup>1</sup>H} NMR (C<sub>6</sub>D<sub>6</sub>): δ 3.8 (Si(CH<sub>3</sub>)<sub>3</sub>), 24.7 ([C(CH<sub>3</sub>)<sub>2</sub>]<sub>2</sub>), 81.7 ([C(CH<sub>3</sub>)<sub>2</sub>]<sub>2</sub>).<sup>S4</sup> <sup>11</sup>B NMR (C<sub>6</sub>D<sub>6</sub>): δ 25.6.<sup>S4</sup>

**Reaction of <sup>t</sup>BuOH with HBpin to afford <sup>t</sup>BuOBpin:** HBpin (1000 μL, 6.892 mmol) was added dropwise to a stirring liquid sample of HO<sup>t</sup>Bu (659.1 μL, 6.892 mmol) at room temperature. Immediate bubbling was observed, and the reaction mixture was stirred for another 15 minutes after the addition of HBpin was complete to afford <sup>t</sup>BuOBpin as a colorless liquid (1.311 g, 95 %). <sup>1</sup>H NMR (C<sub>6</sub>D<sub>6</sub>): δ 1.06 (s, 12H, [C(CH<sub>3</sub>)<sub>2</sub>]<sub>2</sub>), 1.37 (s, 9H, OC(CH<sub>3</sub>)<sub>3</sub>).<sup>S5</sup> <sup>13</sup>C {<sup>1</sup>H} NMR (C<sub>6</sub>D<sub>6</sub>): δ 24.7 ([C(CH<sub>3</sub>)<sub>2</sub>]<sub>2</sub>), 30.3 (OC(CH<sub>3</sub>)<sub>3</sub>), 73.5 (OC(CH<sub>3</sub>)<sub>3</sub>), 81.8 ([C(CH<sub>3</sub>)<sub>2</sub>]<sub>2</sub>). <sup>11</sup>B NMR (C<sub>6</sub>D<sub>6</sub>): δ 21.6.<sup>S5</sup>

**Preparation of Sn[N(SiMe<sub>3</sub>)<sub>2</sub>]<sub>2</sub> (4):** A solution of K[N(SiMe<sub>3</sub>)<sub>2</sub>] (0.673 g, 3.38 mmol) in 5 mL of THF at -35 °C was added dropwise to a stirring solution of SnCl<sub>2</sub> (0.321 g, 1.69 mmol) in 5 mL of THF at the same temperature. The reaction mixture was warmed to room temperature and stirred for 16 hours. The resulting bright orange suspension was filtered through Celite, and the volatiles were removed from the filtrate by vacuum to afford 4 as a bright red-orange liquid (0.514 g, 69 %). NMR data matched those from the literature.<sup>S6</sup>

**Preparation of ImMe<sub>2</sub> for the collection of NMR data in C<sub>6</sub>D<sub>6</sub>:** N,N-dimethylimidazolium iodide (0.183 g, 0.817 mmol) and KH (0.128 g, 3.19 mmol) were suspended in 10 mL of THF and stirred for 4 hours. The resulting brown/grey suspension was filtered to remove KCl and unreacted KH, yielding a light orange solution containing free ImMe<sub>2</sub> (ImMe<sub>2</sub> = (HCNMe)<sub>2</sub>C:). The solvent was then removed from the filtrate by vacuum to afford ImMe<sub>2</sub> as a dark orange liquid (0.078 g, 99 %). <sup>1</sup>H NMR (C<sub>6</sub>D<sub>6</sub>): δ 3.38 (s, 6H, C(CH<sub>3</sub>)<sub>3</sub>), 6.29 (s, 2H, N(CH)<sub>2</sub>N).<sup>S7ab</sup> <sup>13</sup>C {<sup>1</sup>H} NMR (C<sub>6</sub>D<sub>6</sub>): 37.5 (NCH<sub>3</sub>), 119.7 (N(CH)<sub>2</sub>N), 216.6 (NCN).<sup>S7b</sup>

**Reaction of ImMe<sub>2</sub> and <sup>t</sup>BuOBpin in varying ratios:**

**(a) ImMe<sub>2</sub> and <sup>t</sup>BuOBpin (1:0.5):** <sup>t</sup>BuOBpin (0.011 g, 0.055 mmol) was added dropwise to a J-Young NMR tube containing ImMe<sub>2</sub> (0.011 g, 0.11 mmol) in 500 μL of C<sub>6</sub>D<sub>6</sub> to afford a light-yellow solution. The J-Young was then sealed (via a Teflon valve) and inverted several times to ensure homogeneity, and NMR spectra were acquired. <sup>1</sup>H NMR (C<sub>6</sub>D<sub>6</sub>): δ 1.34 (br, 12H, [C(CH<sub>3</sub>)<sub>2</sub>]<sub>2</sub>), 1.36 (s, 9H, OC(CH<sub>3</sub>)<sub>3</sub>), 3.49 (s, 12H, NCH<sub>3</sub>), 6.03 (br, 4H, N(CH)<sub>2</sub>N). <sup>13</sup>C {<sup>1</sup>H} NMR (C<sub>6</sub>D<sub>6</sub>): δ 26.5 ([C(CH<sub>3</sub>)<sub>2</sub>]<sub>2</sub>), 32.5 (OC(CH<sub>3</sub>)<sub>3</sub>), 36.7 (NCH<sub>3</sub>), 68.2 (OC(CH<sub>3</sub>)<sub>3</sub>), 78.9 ([C(CH<sub>3</sub>)<sub>2</sub>]<sub>2</sub>), 119.8 (N(CH)<sub>2</sub>N). <sup>11</sup>B NMR (C<sub>6</sub>D<sub>6</sub>): δ 4.3.

**(b) ImMe<sub>2</sub> and <sup>t</sup>BuOBpin (1:1):** <sup>t</sup>BuOBpin (0.023 g, 0.11 mmol) was added dropwise to a J-Young NMR tube containing ImMe<sub>2</sub> (0.010 g, 0.10 mmol) in 500 μL of C<sub>6</sub>D<sub>6</sub> to afford a light-yellow solution. The J-Young was then sealed (via a Teflon valve) and inverted several times to ensure homogeneity, and NMR spectra were acquired. <sup>1</sup>H NMR (C<sub>6</sub>D<sub>6</sub>): δ 1.31 (br, 12H, [C(CH<sub>3</sub>)<sub>2</sub>]<sub>2</sub>), 1.36 (s, 9H, OC(CH<sub>3</sub>)<sub>3</sub>), 3.60 (s, 6H, NCH<sub>3</sub>), 5.84 (br, 2H, N(CH)<sub>2</sub>N). <sup>13</sup>C {<sup>1</sup>H} NMR (C<sub>6</sub>D<sub>6</sub>): δ 26.4 ([C(CH<sub>3</sub>)<sub>2</sub>]<sub>2</sub>), 32.3 (OC(CH<sub>3</sub>)<sub>3</sub>), 36.1 (NCH<sub>3</sub>), 67.8 (OC(CH<sub>3</sub>)<sub>3</sub>), 79.2 ([C(CH<sub>3</sub>)<sub>2</sub>]<sub>2</sub>), 120.0 (N(CH)<sub>2</sub>N). <sup>11</sup>B NMR (C<sub>6</sub>D<sub>6</sub>): δ 5.7.

**(c) ImMe<sub>2</sub> and <sup>t</sup>BuOBpin (1:2):** <sup>t</sup>BuOBpin (0.046 g, 0.23 mmol) was added dropwise to a J-Young NMR tube containing ImMe<sub>2</sub> (0.011 g, 0.11 mmol) in 500 μL of C<sub>6</sub>D<sub>6</sub> to afford a light-yellow solution. The J-Young was then sealed (via a Teflon valve) and inverted several times to ensure homogeneity, and NMR spectra were acquired. <sup>1</sup>H NMR (C<sub>6</sub>D<sub>6</sub>): δ 1.19 (br, 24H, [C(CH<sub>3</sub>)<sub>2</sub>]<sub>2</sub>), 1.35 (s, 18H, OC(CH<sub>3</sub>)<sub>3</sub>), 3.64 (s, 6H, NCH<sub>3</sub>), 5.85 (s, 2H, N(CH)<sub>2</sub>N). <sup>13</sup>C {<sup>1</sup>H} NMR (C<sub>6</sub>D<sub>6</sub>): δ 25.7 ([C(CH<sub>3</sub>)<sub>2</sub>]<sub>2</sub>), 31.6 (OC(CH<sub>3</sub>)<sub>3</sub>), 36.0 (NCH<sub>3</sub>), 68.1 (OC(CH<sub>3</sub>)<sub>3</sub>), 80.4 ([C(CH<sub>3</sub>)<sub>2</sub>]<sub>2</sub>), 120.1 (N(CH)<sub>2</sub>N). <sup>11</sup>B NMR (C<sub>6</sub>D<sub>6</sub>): δ 12.7.

**Reaction of Sn[N(SiMe<sub>3</sub>)<sub>2</sub>]<sub>2</sub> (4) with HBpin (1 equiv) in the presence of the chelating ligand, PB:** PB (0.009 g, 0.02 mmol), Sn[N(SiMe<sub>3</sub>)<sub>2</sub>]<sub>2</sub> (0.011 g, 0.025 mmol) and HBpin (3.48 μL, 0.0240 mmol) were sequentially added to a J-Young NMR tube containing 500 μL of C<sub>6</sub>D<sub>6</sub>. A black precipitate formed immediately upon inversion of the NMR tube, and the reaction was monitored by NMR spectroscopy over 3 days. NMR data showed the generation of (Me<sub>3</sub>Si)<sub>2</sub>NBpin and HN(SiMe<sub>3</sub>)<sub>2</sub> in the presence of free PB. <sup>1</sup>H NMR (C<sub>6</sub>D<sub>6</sub>, after 3 days): δ 0.10 (s, 18H, HN(Si(CH<sub>3</sub>)<sub>3</sub>)<sub>2</sub>), 0.37 (s, 18H, (Me<sub>3</sub>Si)<sub>2</sub>NBpin, Si(CH<sub>3</sub>)<sub>3</sub>), 1.03 (s, 12H, (Me<sub>3</sub>Si)<sub>2</sub>NBpin, [C(CH<sub>3</sub>)<sub>2</sub>]<sub>2</sub>). Other signals observed matched those from the literature for free PB.<sup>S8</sup> <sup>11</sup>B NMR (C<sub>6</sub>D<sub>6</sub>, after 3 days): δ 21.9 (pinBOBpin, trace hydrolysis), 25.8 ((Me<sub>3</sub>Si)<sub>2</sub>NBpin), 76.4 (free PB).

## 2. NMR spectra

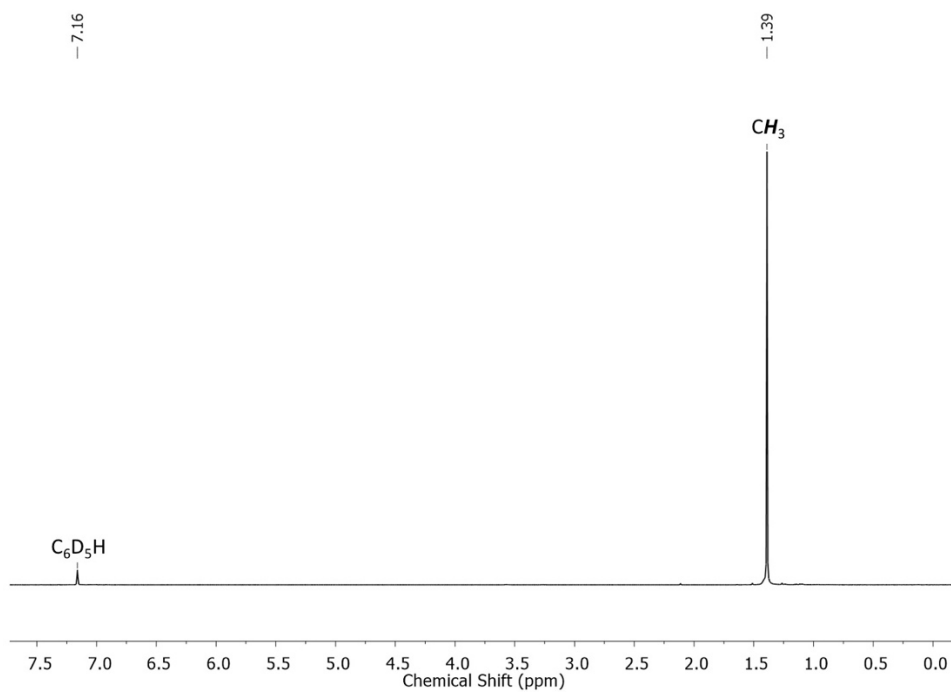


**Fig. S1.**  $^1\text{H}$  NMR spectrum of  $\text{K}[\text{Sn}(\text{O}^t\text{Bu})_3]$  in  $\text{C}_6\text{D}_6$ .

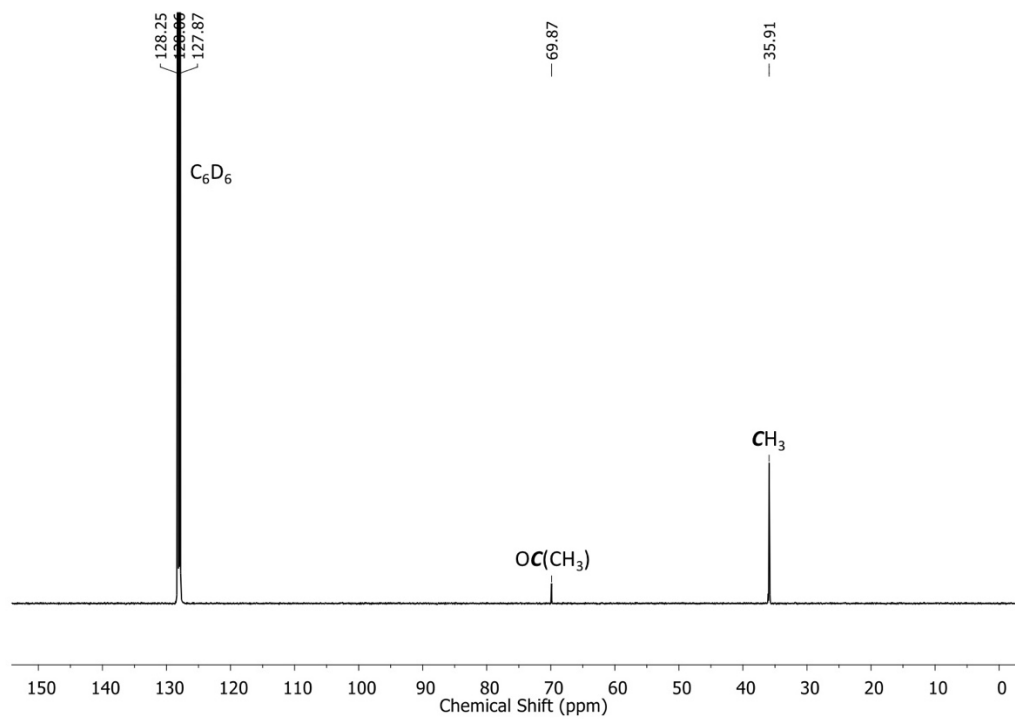


**Fig. S2.**  $^{13}\text{C}\{^1\text{H}\}$  NMR spectrum of  $\text{K}[\text{Sn}(\text{O}^t\text{Bu})_3]$  in  $\text{C}_6\text{D}_6$ .

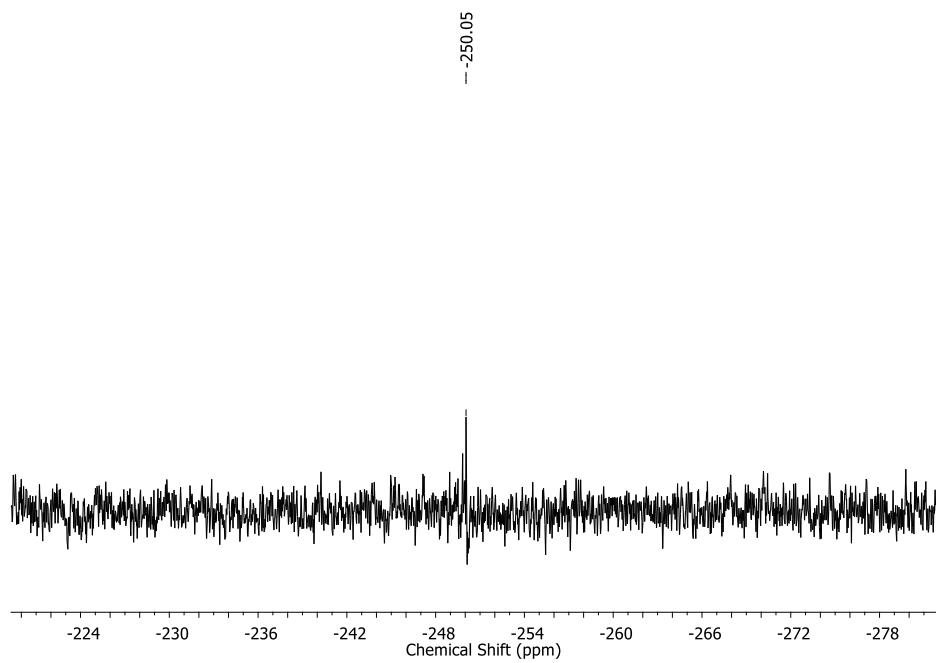


**Fig. S3.**  $^{119}\text{Sn}$  NMR spectrum of  $\text{K}[\text{Sn}(\text{O}^t\text{Bu})_3]$  in  $\text{C}_6\text{D}_6$ .

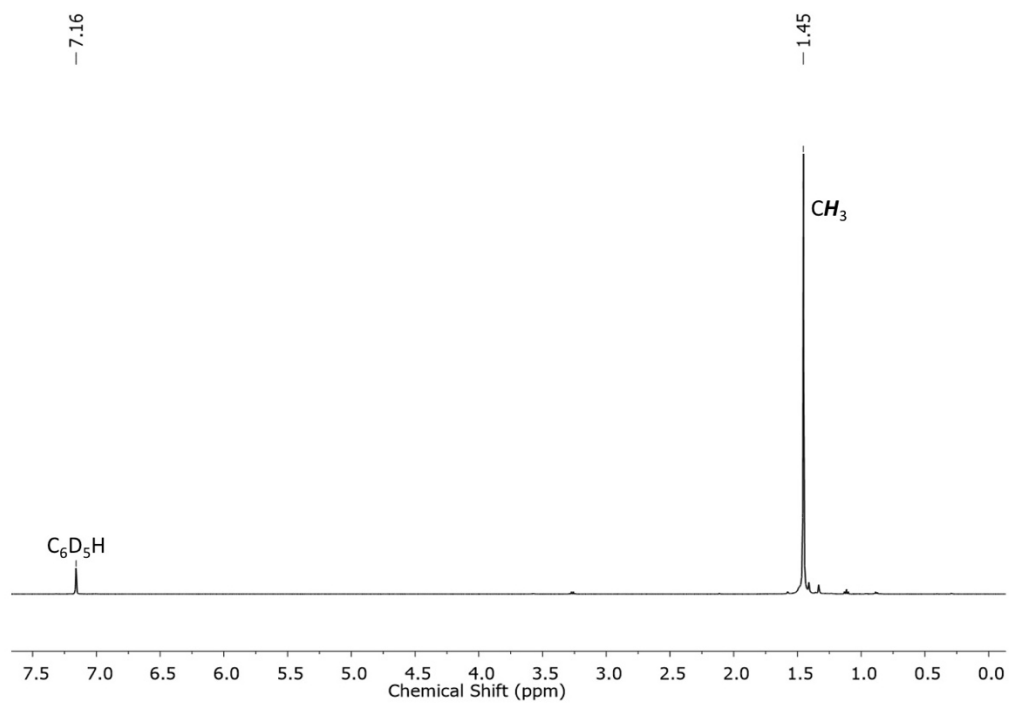


**Fig. S4.**  $^1\text{H}$  NMR spectrum of  $[\text{Sn}(\text{O}^t\text{Bu})_2]$  (**1**) in  $\text{C}_6\text{D}_6$ .

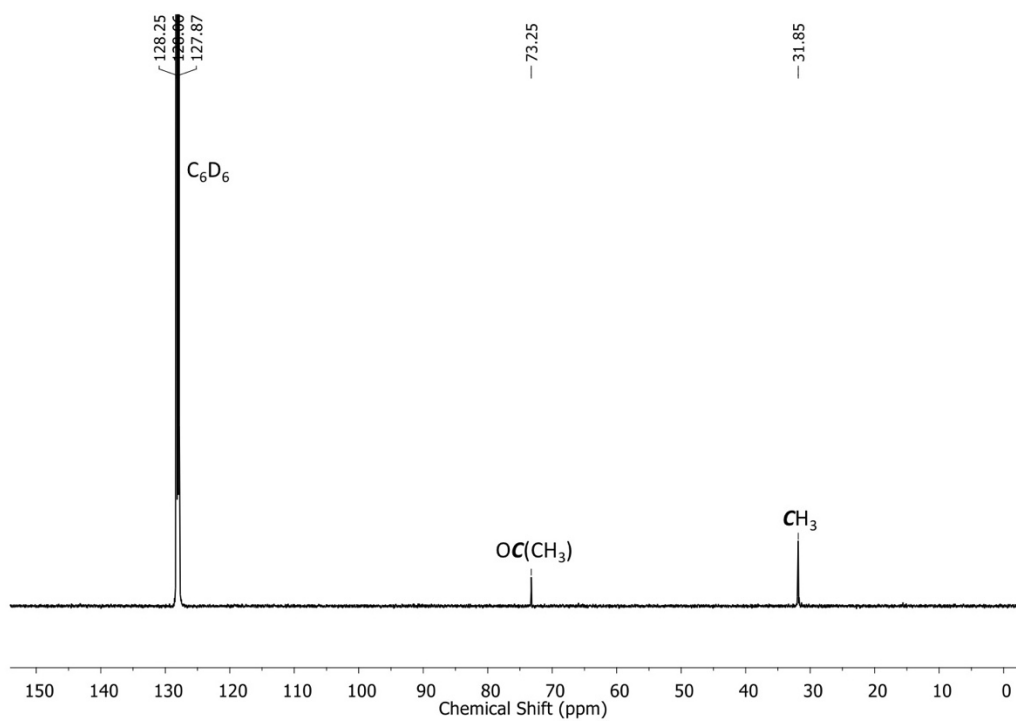


**Fig. S5.**  $^{13}\text{C}\{^1\text{H}\}$  NMR spectrum of  $[\text{Sn}(\text{O}^t\text{Bu})_2]_2$  (**1**) in  $\text{C}_6\text{D}_6$ .

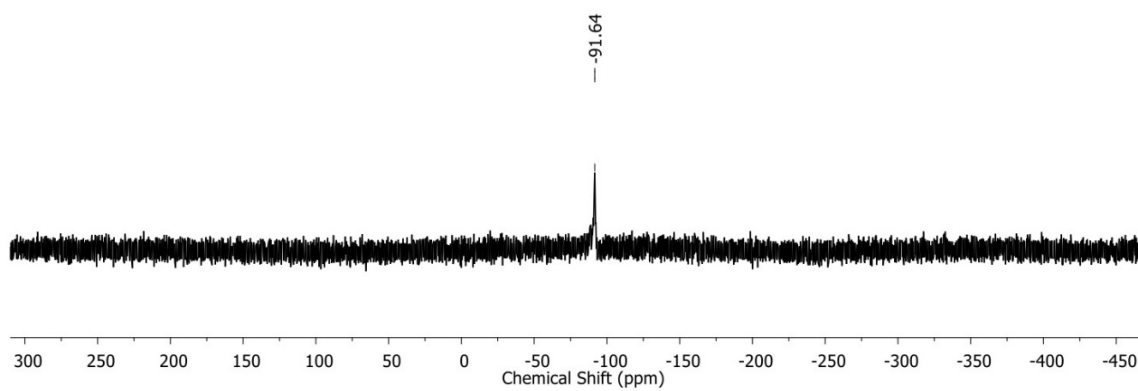


**Fig. S6.**  $^{119}\text{Sn}$  NMR spectrum of  $[\text{Sn}(\text{O}^t\text{Bu})_2]_2$  (**1**) in  $\text{C}_6\text{D}_6$ .

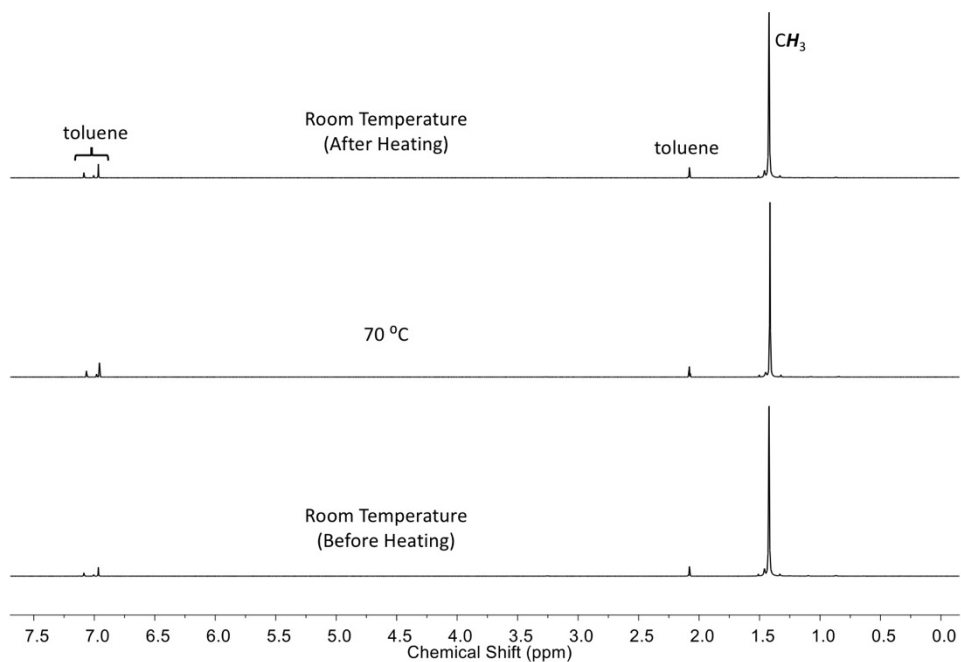


**Fig. S7.** Variable temperature  $^1\text{H}$  NMR spectra of  $[\text{Sn}(\text{O}^t\text{Bu})_2]$  (**1**) in toluene- $d_8$ .

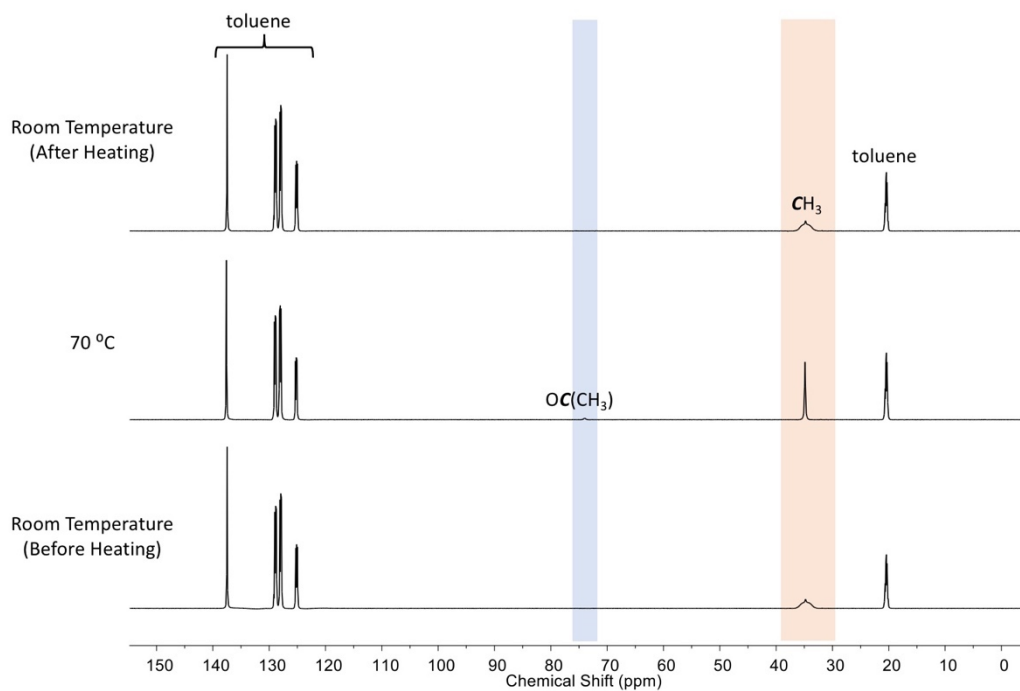


**Fig. S8.** Variable temperature  $^{13}\text{C}\{^1\text{H}\}$  NMR spectra of  $[\text{Sn}(\text{O}^t\text{Bu})_2]$  (**1**) in toluene- $d_8$ . The sharpening of the  $\text{CH}_3$  and  $\text{OC}(\text{CH}_3)$  resonances upon heating is indicative of fluxional behavior at room temperature.

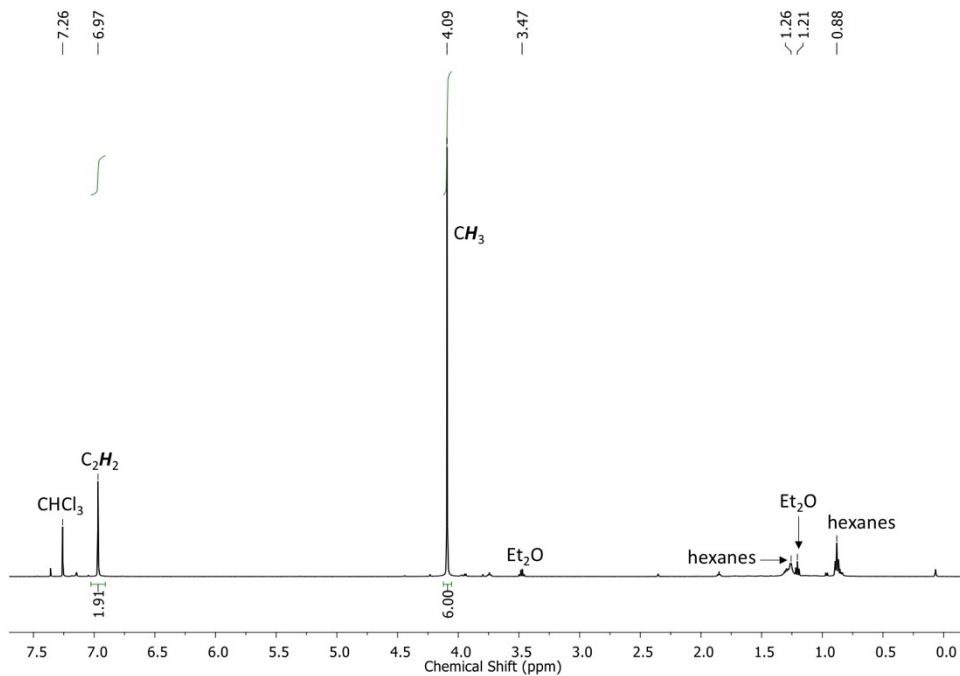


Fig. S9. <sup>1</sup>H NMR spectrum of ImMe<sub>2</sub>·SnCl<sub>2</sub> (**2**) in CDCl<sub>3</sub>.

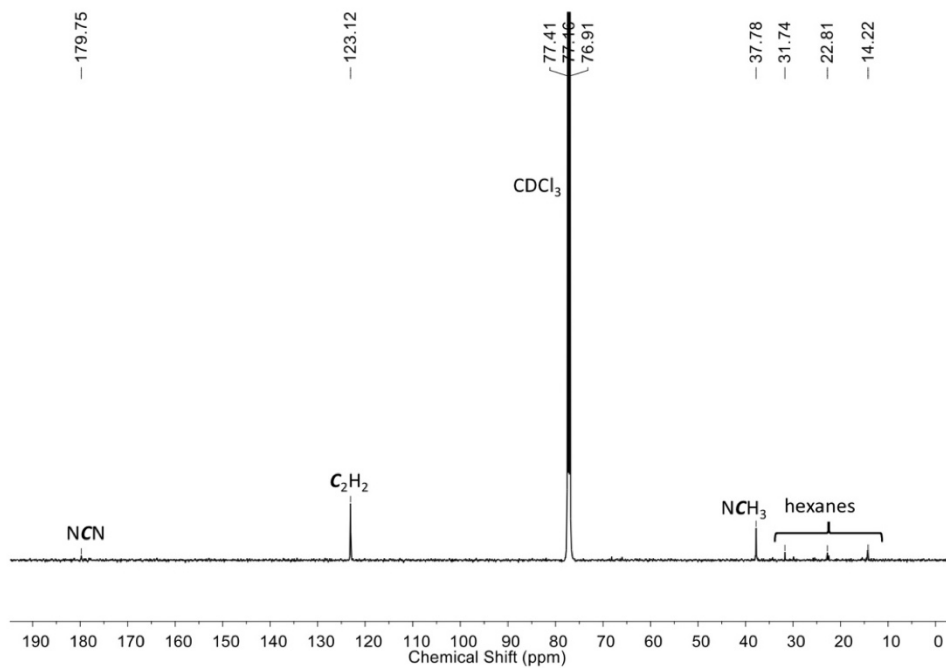
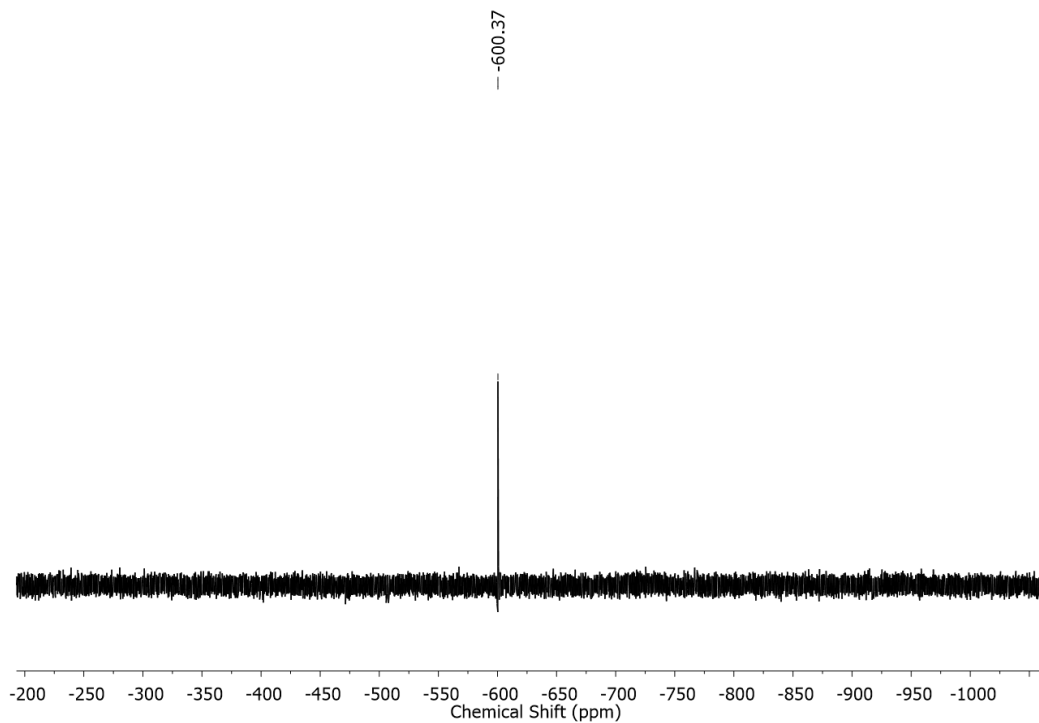
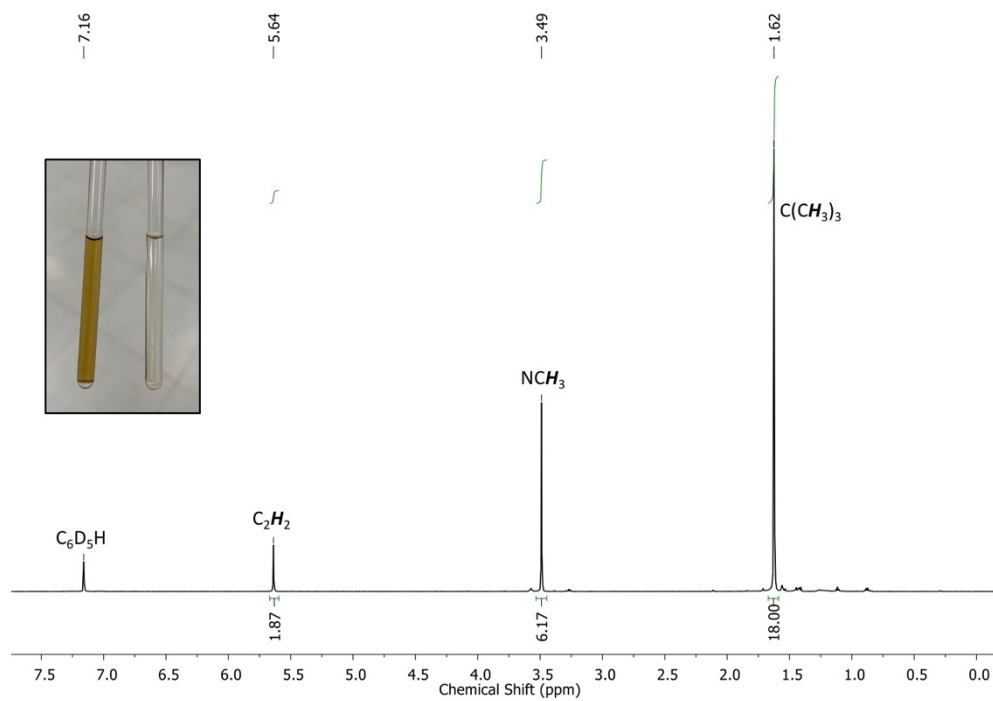


Fig. S10. <sup>13</sup>C{<sup>1</sup>H} NMR spectrum of ImMe<sub>2</sub>·SnCl<sub>2</sub> (**2**) in CDCl<sub>3</sub>.



**Fig. S11.**  $^{119}\text{Sn}$  NMR spectrum of  $\text{ImMe}_2\cdot\text{SnCl}_2$  (**2**) in  $\text{CDCl}_3$ .



**Fig. S12.**  $^1\text{H}$  NMR spectrum of  $\text{ImMe}_2\cdot\text{Sn}(\text{O}^t\text{Bu})_2$  (**3**) in  $\text{C}_6\text{D}_6$ . Inset shows solutions formed upon dissolution of  $\text{ImMe}_2\cdot\text{Sn}(\text{O}^t\text{Bu})_2$  (**3**) in  $\text{CDCl}_3$  (left) or  $\text{C}_6\text{D}_6$  (right). In contrast to  $\text{ImMe}_2\cdot\text{SnCl}_2$  (**2**),  $\text{ImMe}_2\cdot\text{Sn}(\text{O}^t\text{Bu})_2$  (**3**) decomposes in  $\text{CDCl}_3$ .

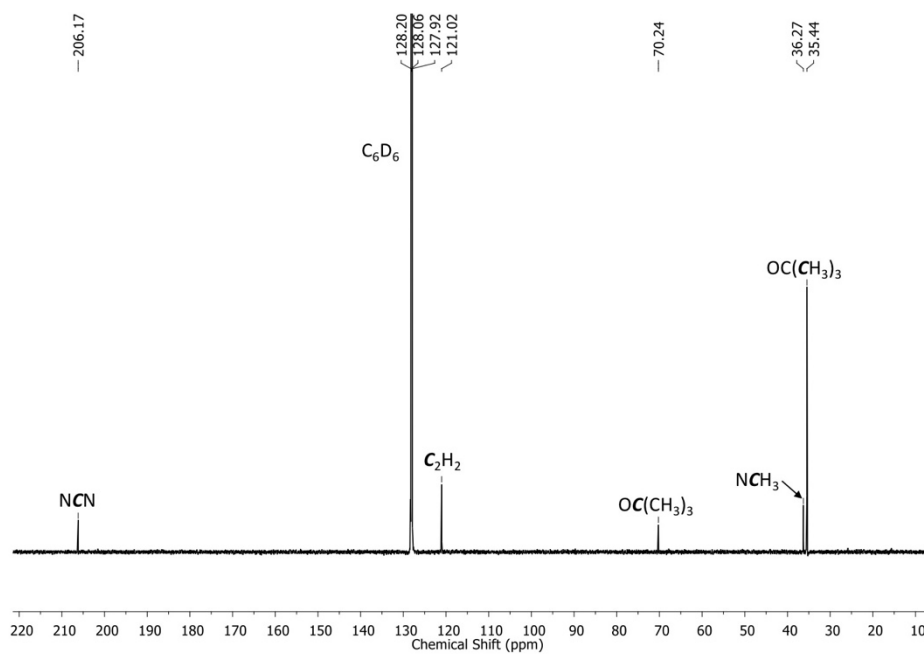


**Fig. S13.**  $^{13}\text{C}\{^1\text{H}\}$  NMR spectrum of  $\text{ImMe}_2\cdot\text{Sn}(\text{O}^t\text{Bu})_2$  (**3**) in  $\text{C}_6\text{D}_6$ .

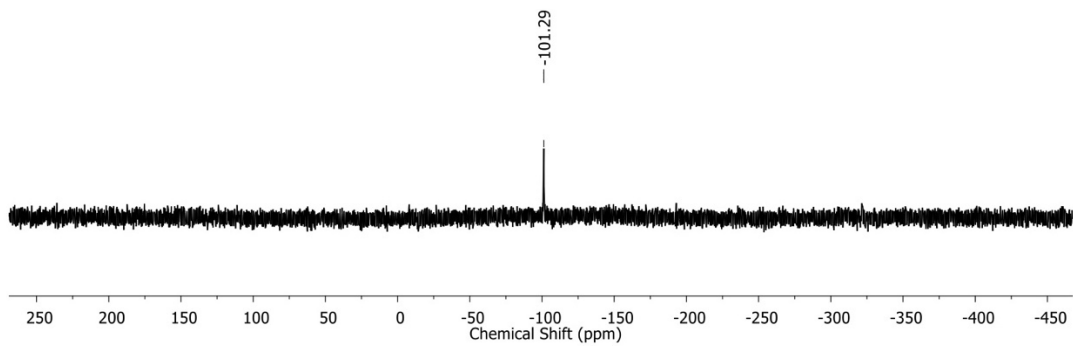


**Fig. S14.**  $^{119}\text{Sn}$  NMR spectrum of  $\text{ImMe}_2\cdot\text{Sn}(\text{O}^t\text{Bu})_2$  (**3**) in  $\text{C}_6\text{D}_6$ .

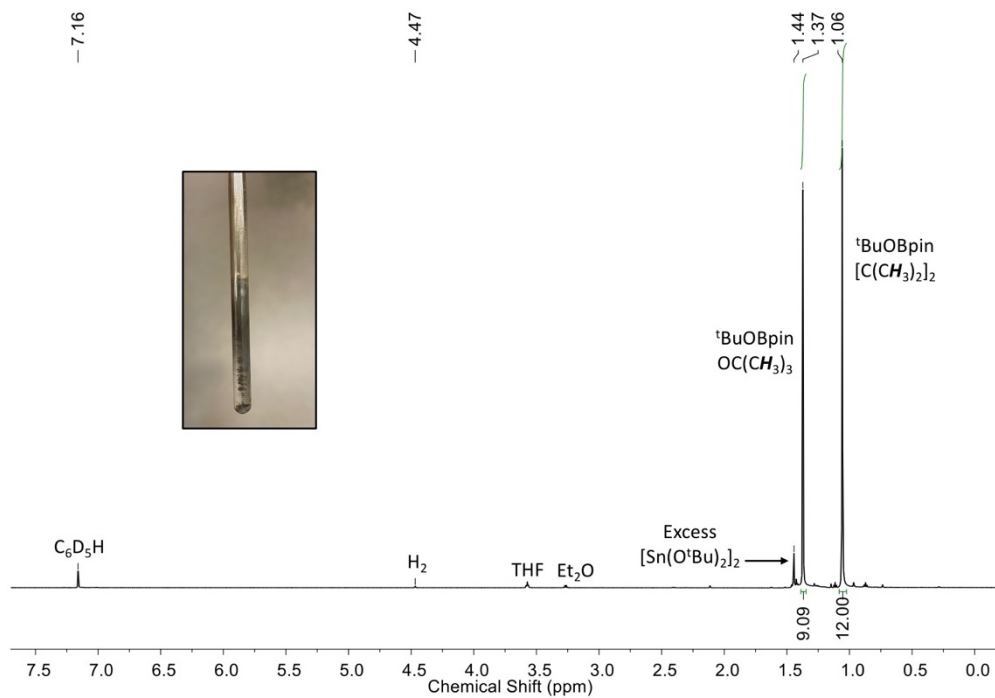


**Fig. S15.**  $^1\text{H}$  NMR spectrum of the soluble products formed upon reaction of  $[\text{Sn}(\text{O}^t\text{Bu})_2]$  (**1**) with 4 equiv of HBpin in  $\text{C}_6\text{D}_6$ . Inset of observed reaction mixture shows the precipitation of crystalline Sn.

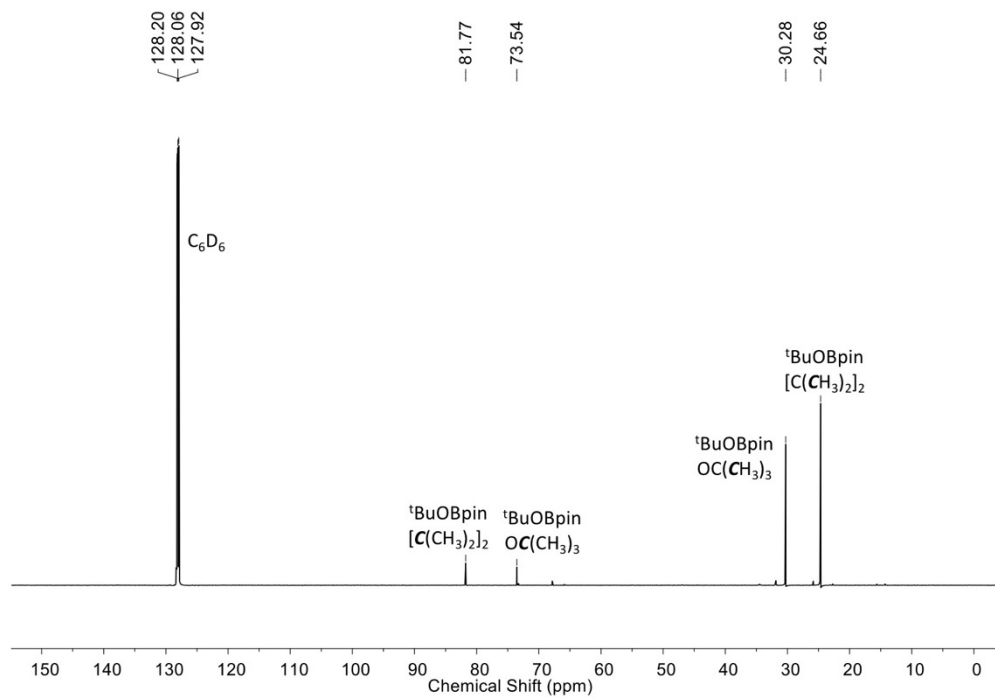


**Fig. S16.**  $^{13}\text{C}\{^1\text{H}\}$  NMR spectrum of the soluble product ( $^t\text{BuOBpin}$ ) formed upon reaction of  $[\text{Sn}(\text{O}^t\text{Bu})_2]$  (**1**) with 4 equiv of HBpin in  $\text{C}_6\text{D}_6$ .

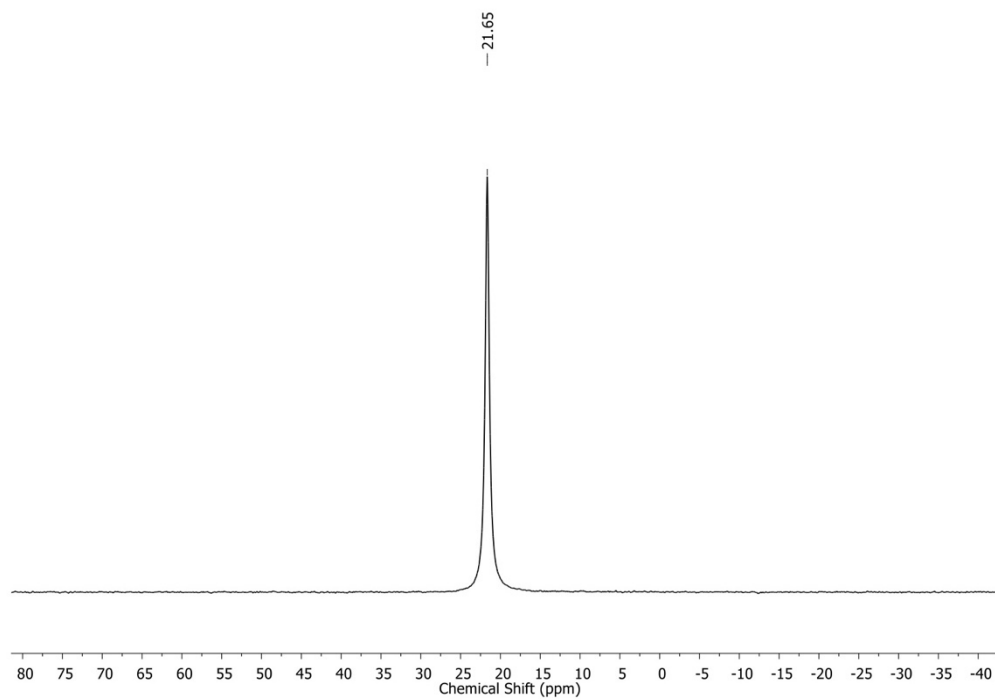


**Fig. S17.**  $^{11}\text{B}$  NMR spectrum of the  $^t\text{BuOBpin}$  formed upon reaction of  $[\text{Sn}(\text{O}^t\text{Bu})_2]$  (**1**) with 4 equiv of HBpin in  $\text{C}_6\text{D}_6$ .

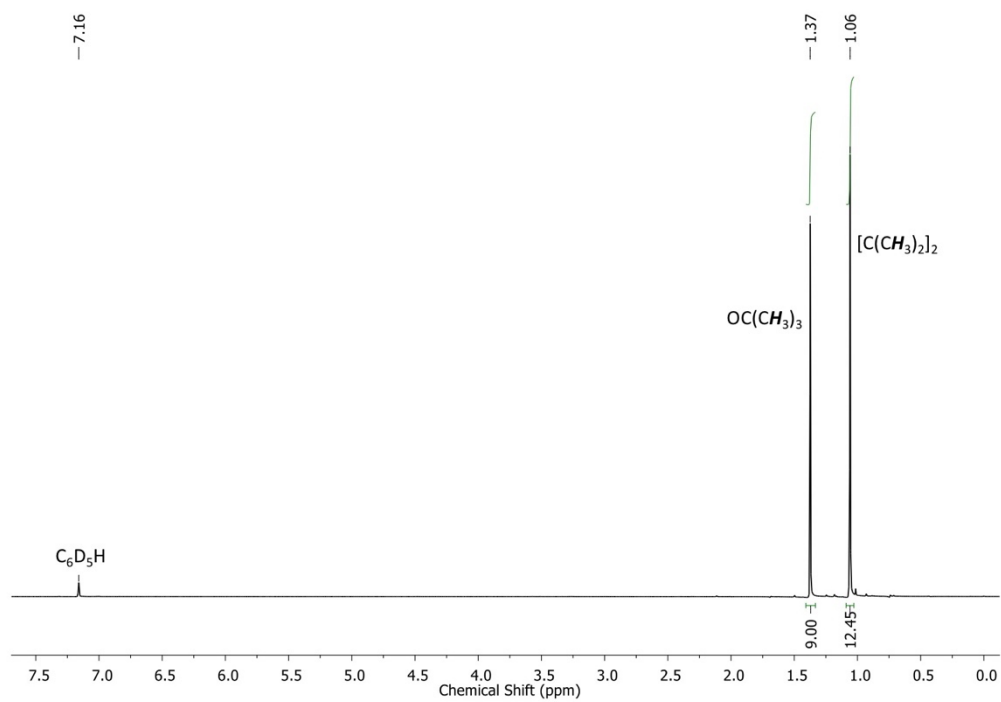


**Fig. S18.**  $^1\text{H}$  NMR spectrum of  $^t\text{BuOBpin}$  (formed from neat  $^t\text{BuOH}$  and HBpin) in  $\text{C}_6\text{D}_6$ .

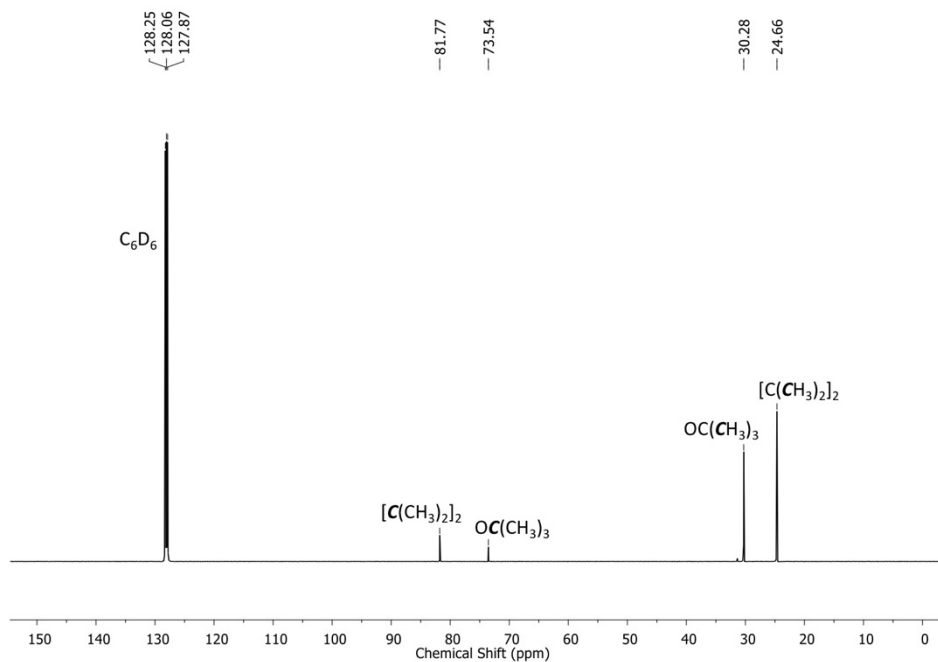


**Fig. S19.**  $^{13}\text{C}\{^1\text{H}\}$  NMR spectrum of  $^t\text{BuOBpin}$  (formed from neat  $^t\text{BuOH}$  and  $\text{HBpin}$ ) in  $\text{C}_6\text{D}_6$ .

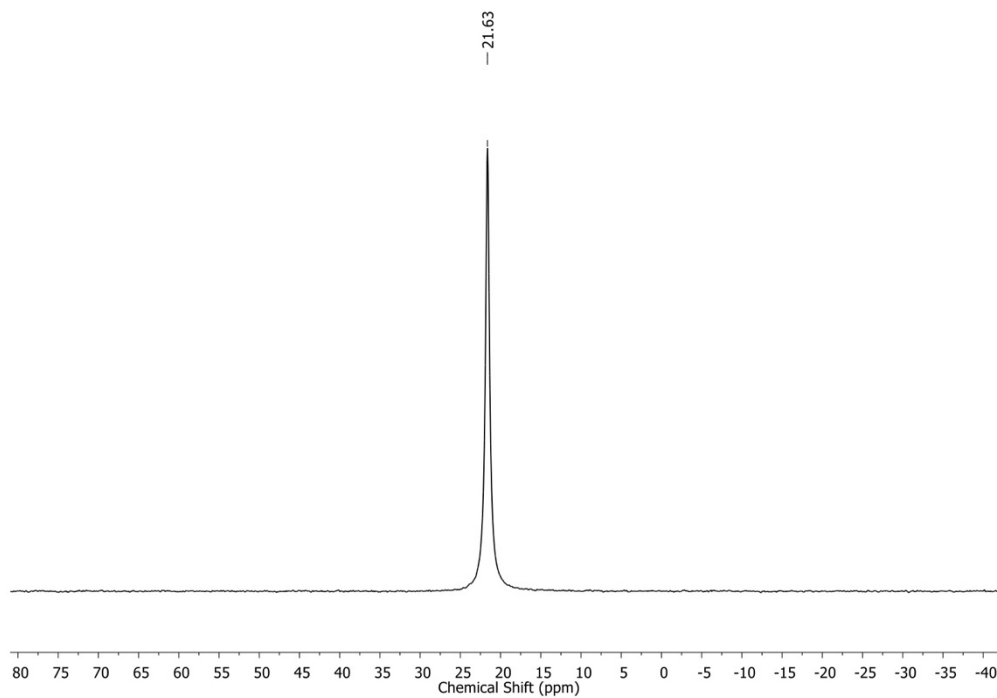


**Fig. S20.**  $^{11}\text{B}$  NMR spectrum of  $^t\text{BuOBpin}$  (formed from neat  $^t\text{BuOH}$  and  $\text{HBpin}$ ) in  $\text{C}_6\text{D}_6$ .

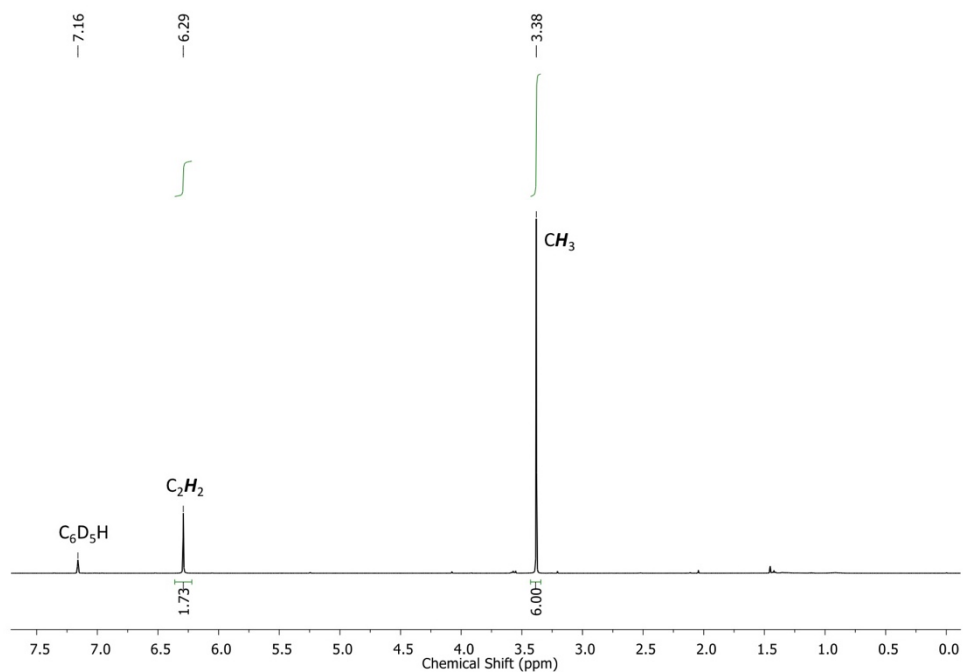


**Fig. S21.**  $^1\text{H}$  NMR spectrum of free  $\text{ImMe}_2$  in  $\text{C}_6\text{D}_6$ .

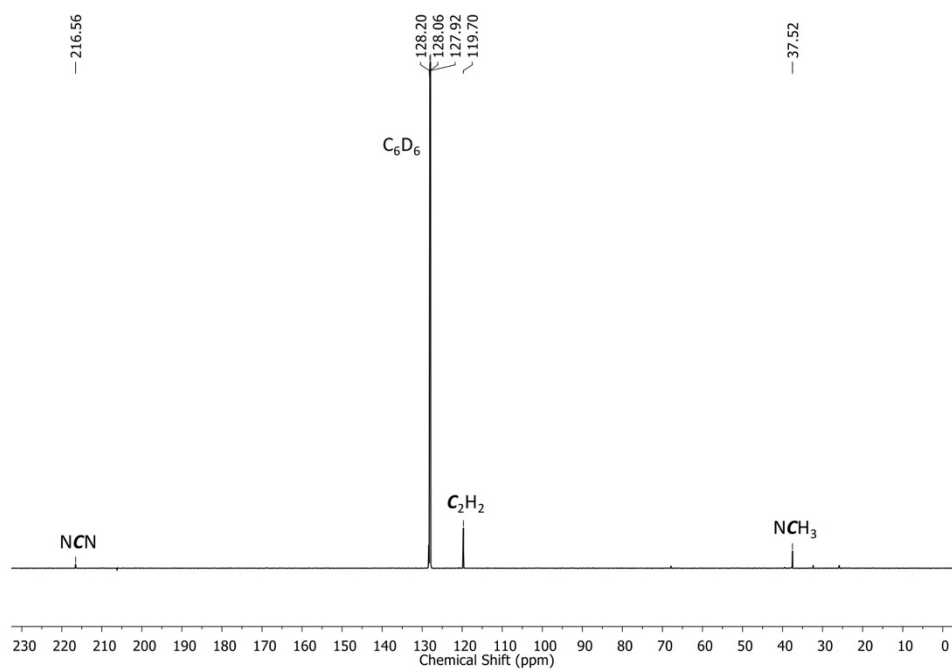


**Fig. S22.**  $^{13}\text{C}\{^1\text{H}\}$  NMR spectrum of free  $\text{ImMe}_2$  in  $\text{C}_6\text{D}_6$ .

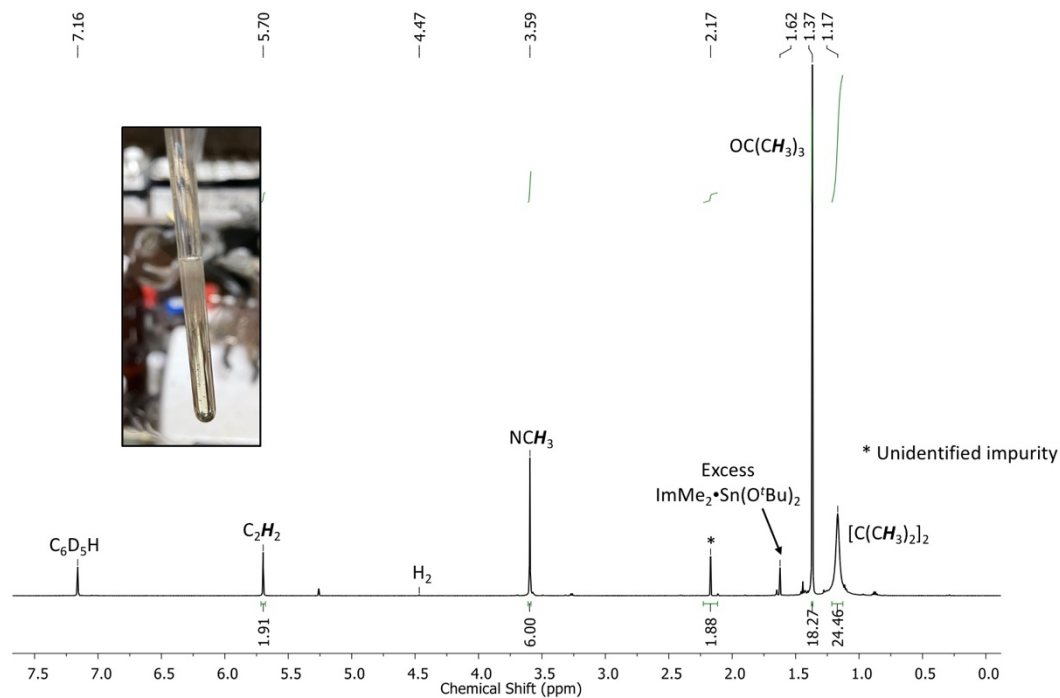


**Fig. S23.**  $^1H$  NMR spectrum of the soluble products formed upon reaction of  $ImMe_2 \cdot Sn(O^tBu)_2$  (**3**) with 2 equiv of HBpin in  $C_6D_6$ . Inset of observed reaction mixture shows the precipitation of crystalline Sn.

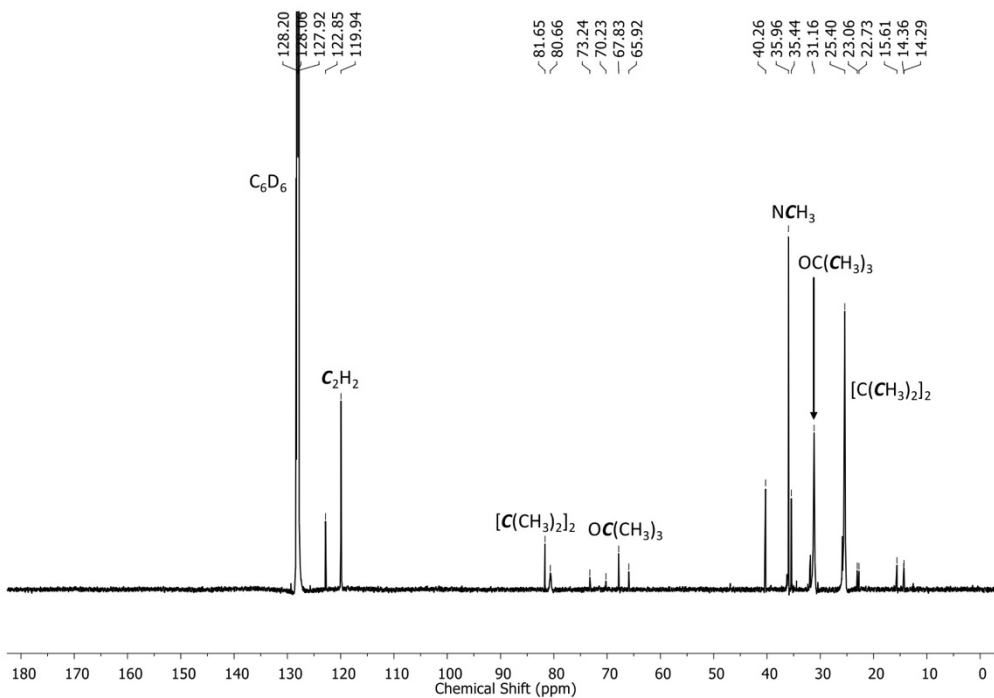


**Fig. S24.**  $^{13}C\{^1H\}$  NMR spectrum of the soluble products formed upon reaction of  $ImMe_2 \cdot Sn(O^tBu)_2$  (**3**) with 2 equiv of HBpin in  $C_6D_6$ .

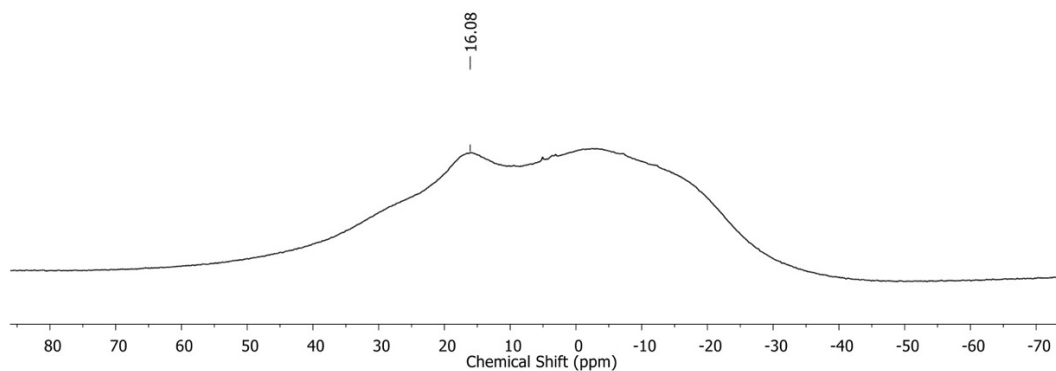


**Fig. S25.**  $^{11}\text{B}$  NMR spectrum of the soluble products formed upon reaction of  $\text{ImMe}_2\cdot\text{Sn}(\text{O}^t\text{Bu})_2$  (**3**) with 2 equiv of HBpin in  $\text{C}_6\text{D}_6$ . Note that the additional broad peaks are from the borosilicate glass NMR tube.

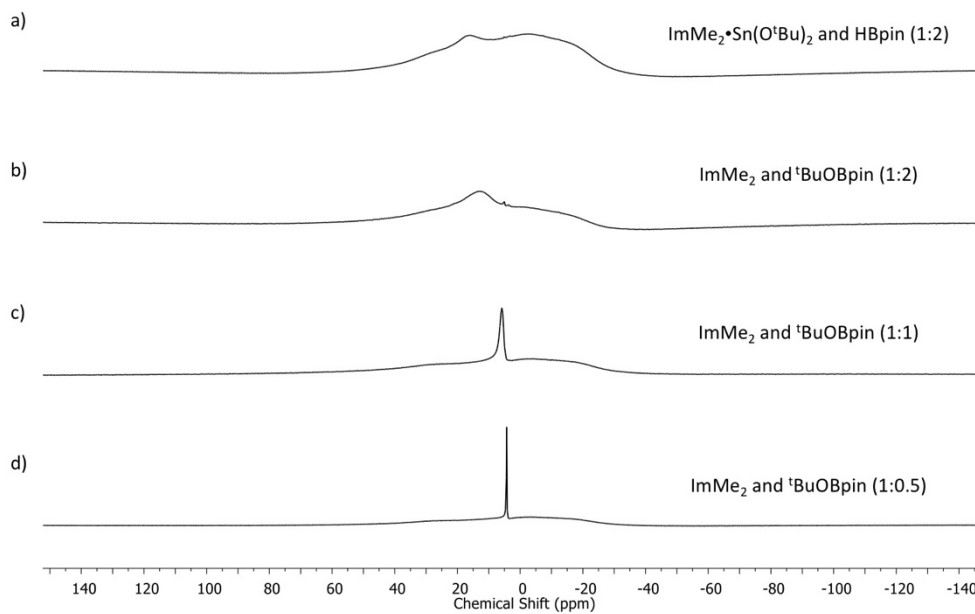


**Fig. S26.** Stacked  $^{11}\text{B}$  NMR spectra (recorded in  $\text{C}_6\text{D}_6$ ) corresponding to the reactions of (a)  $\text{ImMe}_2\cdot\text{Sn}(\text{O}^t\text{Bu})_2$  (**3**) and 2 equiv HBpin, (b) free  $\text{ImMe}_2$  and 2 equiv of  $^t\text{BuOBpin}$ , (c) free  $\text{ImMe}_2$  and 1 equiv of  $^t\text{BuOBpin}$ , and (d) free  $\text{ImMe}_2$  and 0.5 equiv of HBpin. Note that the additional broad peaks are from the borosilicate glass NMR tube.

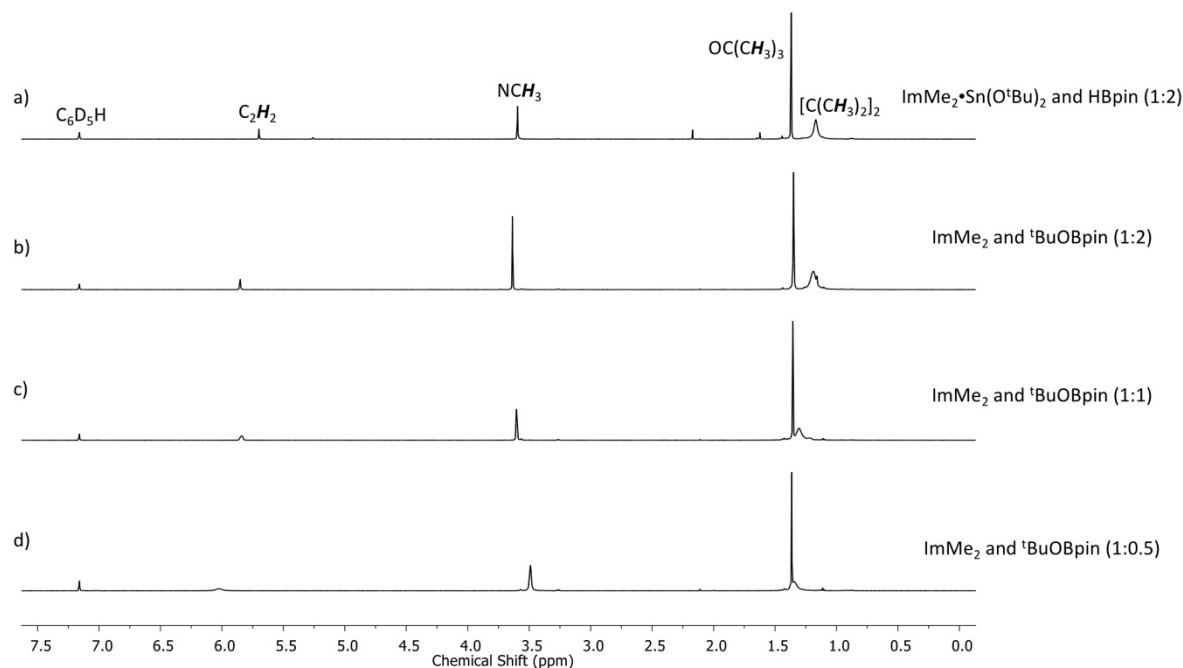


**Fig. S27.** Stacked  $^1\text{H}$  NMR spectra (recorded in  $\text{C}_6\text{D}_6$ ) corresponding to the reactions of (a)  $\text{ImMe}_2\cdot\text{Sn}(\text{O}^t\text{Bu})_2$  (**3**) and 2 equiv HBpin, (b) free  $\text{ImMe}_2$  and 2 equiv of  $^t\text{BuOBpin}$ , (c) free  $\text{ImMe}_2$  and 1 equiv of  $^t\text{BuOBpin}$ , and (d) free  $\text{ImMe}_2$  and 0.5 equiv of HBpin.

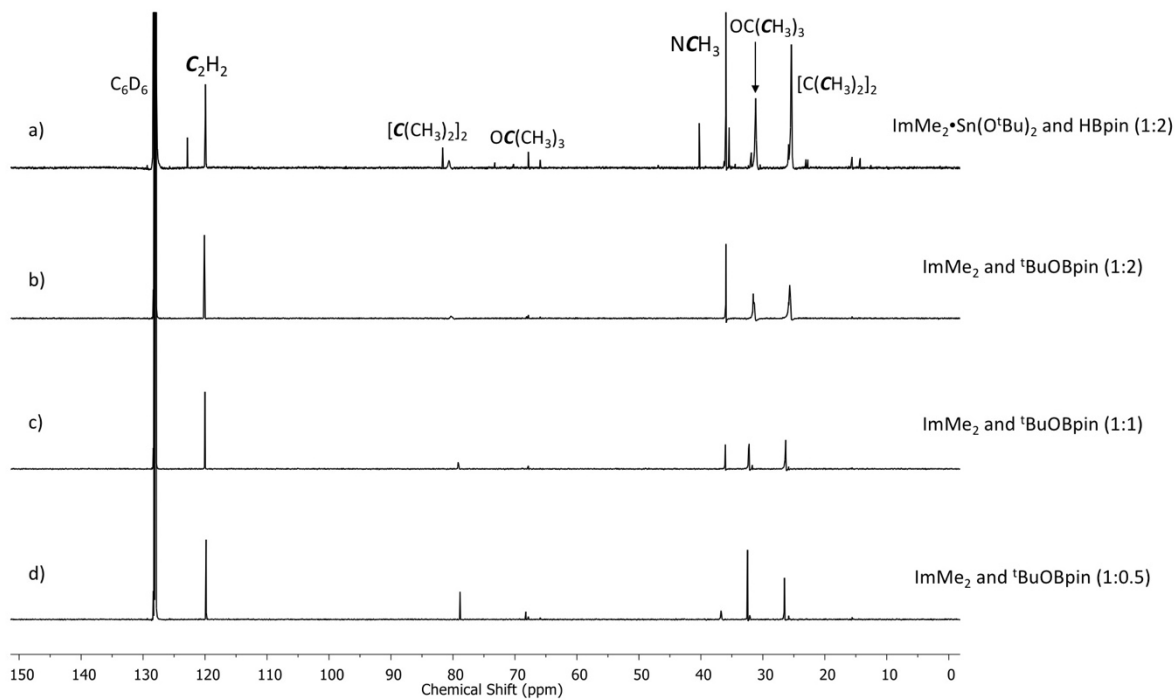


**Fig. S28.** Stacked  $^{13}\text{C}\{^1\text{H}\}$  NMR spectra (recorded in  $\text{C}_6\text{D}_6$ ) corresponding to the reactions of (a)  $\text{ImMe}_2\cdot\text{Sn}(\text{O}^t\text{Bu})_2$  (**3**) and 2 equiv HBpin, (b) free  $\text{ImMe}_2$  and 2 equiv of  $^t\text{BuOBpin}$ , (c) free  $\text{ImMe}_2$  and 1 equiv of  $^t\text{BuOBpin}$ , and (d) free  $\text{ImMe}_2$  and 0.5 equiv of HBpin.

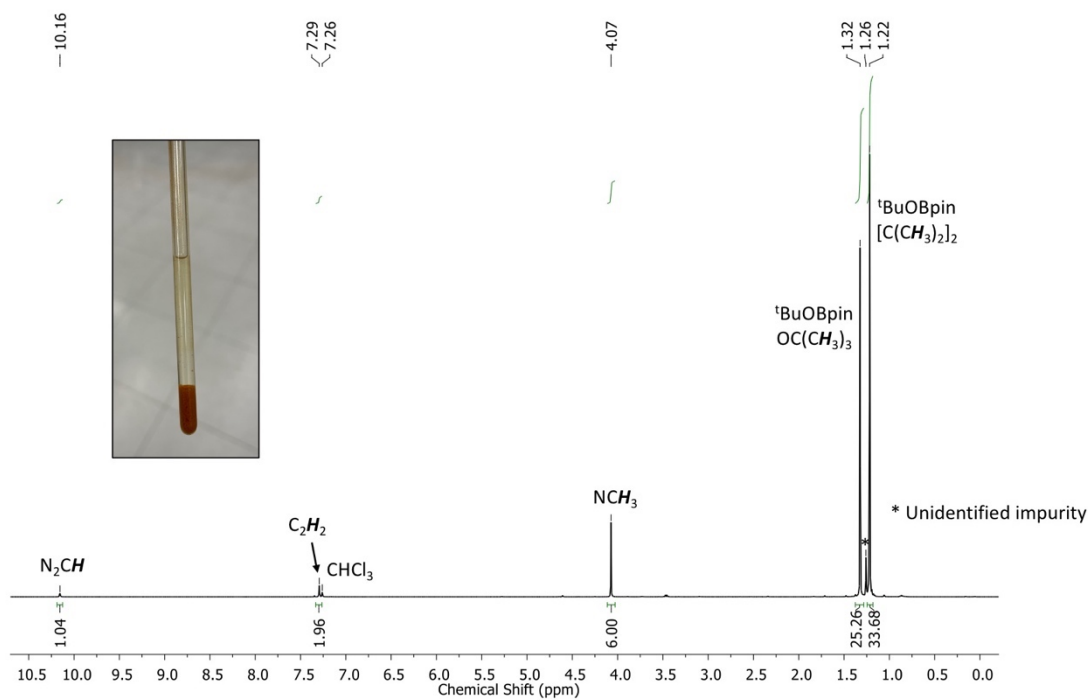


**Fig. S29.**  $^1\text{H}$  NMR spectrum of the soluble products ( $^t\text{BuOBpin}$  and an imidazolium salt) formed upon reaction of  $\text{ImMe}_2\cdot\text{Sn}(\text{O}^t\text{Bu})_2$  (**3**) with 2 equiv of HBpin in  $\text{CDCl}_3$ . Inset of observed reaction mixture shows the precipitation of the imidazolium salt.

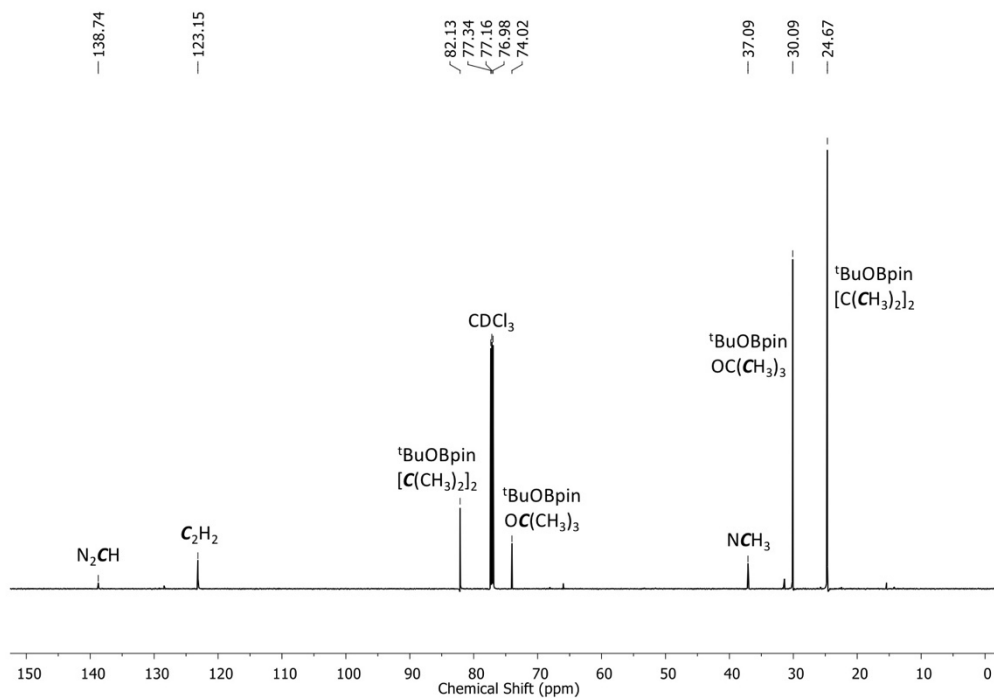


**Fig. S30.**  $^{13}\text{C}\{^1\text{H}\}$  NMR spectrum of the soluble products ( $^t\text{BuOBpin}$  and an imidazolium salt) formed upon reaction of  $\text{ImMe}_2\cdot\text{Sn}(\text{O}^t\text{Bu})_2$  (**3**) with 2 equiv of HBpin in  $\text{CDCl}_3$ .

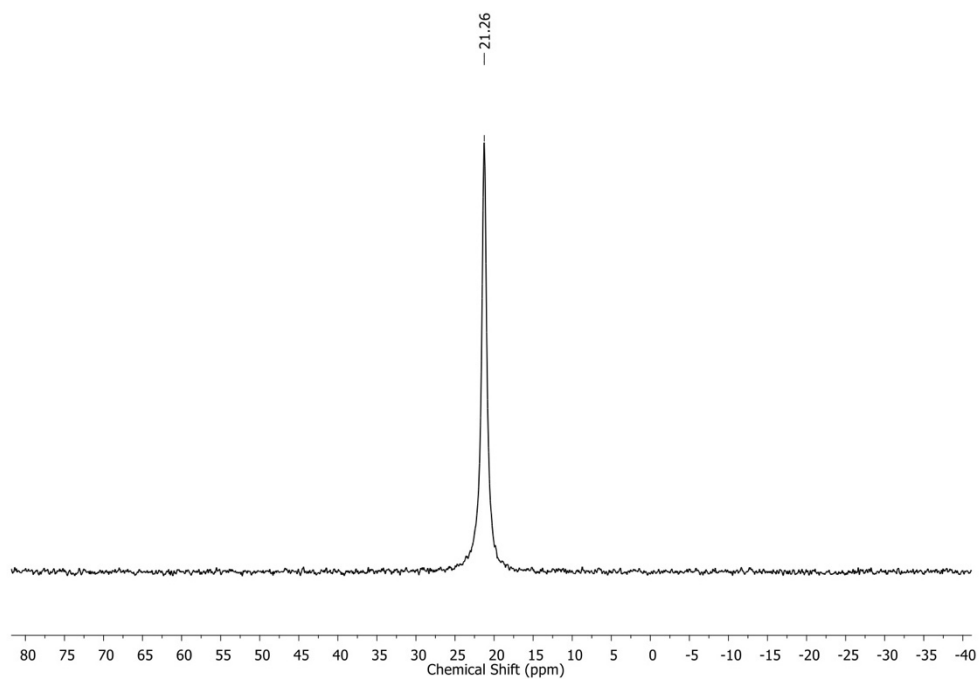


**Fig. S31.**  $^{11}\text{B}$  NMR spectrum of the  $^t\text{BuOBpin}$  formed upon reaction of  $\text{ImMe}_2\cdot\text{Sn}(\text{O}^t\text{Bu})_2$  (**3**) with 2 equiv of HBpin in  $\text{CDCl}_3$ .

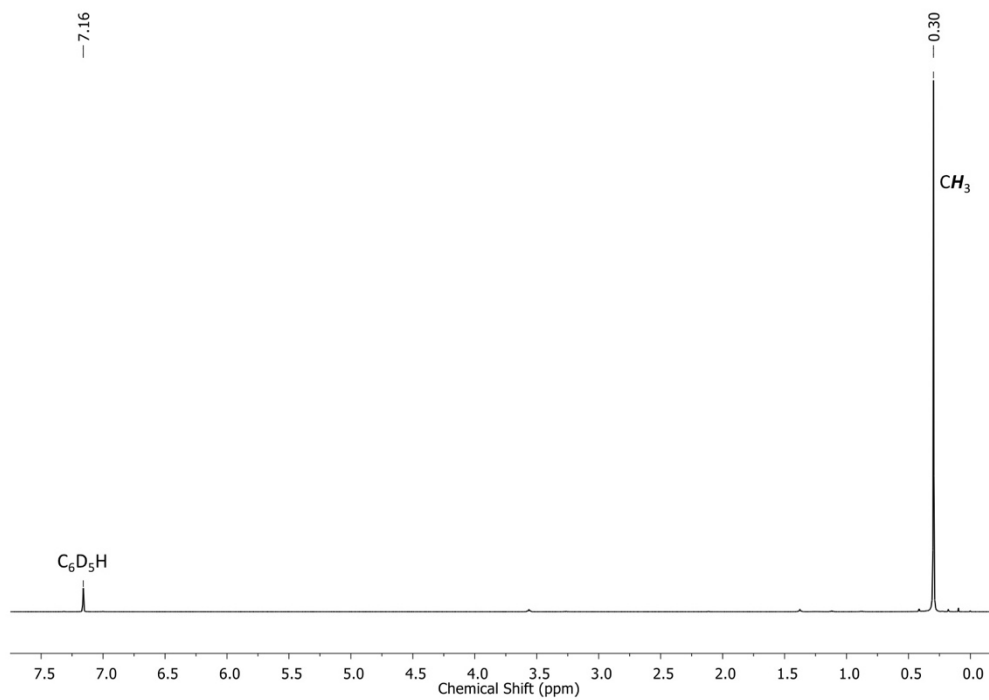


**Fig. S32.**  $^1\text{H}$  NMR spectrum of  $\text{Sn}[\text{N}(\text{SiMe}_3)_2]_2$  (**4**) in  $\text{C}_6\text{D}_6$ .

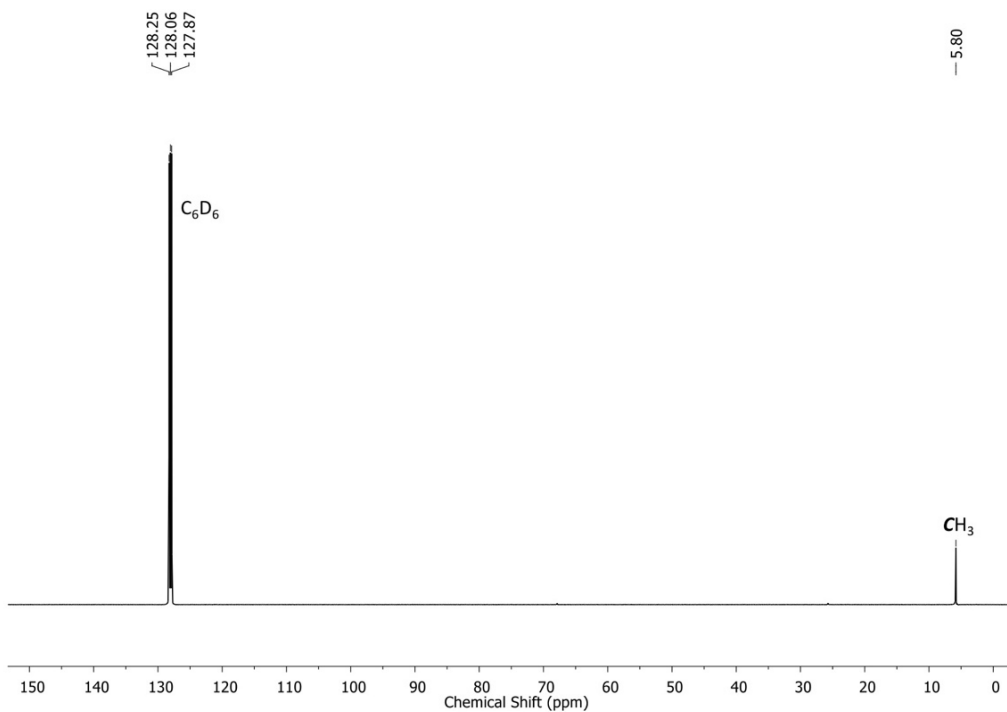


**Fig. S33.**  $^{13}\text{C}\{^1\text{H}\}$  NMR spectrum of  $\text{Sn}[\text{N}(\text{SiMe}_3)_2]_2$  (**4**) in  $\text{C}_6\text{D}_6$ .

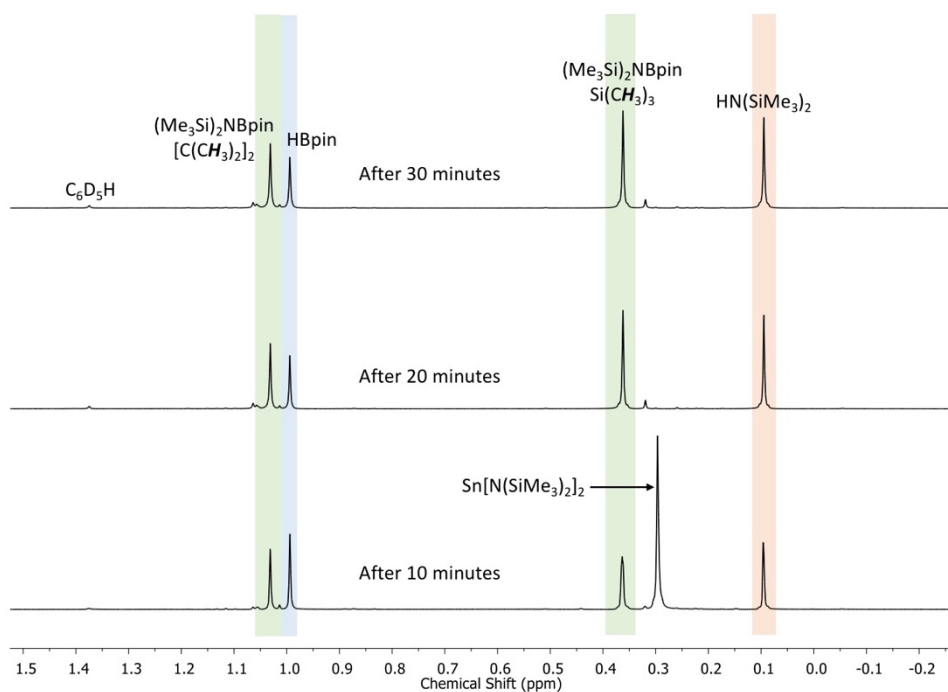


**Fig. S34.**  $^1\text{H}$  NMR spectra of the soluble products formed upon reaction of  $\text{Sn}[\text{N}(\text{SiMe}_3)_2]_2$  (**4**) with 2 equiv of HBpin in  $\text{C}_6\text{D}_6$ . Note that the second equiv of HBpin was not consumed and  $\text{HN}(\text{SiMe}_3)_2$  was generated (as a possible  $\alpha$ -elimination product from transient  $[\text{HSn}\{\text{N}(\text{SiMe}_3)_2\}]_x$ ; see main text for more details).

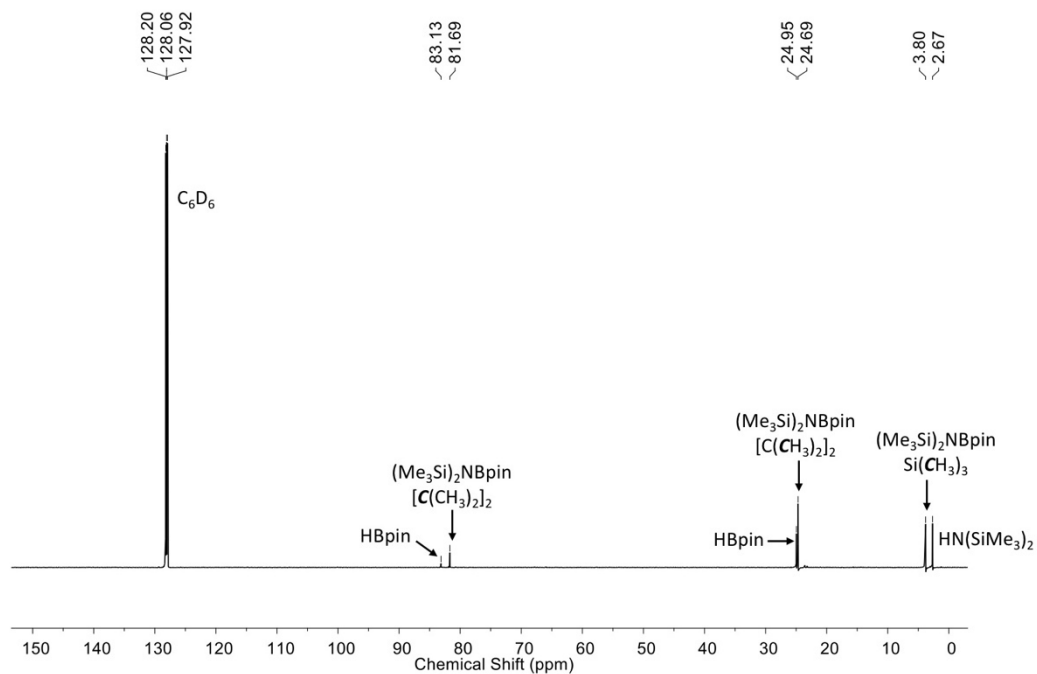


**Fig. S35.**  $^{13}\text{C}\{^1\text{H}\}$  NMR spectrum of the soluble products formed upon reaction of  $\text{Sn}[\text{N}(\text{SiMe}_3)_2]_2$  (**4**) with 2 equiv of HBpin in  $\text{C}_6\text{D}_6$ . This spectrum was acquired after 48 hours.

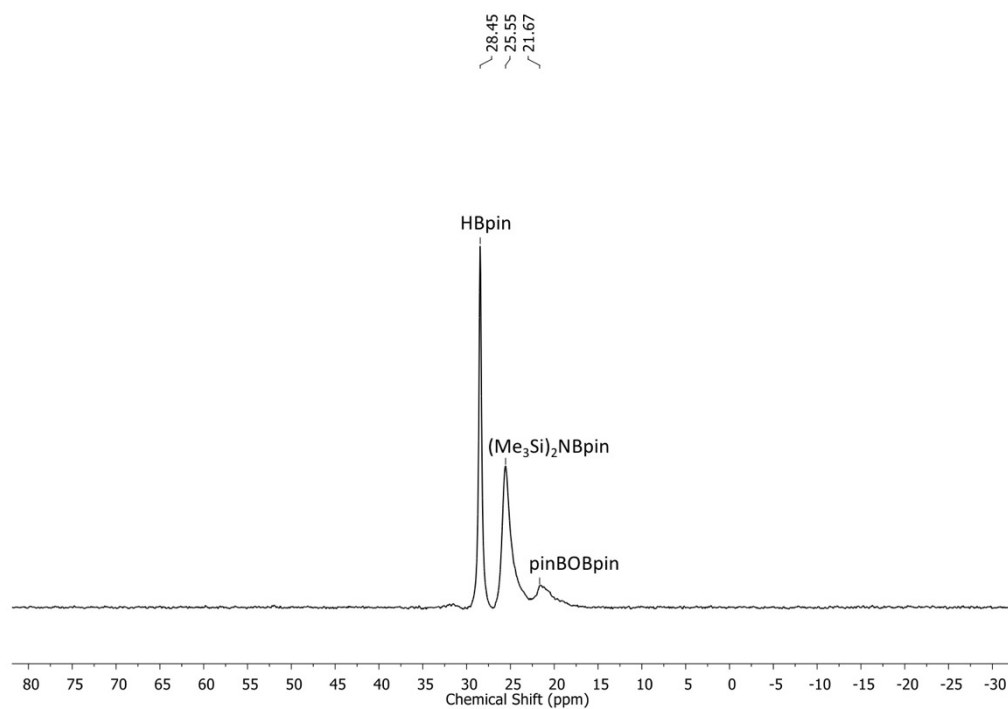


**Fig. S36.**  $^{11}\text{B}$  NMR spectrum of the soluble products formed upon reaction of  $\text{Sn}[\text{N}(\text{SiMe}_3)_2]_2$  (**4**) with 2 equiv of HBpin in  $\text{C}_6\text{D}_6$ . This spectrum was acquired after 48 hours.

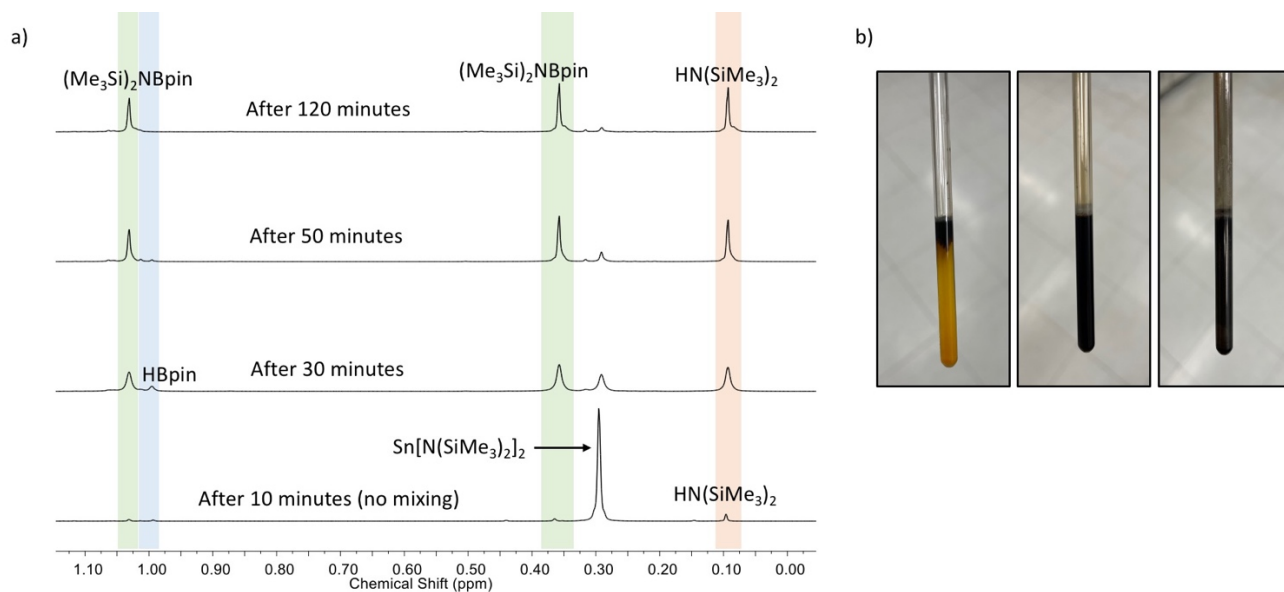


**Fig. S37.** (a) <sup>1</sup>H NMR spectra of the soluble products formed upon reaction of Sn[N(SiMe<sub>3</sub>)<sub>2</sub>]<sub>2</sub> (**4**) with 1 equiv of HBpin in C<sub>6</sub>D<sub>6</sub>. (b) Observed color changes associated with the consumption Sn[N(SiMe<sub>3</sub>)<sub>2</sub>]<sub>2</sub> (**4**) and the formation of crystalline Sn.

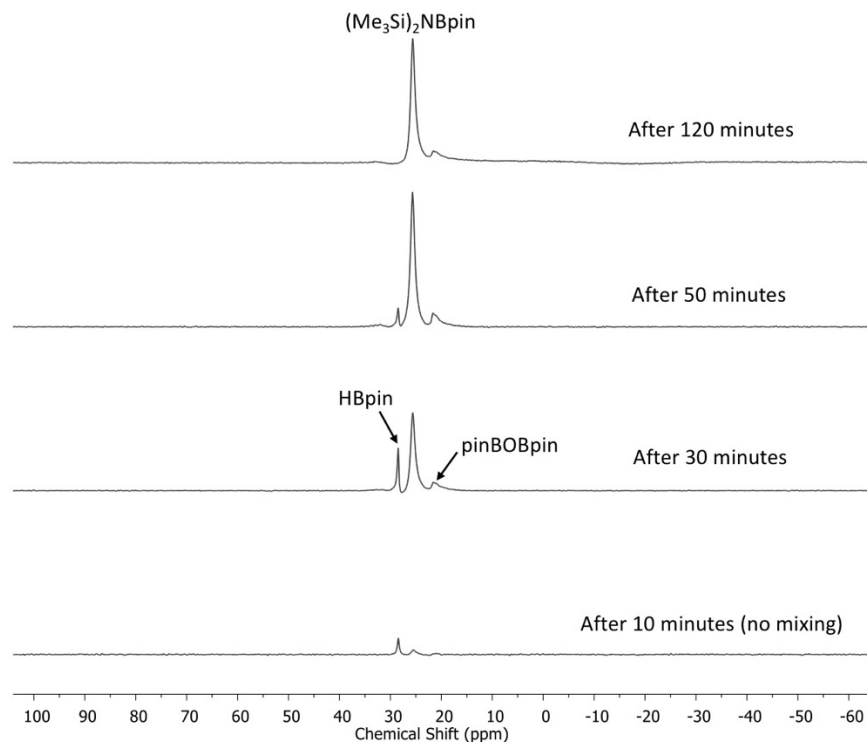


**Fig. S38.** <sup>11</sup>B NMR spectra of the soluble products formed upon reaction of Sn[N(SiMe<sub>3</sub>)<sub>2</sub>]<sub>2</sub> (**4**) with 1 equiv of HBpin in C<sub>6</sub>D<sub>6</sub>.

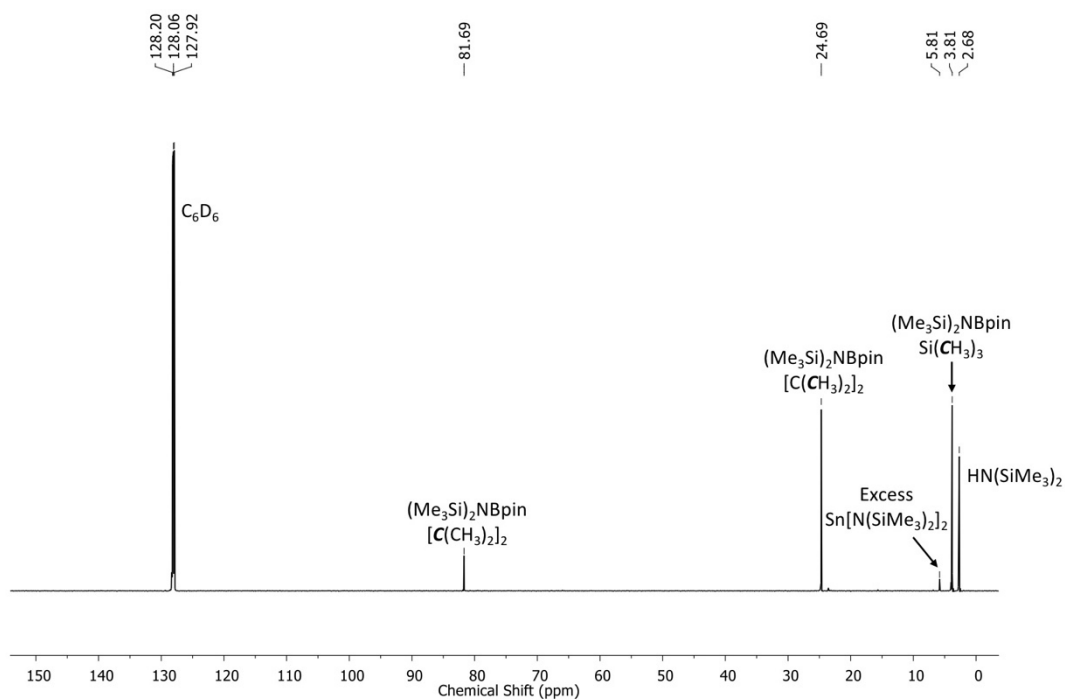


**Fig. S39.**  $^{13}\text{C}\{^1\text{H}\}$  NMR spectrum of the soluble products formed upon reaction of  $\text{Sn}[\text{N}(\text{SiMe}_3)_2]_2$  (**4**) with 1 equiv of HBpin in  $\text{C}_6\text{D}_6$ .

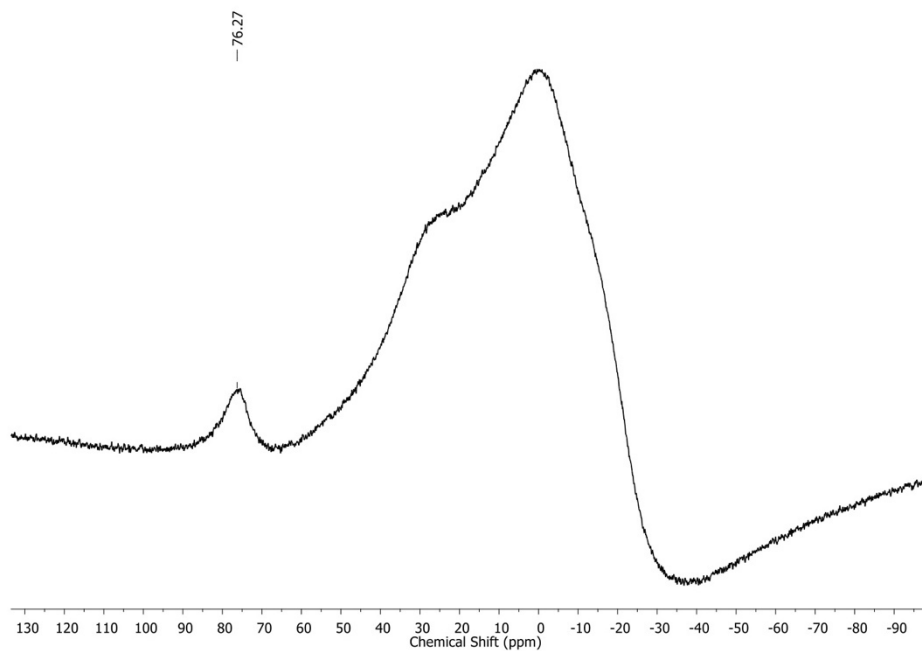


**Fig. S40.**  $^{11}\text{B}$  NMR spectrum of free 1,2- $^i\text{Pr}_2\text{P}(\text{C}_6\text{H}_4)\text{BCy}_2$  (**PB**) in  $\text{C}_6\text{D}_6$ . Note that the additional broad peaks are from the borosilicate glass NMR tube.

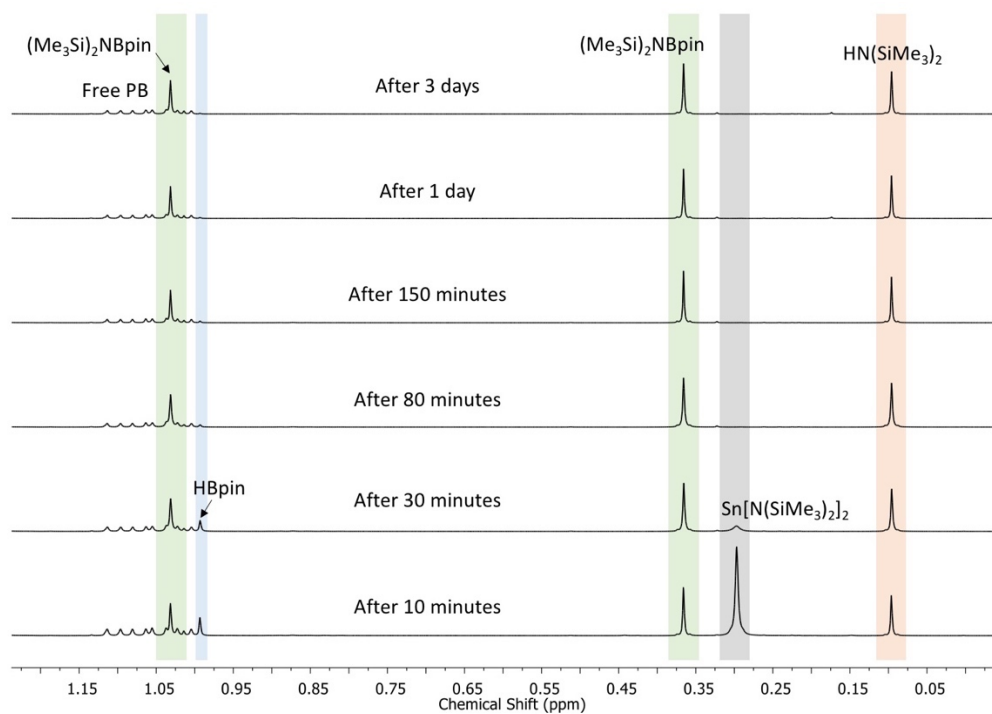


**Fig. S41.** Stacked  $^1\text{H}$  NMR spectra of the soluble by-products formed upon reaction of  $\text{Sn}[\text{N}(\text{SiMe}_3)_2]_2$  (**4**) with 1 equiv of HBpin in the presence of **PB** (in  $\text{C}_6\text{D}_6$ ). No reaction with **PB** was observed.

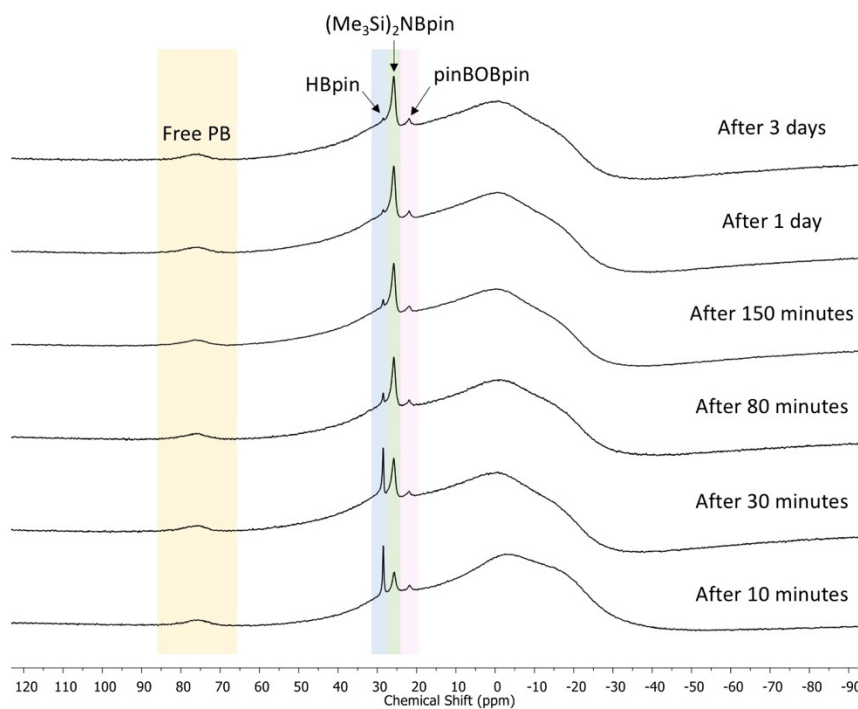


**Fig. S42.**  $^{11}\text{B}$  NMR spectra of the soluble by-products formed upon reaction of  $\text{Sn}[\text{N}(\text{SiMe}_3)_2]_2$  (**4**) with 1 equiv of HBpin in the presence of **PB** (in  $\text{C}_6\text{D}_6$ ). No reaction with **PB** was observed. Note that the additional broad peaks are from the borosilicate glass NMR tube.

### 3. X-ray crystallographic data

Crystals of appropriate quality for single-crystal X-ray diffraction studies were removed from the mother liquor and immediately covered with a thin layer of hydrocarbon oil (Paratone-N) in a sealed vial for transport to the diffractometer. A suitable crystal was then selected, attached to a glass fiber, and mounted under a stream of nitrogen onto the instrument. All data were collected using a Bruker APEX II CCD detector/D8 diffractometer using Cu or Mo  $K\alpha$  radiation. The data were corrected for absorption through Gaussian integration from indexing of the crystal faces. Structures were solved and refinements were completed using direct methods (SHELXT-2014 and SHELXL-2018/3).<sup>S9</sup>

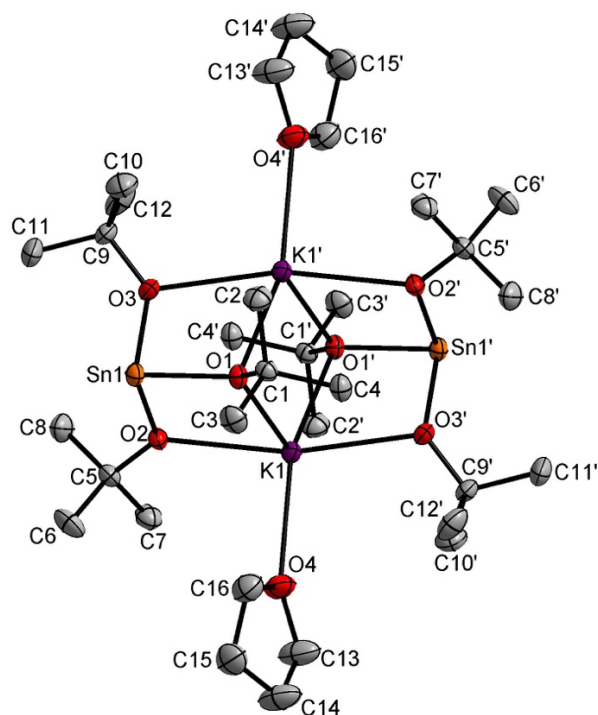


**Fig. S43.** Molecular structure of  $K_2[Sn(O^tBu)_3]_2 \cdot 2THF$  with thermal ellipsoids at 30% probability. Primed atoms are related to the unprimed ones by a crystallographic inversion center at  $(1/2, 1/2, 1/2)$ . Hydrogen atoms have been omitted for clarity. Selected bond lengths [ $\text{\AA}$ ] and angles [ $^\circ$ ]: Sn1–O1 2.0894(17), Sn1–O2 2.0652(17), Sn1–O3 2.0715(19); O1–Sn1–O2 83.58(7), O1–Sn1–O3 88.46(7), O2–Sn1–O3 92.98(8).

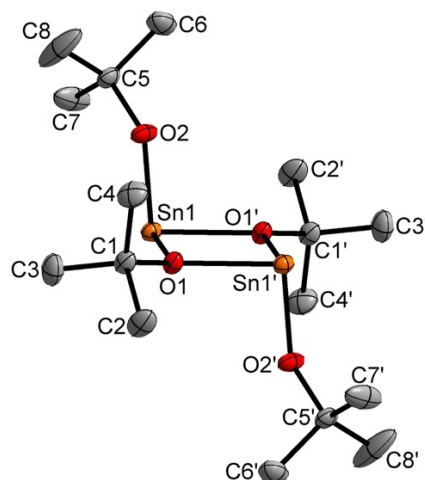


**Fig. S44.** Molecular structure of  $[\text{Sn}(\text{O}^i\text{Bu})_2]$  (**1**) with thermal ellipsoids at 30% probability. Primed atoms are related to the unprimed ones by the inversion center at  $(1/2, 0, 0)$ . Hydrogen atoms have been omitted for clarity. Only the major orientation of the disordered *tert*-butyl group is shown. Selected bond lengths [ $\text{\AA}$ ] and angles [ $^\circ$ ]: Sn1–O1 2.1390(9), Sn1–O1' 2.1544(9), Sn1–O2 2.0051(10); O1–Sn1–O1' 72.78(4), O1–Sn1–O2 89.83(4), O1'–Sn1–O2 92.93(4), Sn1–O1–Sn1' 107.22(4).

**Table S1.** Crystallographic data for  $K_2[Sn(O^iBu)_3]_2 \cdot 2THF$ ,  $[Sn(O^iBu)_2]_2$  (**1**),  $ImMe_2 \cdot SnCl_2$  (**2**), and  $ImMe_2 \cdot Sn(O^iBu)_2$  (**3**).

Compound	$K_2[Sn(O^iBu)_3]_2 \cdot 2THF$	$[Sn(O^iBu)_2]_2$ ( <b>1</b> )	$ImMe_2 \cdot SnCl_2$ ( <b>2</b> )	$ImMe_2 \cdot Sn(O^iBu)_2$ ( <b>3</b> )
Formula	$C_{32}H_{70}K_2O_8Sn_2$	$C_{16}H_{36}O_4Sn_2$	$C_5H_8SnN_2Cl_2$	$C_{13}H_{26}N_2O_2Sn$
Formula weight	898.46	529.83	285.72	361.05
Crystal system	triclinic	triclinic	monoclinic	monoclinic
Space Group	$P\bar{1}$ (No. 2)	$P\bar{1}$ (No. 2)	$P2_1/n$ (No. 14)	$P2_1/n^c$
Crystal dimensions (mm)	$0.28 \times 0.27 \times 0.21$	$0.42 \times 0.24 \times 0.21$	$0.10 \times 0.09 \times 0.02$	$0.13 \times 0.09 \times 0.05$
$a$ (Å)	10.193(2)	8.0779(7)	7.6355(2)	12.568(3)
$b$ (Å)	10.823(2)	8.3405(7)	8.8033(3)	7.7753(19)
$c$ (Å)	11.118(2)	9.8156(8)	13.9001(4)	18.333(5)
$\alpha$ (°)	99.693(3)	114.7162(10)	–	–
$\beta$ (°)	113.801(3)	105.6759(11)	92.7393(8)	107.603(4)
$\gamma$ (°)	96.897(3)	96.9267(11)	–	–
$V$ (Å <sup>3</sup> )	1081.9(4)	557.38(8)	933.26(5)	1707.7(7)
Z	1	1	4	4
$\rho_{calcd}$ (g cm <sup>-3</sup> )	1.379	1.578	2.034	1.404
$\mu$ (mm <sup>-1</sup> )	1.386	2.253	26.52	1.494
T (°C)	–80	–80	–100	–80
$2\theta_{max}$ (°)	61.16	61.12	148.08	51.50
Total data	19027	10236	3559	18947
Unique data ( $R_{int}$ )	6558 (0.0478)	3400 (0.0192)	1876 (0.0296)	3266 (0.0968)
Data <sub>obs</sub> [ $F_o^2 \geq 2\sigma(F_o^2)$ ]	5550	3268	1828	2267
Data/Restraints/Parameters	6558 / 0 / 208	3400 / 48 <sup>b</sup> / 137	1876 / 0 / 93	3266 / 15 <sup>d</sup> / 178
$R_1$ [ $F_o^2 \geq 2\sigma(F_o^2)$ ] <sup>a</sup>	0.0371	0.0150	0.0186	0.0419
$wR_2$ [all data] <sup>a</sup>	0.0990	0.0380	0.0482	0.1015
Max/min $\Delta\rho$ (e <sup>-</sup> Å <sup>-3</sup> )	1.247/–0.953	0.374/–0.422	0.291/–1.093	1.100/–0.448

$$^a R_1 = \frac{\sum ||F_o| - |F_c||}{\sum |F_o|}; wR_2 = \left[ \frac{\sum w(F_o^2 - F_c^2)^2}{\sum w(F_o^4)} \right]^{1/2}$$

<sup>b</sup> The C–C distances within the disordered *tert*-butyl group were restrained to be approximately the same by use of the *SHELXL SADI* instruction. Similarly, the C···C distances within the minor orientation of the disordered *tert*-butyl group were restrained to be approximately the same. Finally, the rigid-bond restraint (**RIGU**) was applied to carbon atoms C5, C6A, C7A, C8A, and **SIMU** was applied to the near overlapping pairs of atoms C6 & C6A and C7 & C7A.

<sup>c</sup> An alternate setting of  $P2_1/c$  [No. 14]).

<sup>d</sup> The C–C distances within the disordered *tert*-butyl group were restrained to be approximately the same by the *SHELXL SADI* instruction.

#### 4. SEM and EDX images of deposited Sn

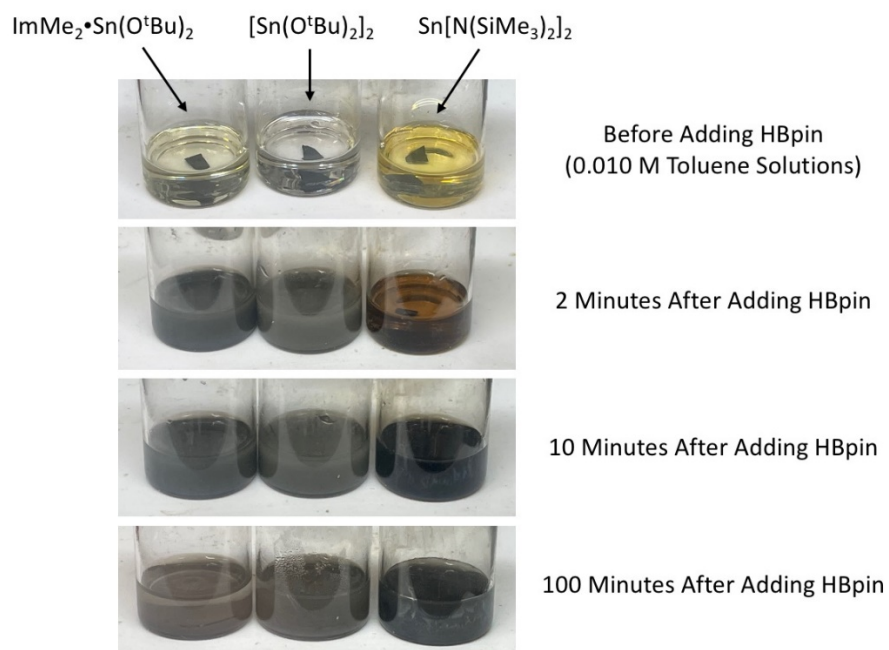


**Fig. S45.** Reaction of [Sn(O<sup>t</sup>Bu)<sub>2</sub>]<sub>2</sub> (**1**), ImMe<sub>2</sub>•Sn(O<sup>t</sup>Bu)<sub>2</sub> (**3**), and Sn[N(SiMe<sub>3</sub>)<sub>2</sub>]<sub>2</sub> (**4**) with HBpin to deposit Sn on top of *n*-type Si wafers. Pronounced color changes are observed as the reactions progress.

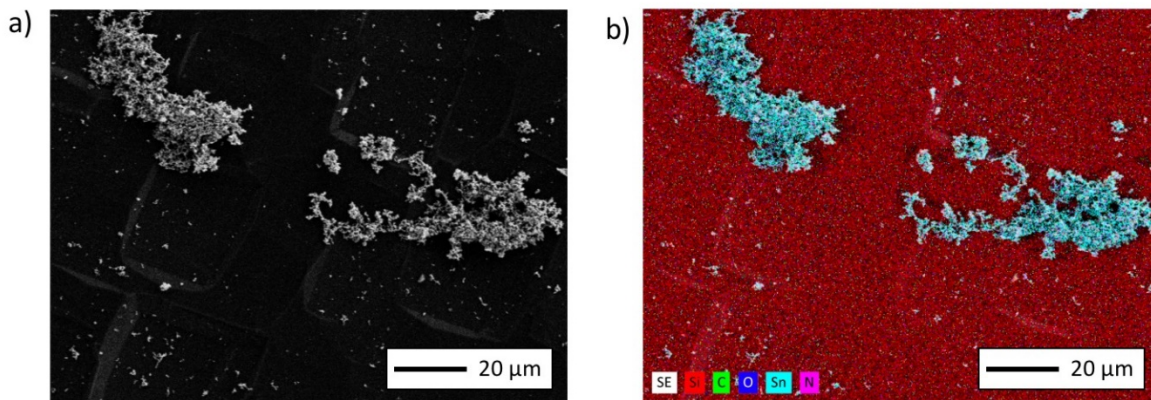


**Fig. S46.** SEM image of Sn deposited on a Si wafer, prepared upon reaction of [Sn(O<sup>t</sup>Bu)<sub>2</sub>]<sub>2</sub> (**1**) (0.010 M solution in toluene) with 4 equiv of HBpin. (b) EDX map of the same sample, showing the spatial distribution of Si, C, O, Sn, and N.

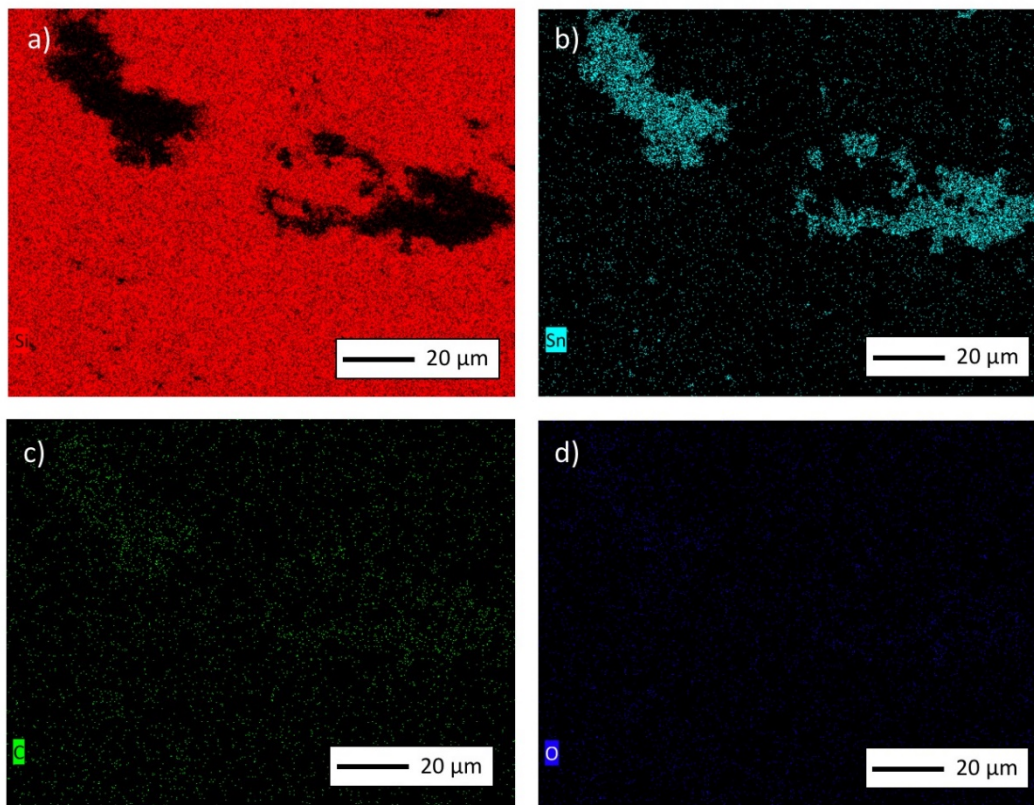


**Fig. S47.** (a) EDX maps of Sn deposited on a Si wafer, showing the spatial distribution of (a) Si, (b) Sn, (c) C, and (d) O (same sample as Fig. S46, *vide supra*).

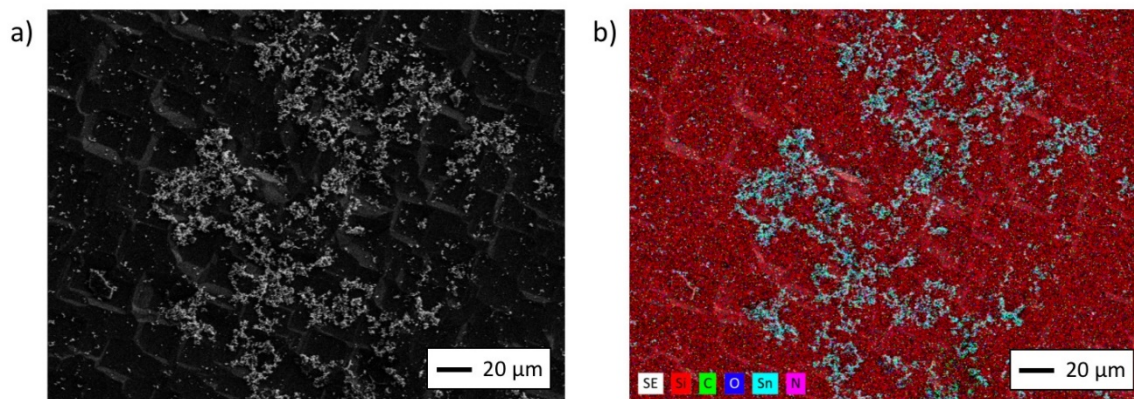


**Fig. S48.** (a) SEM image of Sn deposited on a Si wafer, prepared upon reaction of  $\text{ImMe}_2\cdot\text{Sn}(\text{O}^t\text{Bu})_2$  (**3**) (0.010 M solution in toluene) with 2 equiv of HBpin. (b) EDX map of the same sample, showing the spatial distribution of Si, C, O, Sn, and N.

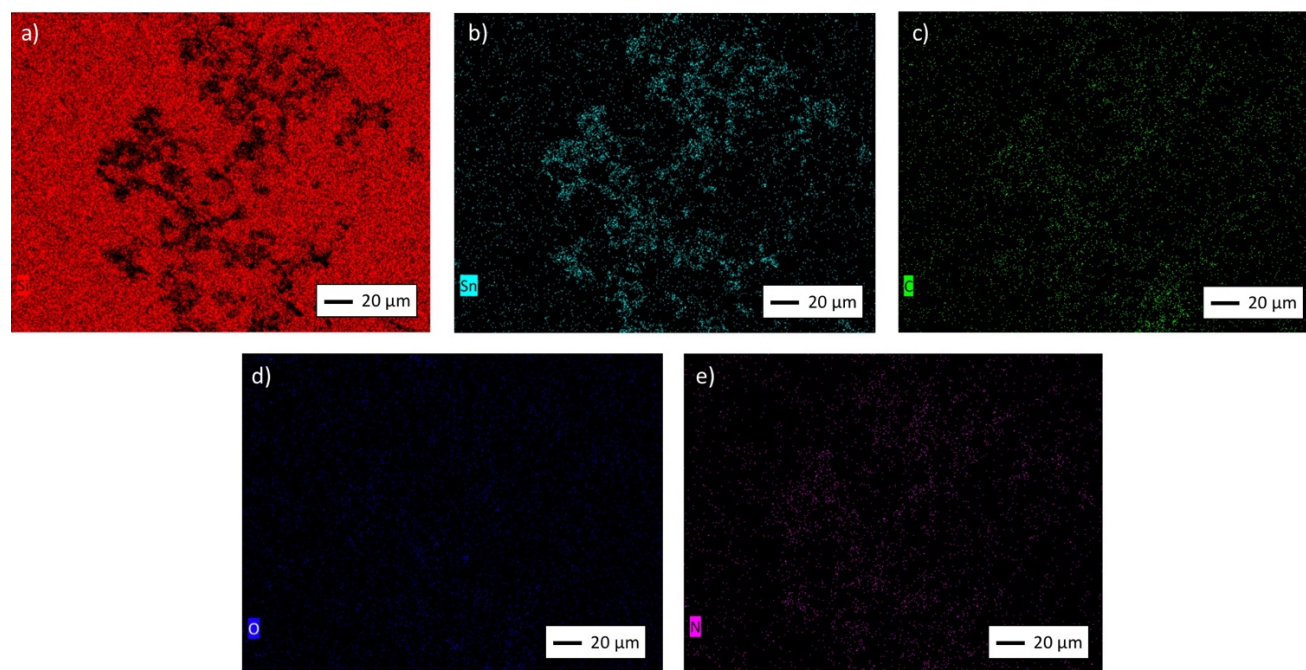


**Fig. S49.** (a) EDX maps of Sn deposited on a Si wafer, showing the spatial distribution of (a) Si, (b) Sn, (c) C, (d) O, and (e) N (same sample as Fig. S48, *vide supra*).

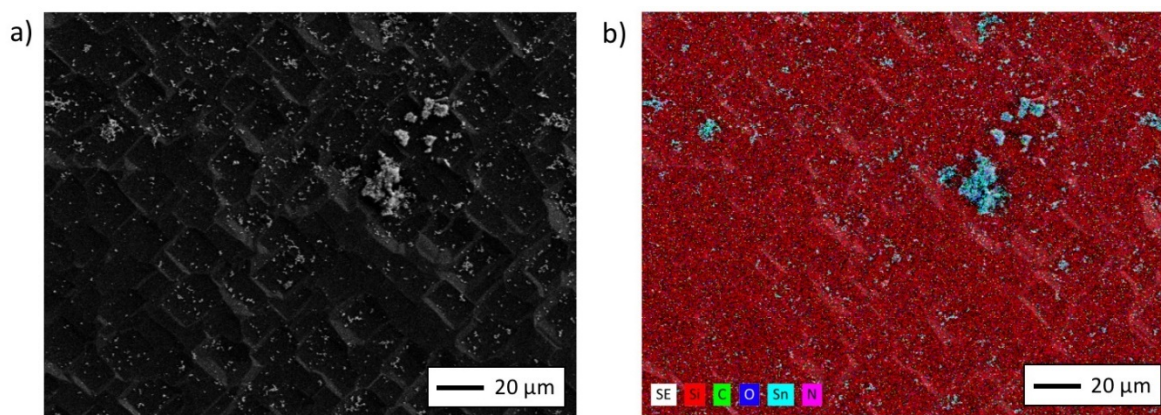


**Fig. S50.** (a) SEM image of Sn deposited on a Si wafer, prepared upon reaction of  $\text{Sn}[\text{N}(\text{SiMe}_3)_2]_2$  (**4**) (0.010 M solution in toluene) with 2 equiv of HBpin. (b) EDX map of the same sample, showing the spatial distribution of Si, C, O, Sn, and N.

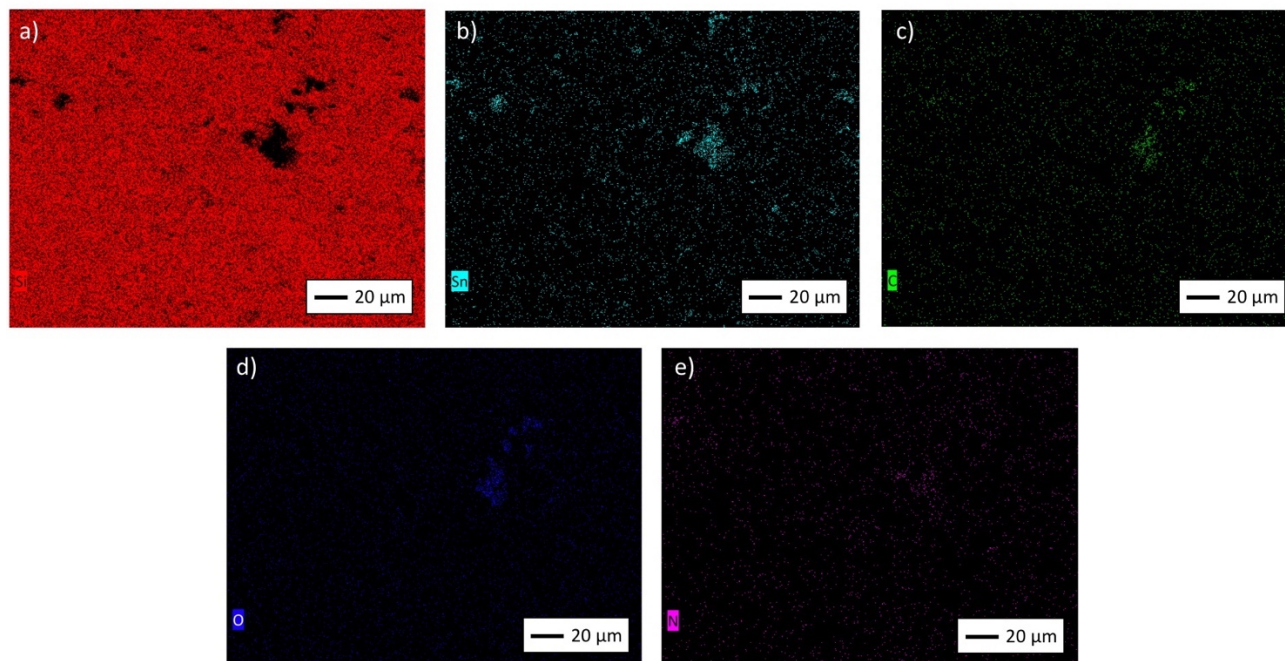


**Fig. S51.** (a) EDX maps of Sn deposited on a Si wafer, showing the spatial distribution of (a) Si, (b) Sn, (c) C, (d) O, and (e) N (same sample as Fig. S50, *vide supra*).

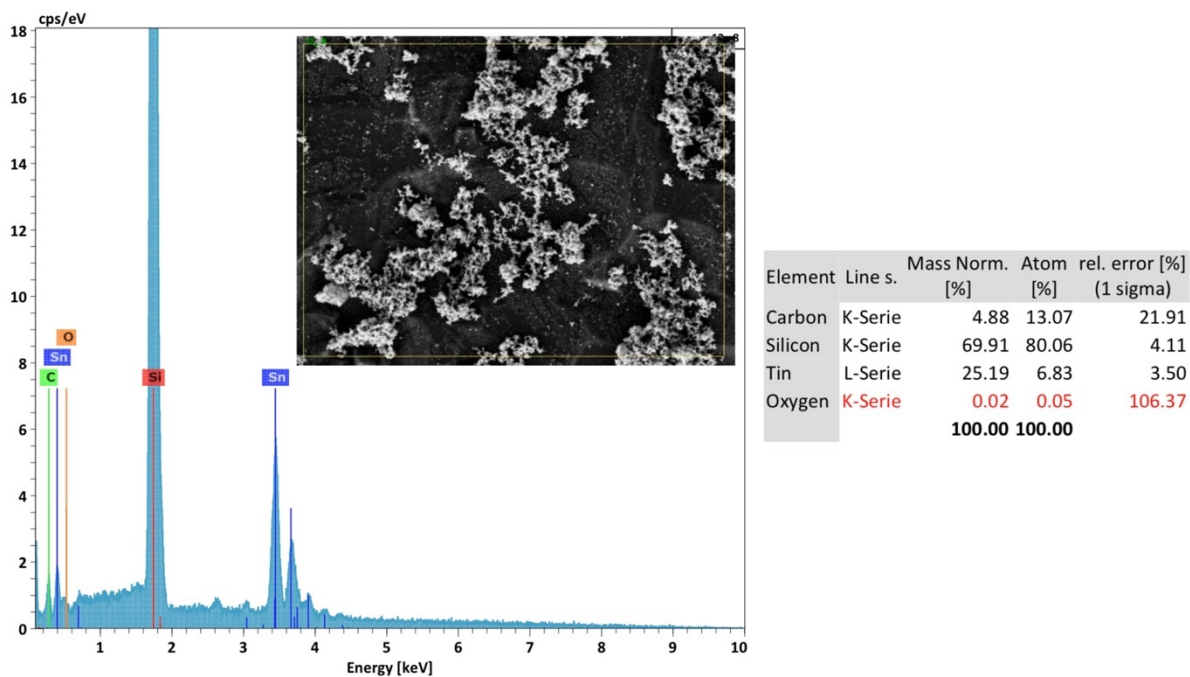


**Fig. S52.** EDX survey spectrum of a sample of elemental Sn deposited on a Si wafer, prepared upon reaction of  $\text{Sn}[\text{N}(\text{SiMe}_3)_2]_2$  (**4**) (0.30 M solution in toluene) with 2 equiv of HBpin.

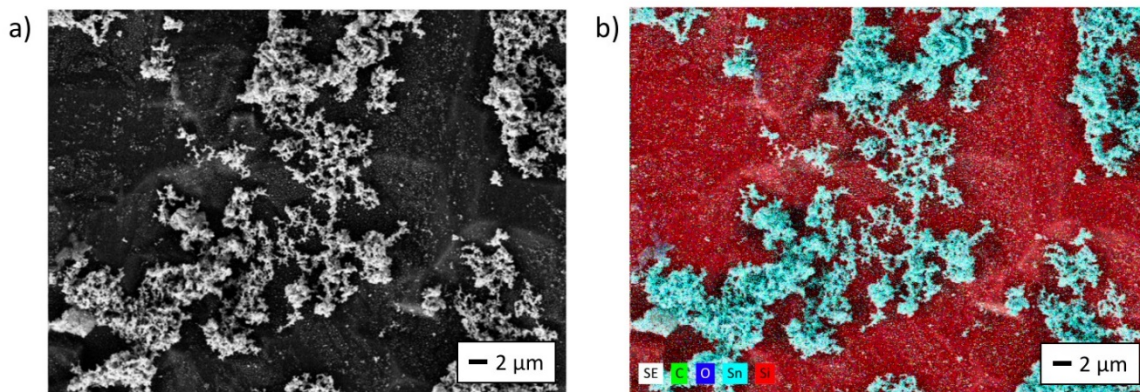


**Fig. S53.** (a) SEM image of Sn deposited on a Si wafer, prepared upon reaction of  $\text{Sn}[\text{N}(\text{SiMe}_3)_2]_2$  (**4**) (0.30 M solution in toluene) with 2 equiv of HBpin (same sample as Fig. S52, *vide supra*). (b) EDX map of the same sample, showing the spatial distribution of C, O, Sn, and Si.

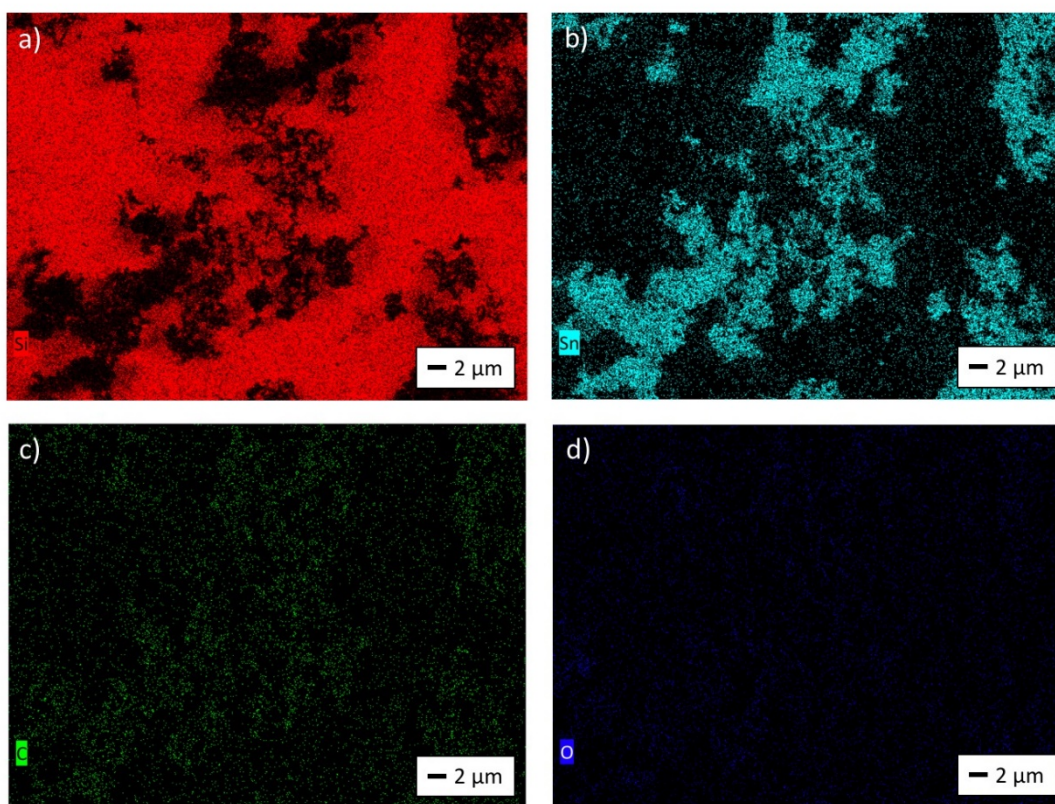


**Fig. S54.** (a) EDX maps of Sn deposited on a Si wafer, showing the spatial distribution of (a) Si, (b) Sn, (c) C, and (d) O (same sample as Figs. S52 and S53, *vide supra*).

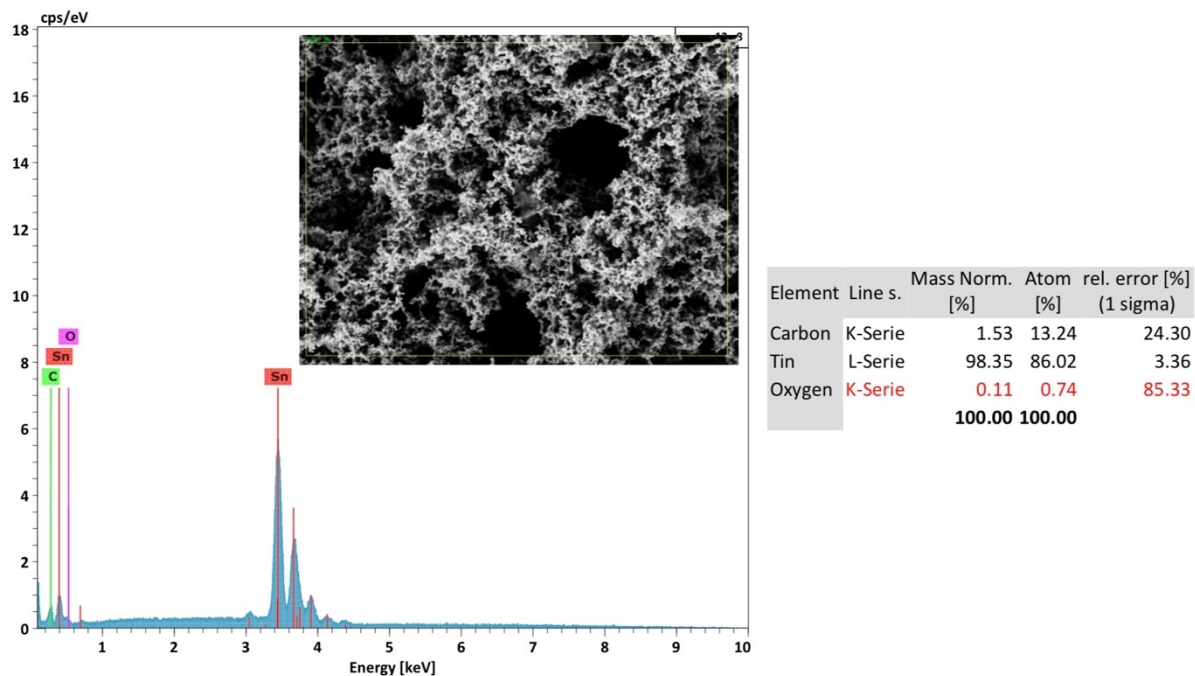


**Fig. S55.** EDX survey spectrum of a sample of elemental Sn deposited on a Cu plate, prepared upon reaction of  $[\text{Sn}(\text{O}^t\text{Bu})_2]_2$  (**1**) (0.10 M solution in toluene) with 4 equiv of HBpin.

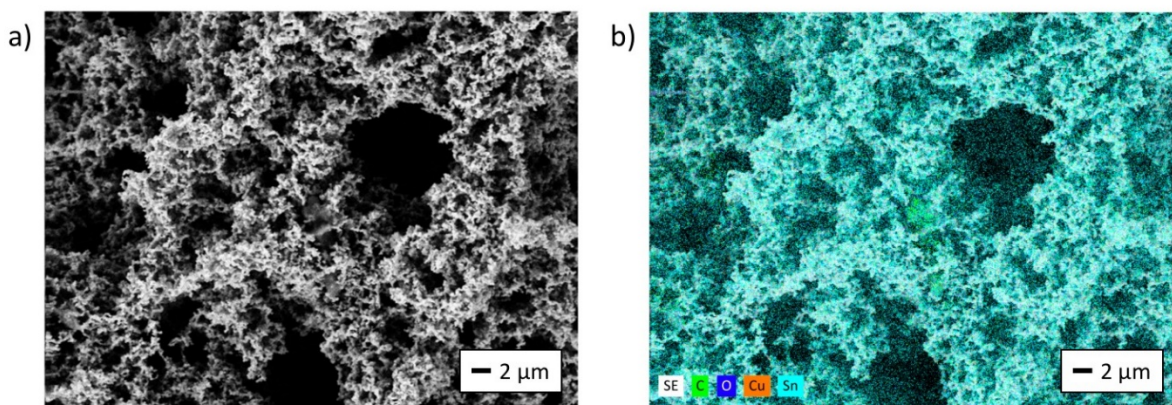


**Fig. S56.** (a) SEM image of Sn deposited on a Cu plate, prepared upon reaction of  $[\text{Sn}(\text{O}^t\text{Bu})_2]_2$  (**1**) (0.10 M solution in toluene) with 4 equiv of HBpin (same sample as Fig. S55, *vide supra*). (b) EDX map of the same sample, showing the spatial distribution of C, O, Cu, and Sn.

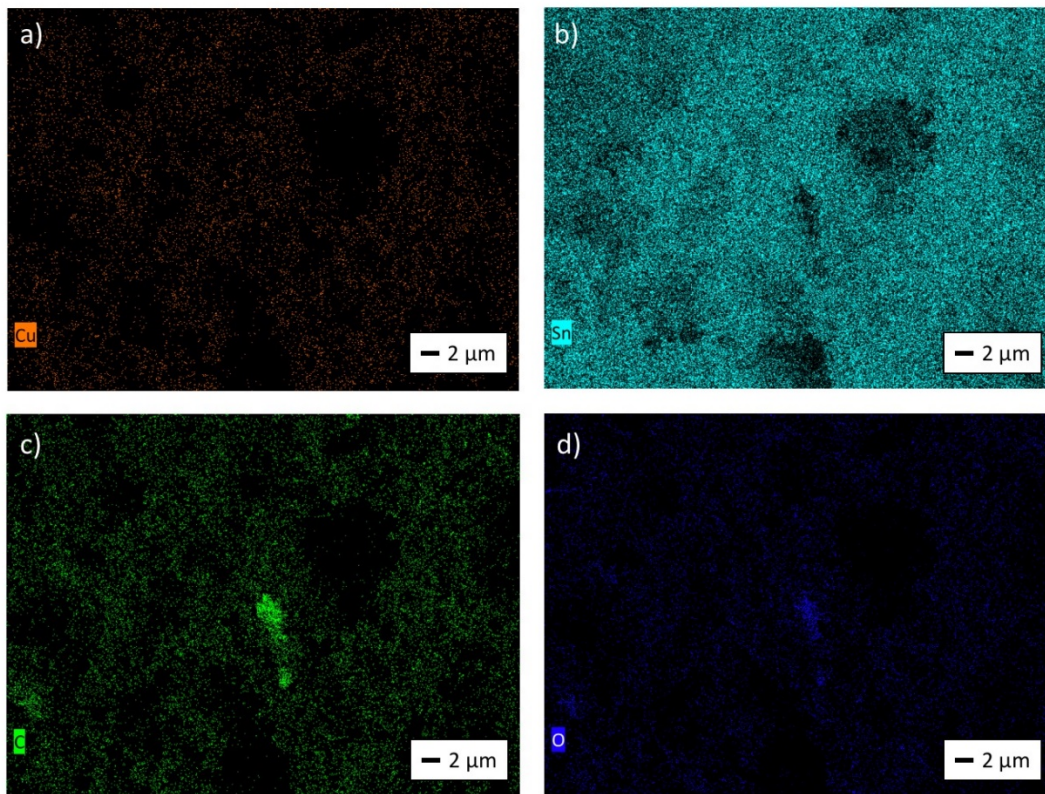


**Fig. S57.** (a) EDX maps of Sn deposited on a Cu plate, showing the spatial distribution of (a) Cu, (b) Sn, (c) C, and (d) O (same sample as Figs. S55 and S56, *vide supra*).

## 5. X-ray photoelectron spectroscopy and powder X-ray diffraction

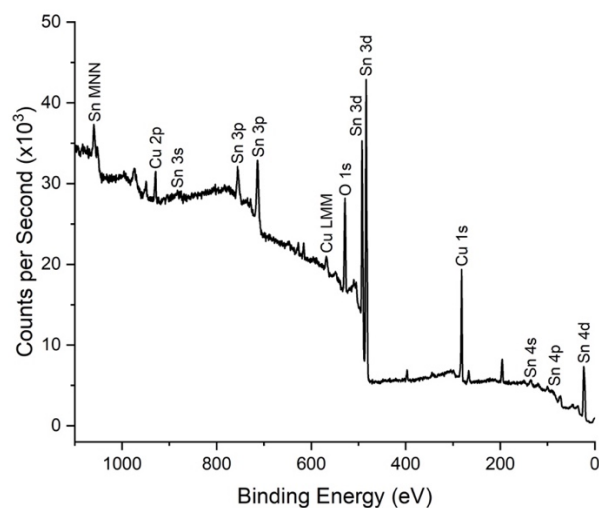


**Fig. S58.** Survey XPS spectrum of a sample of crystalline Sn, prepared upon reaction of  $[\text{Sn}(\text{O}^t\text{Bu})_2]_2$  (**1**) with 4 equiv of HBpin in toluene. This sample contains significant surface oxidation due to air exposure before and during sample measurement (sample was exposed to air for 24 hours before spectral acquisition commenced).

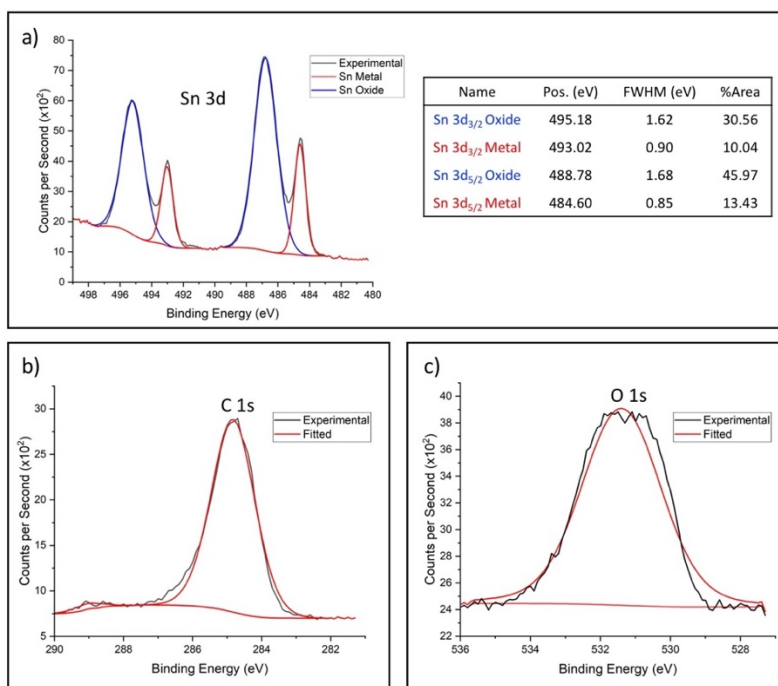


**Fig. S59.** High resolution XPS spectra of a sample of crystalline Sn (same sample as Fig. S58, *vide supra*), showing the (a) Sn 3d, (b) C 1s, and (c) O 1s regions. Significant surface oxidation is observed due to air exposure before and during sample measurement.

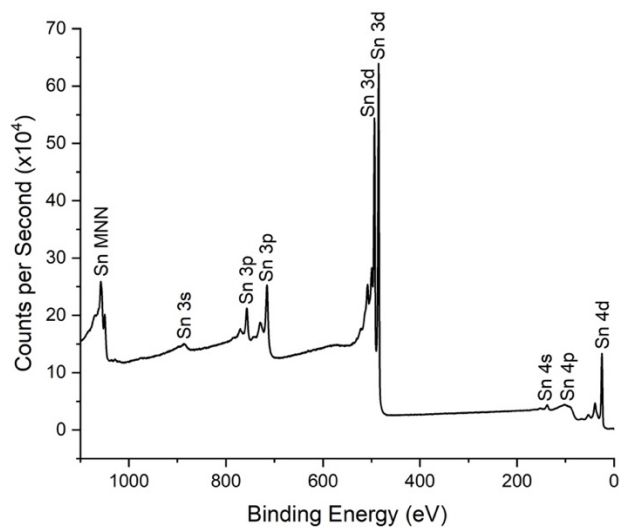


**Fig. S60.** Survey XPS spectrum of a sample of crystalline Sn, prepared upon reaction of  $[\text{Sn}(\text{O}^t\text{Bu})_2]_2$  (**1**) with 4 equiv of HBpin in toluene. Although a thick surface oxide layer formed readily upon exposure to air, this passivation layer could be removed after Ar sputtering for 12 minutes (sputtering rate of 6 nm/min).

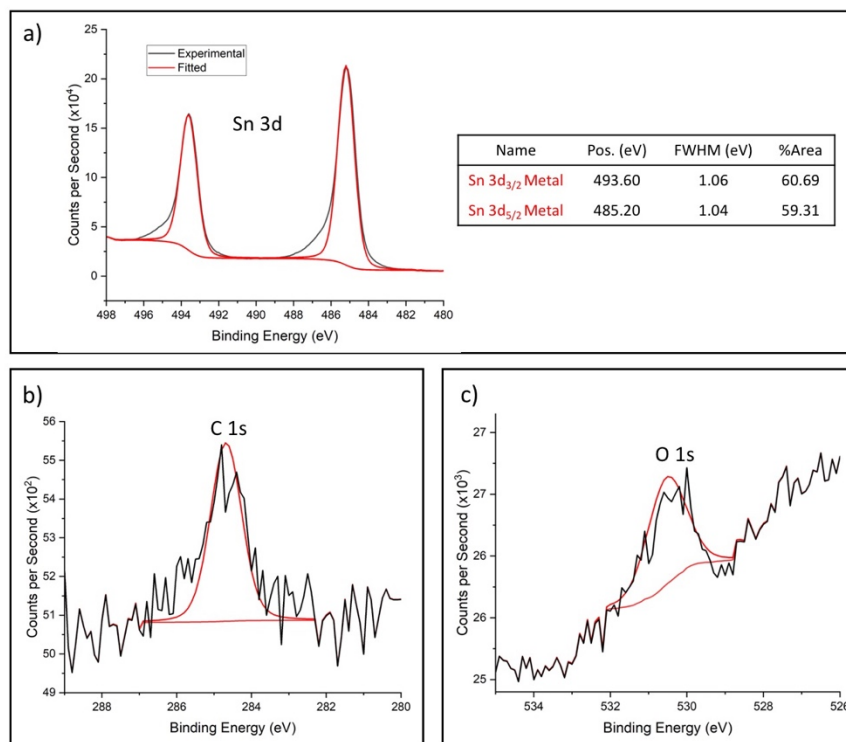


**Fig. S61.** High resolution XPS spectra of a sample of crystalline Sn (same sample as Fig. S60, *vide supra*), showing the (a) Sn 3d, (b) C 1s, and (c) O 1s regions. The thick surface oxide layer was removed after Ar sputtering for 12 minutes (sputtering rate of 6 nm/min).

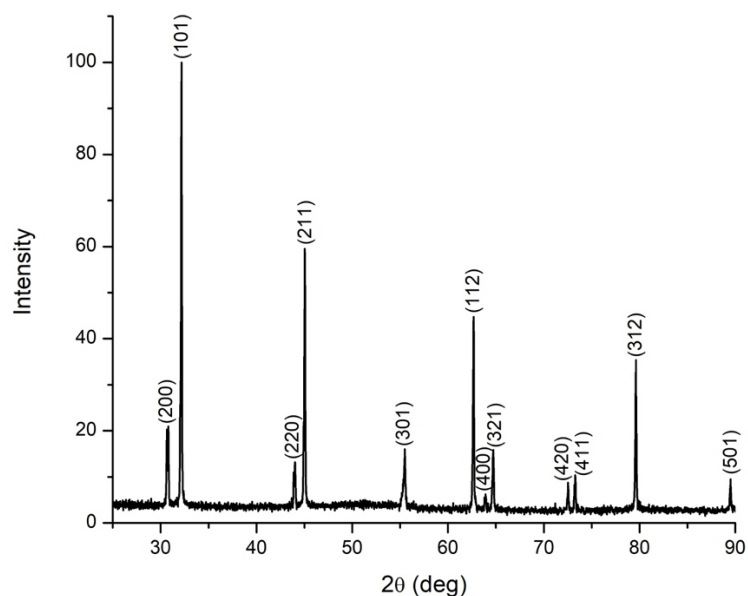


**Fig. S62.** PXRD spectrum of a sample of crystalline Sn left exposed to air for 3 days. This sample was prepared by treating  $[\text{Sn}(\text{O}^t\text{Bu})_2]_2$  (**1**) (0.010 M solution in toluene) with 4 equiv of HBpin. The preservation of crystallinity is attributed to the formation of passivating oxide layer.

## 6. Raman spectra of deposited Sn

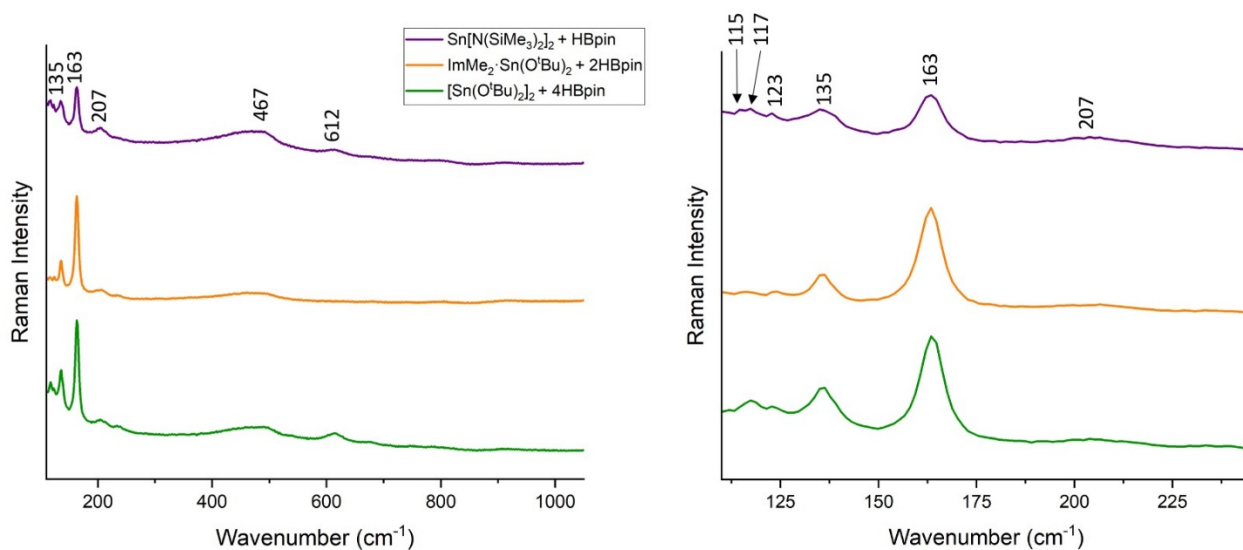


**Fig. S63.** Raman spectra (full view and lower wavenumber region) of the crystalline Sn deposited upon reaction of  $[\text{Sn}(\text{O}^t\text{Bu})_2]_2$  (**1**),  $\text{ImMe}_2 \cdot \text{Sn}(\text{O}^t\text{Bu})_2$  (**3**), and  $\text{Sn}[\text{N}(\text{SiMe}_3)_2]_2$  (**4**) with HBpin in toluene. The broad signals at 467 and 612  $\text{cm}^{-1}$  correspond to the background.

## 7. Computational data

### General methods

Computations were carried out using the Gaussian 16 software package.<sup>S10</sup> All calculations were performed using density functional theory (DFT) with the M06-2X functional<sup>S11</sup> and either the cc-PVDZ (H, B, C, N, O, Si, P, Ge) or cc-PVDZ-PP (Sn, Pb) basis sets.<sup>S12</sup> Where possible, Cartesian coordinates from experimentally determined molecular structures were used as starting points for the geometry optimizations. Harmonic vibrational analyses were also conducted to calculate thermochemical data ( $\Delta_r G$ ) and ensure that all optimized structures corresponded to energy minima.

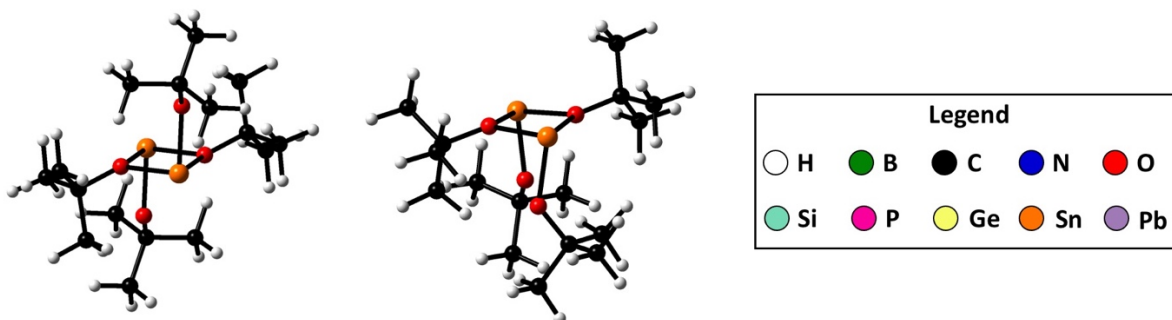


**Fig. S64.** Optimized gas phase geometries of the *trans* (left) and *cis* (right) isomers of [Sn(O<sup>t</sup>Bu)<sub>2</sub>]<sub>2</sub> (**1**). A legend is also provided to delineate the coloring scheme used in all optimized structures illustrated herein.

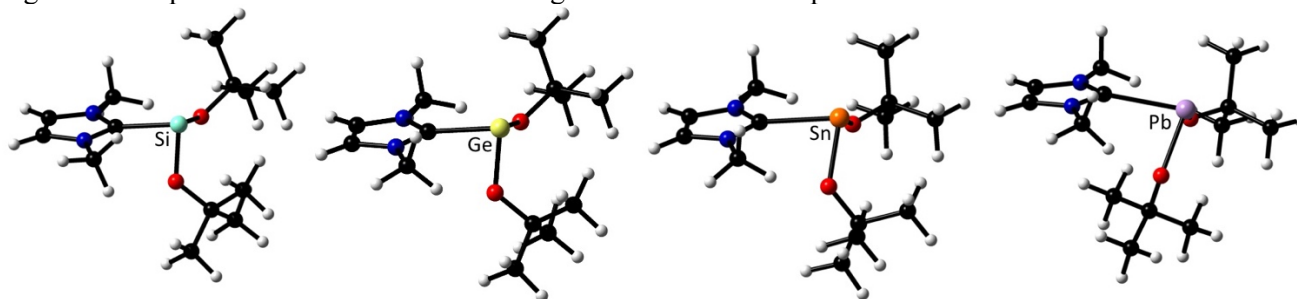


**Fig. S65.** Optimized gas phase geometries of ImMe<sub>2</sub>•E(O<sup>t</sup>Bu)<sub>2</sub> (E = Si, Ge, Sn, Pb). Selected bond lengths [Å] and angles [°]: E = Si: Si-C 2.033; O-Si-O 100.6. E = Ge: Ge-C 2.161; O-Ge-O 98.4. E = Sn: Sn-C 2.401; O-Sn-O 97.5. E = Pb: Pb-C 2.542; O-Pb-O 97.3.

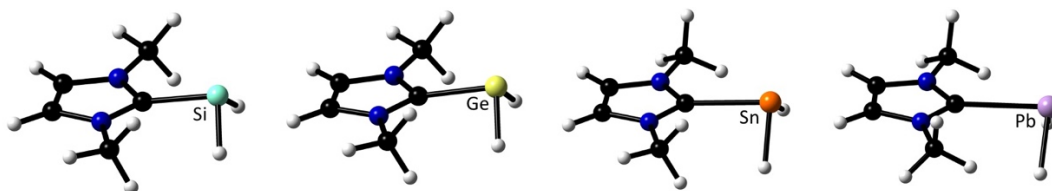


**Fig. S66.** Optimized gas phase geometries of ImMe<sub>2</sub>•EH<sub>2</sub> (E = Si, Ge, Sn, Pb). Selected bond lengths [Å] and angles [°]: E = Si: Si-C 1.942; H-Si-H 97.4. E = Ge: Ge-C 2.057; H-Ge-H 96.1. E = Sn: Sn-C 2.343; H-Sn-H 94.1. E = Pb: Pb-C 2.511, H-Pb-H 92.3.

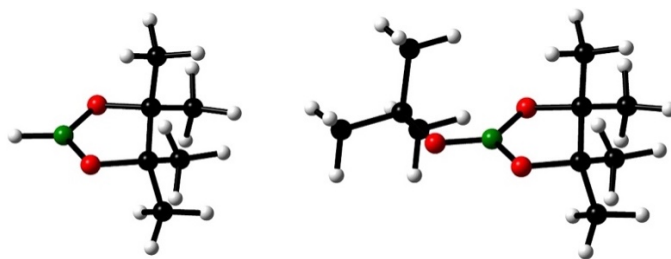


**Fig. S67.** Optimized gas-phase geometries of HBpin (left) and <sup>t</sup>BuOBpin (right).

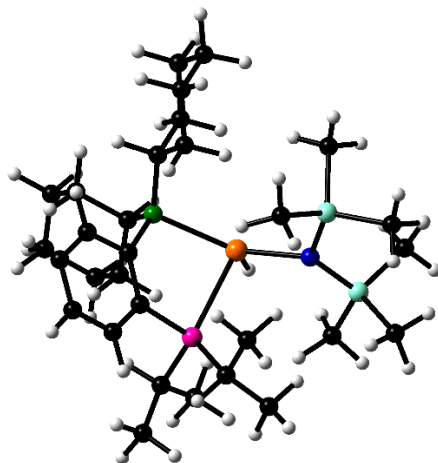


**Fig. S68.** Optimized gas-phase geometry of {PB}SnH{N(SiMe<sub>3</sub>)<sub>2</sub>} (**PB** = 1,2-<sup>i</sup>Pr<sub>2</sub>P(C<sub>6</sub>H<sub>4</sub>)BCy<sub>2</sub>). Selected bond lengths [Å] and angles [°]: Sn–P 2.729, Sn–B 2.427, Sn–N 2.113; P–Sn–B 83.2, N–Sn–H 100.3.

**Table S2.** Coordinates for the optimized gas-phase geometry of *trans*-[Sn(O<sup>t</sup>Bu)<sub>2</sub>]<sub>2</sub> (**1**) (total energy: -1360.546444 a.u.).

Atoms	Coordinates		
	<i>X</i>	<i>Y</i>	<i>Z</i>
Sn	-0.217314	-1.430218	0.986906
Sn	0.217314	1.430218	-0.986906
O	-2.100521	-0.787774	1.456295
O	0.322799	0.671213	1.057783
O	2.100521	0.787774	-1.456295
O	-0.322799	-0.671213	-1.057783
C	-3.195927	-1.549432	1.919686
C	-2.772450	-2.510053	3.037729
C	-4.223235	-0.554125	2.462588
C	-3.802285	-2.339745	0.757151
C	0.188907	1.520552	2.214440
C	1.343305	2.519315	2.190677
C	0.274082	0.648784	3.466767

C	-1.162835	2.234146	2.169963
C	3.195927	1.549432	-1.919686
C	4.223235	0.554125	-2.462588
C	2.772450	2.510053	-3.037729
C	3.802285	2.339745	-0.757151
C	-0.188907	-1.520552	-2.214440
C	-1.343305	-2.519315	-2.190677
C	1.162835	-2.234146	-2.169963
C	-0.274082	-0.648784	-3.466767
H	-2.050412	-3.256142	2.666483
H	-3.636850	-3.056850	3.444364
H	-2.300487	-1.950149	3.860304
H	-4.500186	0.156737	1.670610
H	-3.786219	0.013971	3.297699
H	-5.131650	-1.063332	2.819383
H	-3.073675	-3.072516	0.372493
H	-4.061354	-1.651459	-0.060576
H	-4.706803	-2.888073	1.062608
H	0.265459	1.273431	4.371716
H	1.203570	0.057866	3.464078
H	-0.596094	-0.025060	3.514339
H	1.315817	3.169719	3.077581
H	2.306617	1.990344	2.161084
H	1.275301	3.168883	1.301980
H	-1.212992	2.924318	1.312642
H	-1.958894	1.483381	2.069251
H	-1.317595	2.824494	3.086056
H	4.706803	2.888073	-1.062608
H	3.073675	3.072516	-0.372493
H	4.061354	1.651459	0.060576
H	2.050412	3.256142	-2.666483
H	3.636850	3.056850	-3.444364
H	2.300487	1.950149	-3.860304
H	5.131650	1.063332	-2.819383
H	3.786219	-0.013971	-3.297699
H	4.500186	-0.156737	-1.670610
H	-0.265459	-1.273431	-4.371716
H	0.596094	0.025060	-3.514339
H	-1.203570	-0.057866	-3.464078
H	1.212992	-2.924318	-1.312642
H	1.958894	-1.483381	-2.069251
H	1.317595	-2.824494	-3.086056
H	-1.275301	-3.168883	-1.301980

H	-1.315817	-3.169719	-3.077581
H	-2.306617	-1.990344	-2.161084

**Table S3.** Coordinates for the optimized gas-phase geometry of *cis*-[Sn(O<sup>t</sup>Bu)<sub>2</sub>]<sub>2</sub> (total energy: -1360.542343 a.u.).

Atoms	Coordinates		
	<i>X</i>	<i>Y</i>	<i>Z</i>
Sn	-2.025717	0.117820	-0.617073
Sn	1.450518	0.534683	-1.054361
O	-1.695611	-1.144660	0.933400
O	-0.354060	1.524365	-0.333741
O	1.748016	-0.305797	0.775877
O	-0.240457	-0.762389	-1.507506
C	-1.809888	-1.024299	2.335613
C	-3.273946	-0.799634	2.723668
C	-1.303739	-2.341075	2.926180
C	-0.936008	0.129838	2.830906
C	-0.402131	2.924150	-0.017681
C	0.616466	3.196677	1.087980
C	-1.808865	3.286622	0.460302
C	-0.072584	3.732318	-1.274330
C	2.977672	-0.516711	1.441984
C	2.719072	-1.575039	2.515958
C	4.064529	-1.018008	0.481782
C	3.433088	0.791555	2.095310
C	-0.123635	-2.160933	-1.843994
C	-1.530100	-2.726874	-2.040153
C	0.571844	-2.904095	-0.705538
C	0.669458	-2.261026	-3.145349
H	-3.645906	0.142433	2.285254
H	-3.399679	-0.736425	3.815558
H	-3.895203	-1.623881	2.342712
H	-0.244419	-2.474519	2.661847
H	-1.877399	-3.180662	2.506446
H	-1.400994	-2.354843	4.022740
H	-1.361973	1.093502	2.505172
H	0.067250	0.031321	2.388373
H	-0.870970	0.146038	3.930514
H	-1.848548	4.344507	0.758141
H	-2.097588	2.680143	1.332553
H	-2.548488	3.134170	-0.340731

H	0.585124	4.251013	1.401003
H	0.413908	2.552252	1.954723
H	1.638871	2.981479	0.736558
H	0.947779	3.515777	-1.626941
H	-0.777919	3.480909	-2.080636
H	-0.139387	4.811990	-1.073543
H	4.347475	0.652582	2.692719
H	3.643338	1.550990	1.323389
H	2.637107	1.175669	2.750480
H	4.289735	-0.264583	-0.291112
H	5.000904	-1.231567	1.019312
H	3.738345	-1.944095	-0.016927
H	3.632542	-1.801419	3.087310
H	2.355646	-2.499938	2.043547
H	1.945230	-1.218412	3.211417
H	0.770460	-3.310374	-3.459657
H	1.684755	-1.851393	-3.017002
H	0.167031	-1.696023	-3.944200
H	0.045633	-2.683590	0.233526
H	1.613881	-2.569614	-0.597665
H	0.570536	-3.987487	-0.901069
H	-2.077218	-2.716368	-1.083371
H	-1.477348	-3.770658	-2.382259
H	-2.083090	-2.146998	-2.796562

**Table S4.** Coordinates for the optimized gas-phase geometry of ImMe<sub>2</sub>•Si(O<sup>t</sup>Bu)<sub>2</sub> (total energy: -1060.212248 a.u.).

Atoms	Coordinates		
	<i>X</i>	<i>Y</i>	<i>Z</i>
Si	0.161205	0.107015	-0.824584
O	1.068940	-0.966491	0.242814
O	-0.003133	1.523396	0.204265
N	-2.187668	-1.477588	0.520252
N	-2.760808	0.324388	-0.489834
C	-1.681098	-0.412712	-0.139277
C	-3.565647	-1.410694	0.582699
C	-3.927019	-0.266948	-0.054040
C	-1.399286	-2.540517	1.131330
C	-2.682341	1.599805	-1.191789
C	2.131499	-1.797346	-0.219182
C	3.224983	-0.964578	-0.894711

C	1.601938	-2.849721	-1.198791
C	2.699274	-2.476713	1.026158
C	0.999445	2.504200	0.413214
C	1.883646	2.046094	1.575931
C	0.264844	3.791728	0.786654
C	1.849932	2.745234	-0.837525
H	-4.159268	-2.171887	1.076292
H	-4.901599	0.174518	-0.229006
H	-0.353710	-2.213719	1.134910
H	-1.511116	-3.468956	0.554568
H	-1.753746	-2.701428	2.157240
H	-2.020763	1.485545	-2.061357
H	-2.254332	2.357918	-0.527223
H	-3.690760	1.877118	-1.519244
H	4.071070	-1.602110	-1.193734
H	2.829773	-0.467617	-1.793669
H	3.597410	-0.194670	-0.201874
H	2.406435	-3.528198	-1.521966
H	0.813887	-3.452836	-0.721944
H	1.176353	-2.360583	-2.087920
H	3.545478	-3.132271	0.770430
H	3.040770	-1.715724	1.742575
H	1.923608	-3.085063	1.516201
H	2.682625	2.773716	1.788139
H	1.267453	1.917893	2.477980
H	2.328014	1.069716	1.335845
H	0.969487	4.590100	1.064647
H	-0.340664	4.142139	-0.063812
H	-0.405735	3.597410	1.636527
H	2.547075	3.580380	-0.669659
H	2.440737	1.853483	-1.096228
H	1.206514	2.987082	-1.697117

**Table S5.** Coordinates for the optimized gas-phase geometry of ImMe<sub>2</sub>•Ge(O<sup>t</sup>Bu)<sub>2</sub> (total energy: -2847.718637 a.u.).

Atoms	Coordinates		
	<i>X</i>	<i>Y</i>	<i>Z</i>
Ge	0.153565	0.114272	-0.899584
O	1.143535	-0.931922	0.322109
O	-0.129274	1.615471	0.191702
N	-2.167959	-1.573410	0.629656

N	-2.882184	0.163761	-0.399408
C	-1.752648	-0.516961	-0.100615
C	-3.539405	-1.557933	0.788676
C	-3.991141	-0.455442	0.136101
C	-1.290501	-2.581348	1.213635
C	-2.905339	1.403304	-1.170229
C	2.249599	-1.723360	-0.086266
C	3.343180	-0.851181	-0.711571
C	1.808538	-2.799064	-1.086614
C	2.788809	-2.384722	1.182893
C	0.869500	2.546649	0.562365
C	1.601689	2.020778	1.800766
C	0.140359	3.848832	0.896383
C	1.866125	2.796928	-0.574382
H	-4.064446	-2.316969	1.357655
H	-4.992435	-0.056822	0.018066
H	-0.265129	-2.195168	1.157228
H	-1.381906	-3.524610	0.657768
H	-1.581479	-2.742559	2.259181
H	-2.753639	1.185578	-2.236109
H	-2.098246	2.047612	-0.800698
H	-3.879715	1.883514	-1.026003
H	4.224363	-1.453336	-0.981536
H	2.971774	-0.360552	-1.625258
H	3.657216	-0.073630	0.001356
H	2.647558	-3.457750	-1.359267
H	1.011322	-3.420180	-0.649376
H	1.421321	-2.334481	-2.006569
H	3.670456	-3.007339	0.966511
H	3.067926	-1.612432	1.914122
H	2.015202	-3.022828	1.637085
H	2.391789	2.714345	2.129524
H	0.881466	1.886773	2.621595
H	2.038163	1.036954	1.577339
H	0.835321	4.614926	1.273149
H	-0.361536	4.241436	-0.001639
H	-0.623002	3.653367	1.663604
H	2.581517	3.587669	-0.301267
H	2.443142	1.886443	-0.801188
H	1.333226	3.103606	-1.487686

---

**Table S6.** Coordinates for the optimized gas-phase geometry of ImMe<sub>2</sub>•Sn(O<sup>t</sup>Bu)<sub>2</sub> (**3**) (total energy: -984.972472 a.u.).

Atoms	Coordinates		
	<i>X</i>	<i>Y</i>	<i>Z</i>
Sn	0.187806	0.099266	-1.083847
O	1.260064	-0.888726	0.408127
O	-0.353001	1.760291	0.027557
N	-2.071360	-1.898020	0.588664
N	-3.018277	-0.123681	-0.142308
C	-1.822381	-0.754322	-0.087245
C	-3.399163	-1.985325	0.953023
C	-3.999738	-0.858653	0.488037
C	-1.063060	-2.902365	0.906763
C	-3.235485	1.171001	-0.781326
C	2.529543	-1.481916	0.229077
C	3.567883	-0.429353	-0.175014
C	2.472270	-2.584425	-0.837457
C	2.923797	-2.090991	1.577320
C	0.490116	2.668890	0.698521
C	0.946327	2.054643	2.026261
C	-0.333870	3.932120	0.958565
C	1.706429	3.023640	-0.164456
H	-3.791933	-2.822794	1.518730
H	-5.024880	-0.513764	0.563899
H	-0.084355	-2.403449	0.887709
H	-1.100339	-3.720720	0.174344
H	-1.264059	-3.300530	1.908969
H	-3.408469	1.037015	-1.858132
H	-2.347403	1.791536	-0.598082
H	-4.117712	1.638488	-0.328224
H	4.571879	-0.869697	-0.277042
H	3.301191	0.026530	-1.143571
H	3.609937	0.366112	0.584302
H	3.441421	-3.096702	-0.940994
H	1.713455	-3.335201	-0.566384
H	2.204597	-2.162345	-1.819498
H	3.918458	-2.561295	1.534488
H	2.932303	-1.306897	2.348163
H	2.189266	-2.855007	1.875078
H	1.616370	2.731769	2.579838
H	0.065215	1.841081	2.650279
H	1.457369	1.099953	1.832198

H	0.244066	4.686078	1.515309
H	-0.659110	4.370338	0.002677
H	-1.228876	3.671726	1.543232
H	2.341306	3.781676	0.319849
H	2.330116	2.130990	-0.337709
H	1.374842	3.413499	-1.139461

**Table S7.** Coordinates for the optimized gas-phase geometry of ImMe<sub>2</sub>•Pb(O<sup>t</sup>Bu)<sub>2</sub> (total energy: -963.469431 a.u.).

Atoms	Coordinates		
	<i>X</i>	<i>Y</i>	<i>Z</i>
Pb	0.352717	0.172317	-1.123606
O	1.497830	-0.430650	0.662786
O	-0.742969	1.809312	-0.209629
N	-1.576048	-2.186097	0.783844
N	-2.844242	-0.858642	-0.310984
C	-1.546106	-1.209959	-0.150549
C	-2.863997	-2.438230	1.209066
C	-3.670366	-1.593443	0.513219
C	-0.389301	-2.856406	1.300723
C	-3.284411	0.224899	-1.183510
C	2.888977	-0.642052	0.635618
C	3.621544	0.555221	0.012833
C	3.221042	-1.911034	-0.163214
C	3.345180	-0.814062	2.087825
C	-0.755820	2.245580	1.130561
C	-1.143531	1.108097	2.085488
C	-1.787807	3.374116	1.216474
C	0.629665	2.773959	1.519200
H	-3.092244	-3.180324	1.965945
H	-4.744549	-1.448349	0.541844
H	0.464036	-2.176123	1.160667
H	-0.229748	-3.807322	0.773574
H	-0.532344	-3.052754	2.370643
H	-3.238501	-0.091747	-2.234630
H	-2.630653	1.092512	-1.004960
H	-4.321137	0.477398	-0.931718
H	4.714154	0.420609	0.036456
H	3.330559	0.686027	-1.044112
H	3.371590	1.478170	0.556472
H	4.302300	-2.120002	-0.174988

H	2.706042	-2.779856	0.275157
H	2.886991	-1.806118	-1.209478
H	4.429537	-0.993224	2.158621
H	3.094388	0.090055	2.661568
H	2.816669	-1.664652	2.544321
H	-1.186458	1.463163	3.127638
H	-2.134575	0.703786	1.819076
H	-0.393564	0.303378	2.020412
H	-1.836922	3.805078	2.228836
H	-1.523898	4.167725	0.502322
H	-2.786006	2.991608	0.950655
H	0.635190	3.203064	2.533877
H	1.347718	1.940600	1.485367
H	0.941392	3.551068	0.804414

**Table S8.** Coordinates for the optimized gas-phase geometry of ImMe<sub>2</sub>•SiH<sub>2</sub> (total energy: -595.358532 a.u.).

Atoms	Coordinates		
	<i>X</i>	<i>Y</i>	<i>Z</i>
Si	0.090051	-2.186847	-0.154894
N	-1.097476	0.525819	0.022692
N	1.051144	0.611020	0.022822
C	0.009594	-0.258254	0.056654
C	-0.753447	1.863905	-0.025156
C	0.602464	1.917669	-0.024939
C	-2.446382	-0.007858	0.015977
C	2.437708	0.184779	0.015578
H	-1.496583	2.652402	-0.054284
H	1.281035	2.762403	-0.053764
H	-2.649084	-0.530409	0.959763
H	-2.549902	-0.725623	-0.810003
H	-3.152291	0.819132	-0.119199
H	2.592954	-0.531889	-0.803319
H	2.685137	-0.309835	0.963784
H	3.076216	1.062809	-0.132354
H	1.233519	-2.323432	0.846330
H	-1.057007	-2.419021	0.824284

**Table S9.** Coordinates for the optimized gas-phase geometry of ImMe<sub>2</sub>•GeH<sub>2</sub> (total energy: -2382.878217 a.u.).

Atoms	Coordinates		
	<i>X</i>	<i>Y</i>	<i>Z</i>
Ge	1.803649	0.000000	-0.084116
N	-1.071357	-1.073031	0.025399
N	-1.071356	1.073031	0.025398
C	-0.247253	0.000000	0.077213
C	-2.394010	-0.678843	-0.047384
H	-3.210302	-1.390546	-0.093276
C	-2.394009	0.678844	-0.047384
H	-3.210301	1.390547	-0.093277
C	-0.592400	-2.444313	0.037795
H	-0.103109	-2.661566	0.995740
H	0.140079	-2.581570	-0.769250
H	-1.444178	-3.116249	-0.115454
C	-0.592399	2.444313	0.037795
H	0.140087	2.581569	-0.769244
H	-0.103115	2.661569	0.995743
H	-1.444175	3.116249	-0.115463
H	1.918824	1.186635	0.976203
H	1.918825	-1.186634	0.976205

**Table S10.** Coordinates for the optimized gas-phase geometry of ImMe<sub>2</sub>•SnH<sub>2</sub> (total energy: -520.122528 a.u.).

Atoms	Coordinates		
	<i>X</i>	<i>Y</i>	<i>Z</i>
Sn	1.643296	-0.028896	-0.054474
N	-1.580451	-1.040472	0.026304
N	-1.468634	1.096681	0.005354
C	-0.697430	-0.015195	0.052427
C	-2.882036	-0.580421	-0.031238
C	-2.810879	0.775619	-0.041260
C	-1.197794	-2.443592	0.018174
C	-0.926279	2.446377	0.027827
H	-3.735009	-1.249177	-0.056025
H	-3.589599	1.529351	-0.071337
H	-0.236234	-2.540384	0.536563
H	-1.098106	-2.807156	-1.013565
H	-1.963595	-3.027543	0.542573
H	-0.220245	2.572209	-0.804089

H	-0.393853	2.617534	0.971787
H	-1.751010	3.159659	-0.079620
H	1.613973	1.155788	1.290868
H	1.639008	-1.455651	1.029363

**Table S11.** Coordinates for the optimized gas-phase geometry of ImMe<sub>2</sub>•PbH<sub>2</sub> (total energy: -498.621706 a.u.).

Atoms	Coordinates		
	<i>X</i>	<i>Y</i>	<i>Z</i>
Pb	1.326539	0.000001	-0.031832
N	-2.016711	-1.067984	0.008016
N	-2.016721	1.067980	0.008015
C	-1.183580	0.000002	0.024563
C	-3.342361	-0.678812	-0.018283
C	-3.342368	0.678794	-0.018284
C	-1.564066	-2.450229	0.002923
C	-1.564089	2.450229	0.002923
H	-4.159878	-1.391221	-0.022455
H	-4.159892	1.391196	-0.022456
H	-0.583066	-2.491777	0.492110
H	-1.484563	-2.825462	-1.026403
H	-2.278959	-3.065337	0.562873
H	-1.484592	2.825465	-1.026402
H	-0.583089	2.491788	0.492109
H	-2.278987	3.065330	0.562875
H	1.224840	1.349881	1.261351
H	1.224835	-1.349840	1.261391

**Table S12.** Coordinates for the optimized gas-phase geometry of HBpin (total energy: -411.715514 a.u.).

Atoms	Coordinates		
	<i>X</i>	<i>Y</i>	<i>Z</i>
B	0.000003	1.937648	0.000008
O	-1.067448	1.186471	0.410331
O	1.067454	1.186471	-0.410317
C	0.780338	-0.186841	-0.052980
C	-0.780340	-0.186836	0.052980
C	-1.346879	-1.103052	1.124161
C	-1.465700	-0.443207	-1.286694
C	1.465697	-0.443227	1.286691
C	1.346876	-1.103040	-1.124174

H	-2.443376	-1.033471	1.122983
H	-1.066739	-2.148296	0.924132
H	-0.986882	-0.823026	2.121384
H	-1.357519	-1.491020	-1.600666
H	-2.534885	-0.213140	-1.184388
H	-1.047982	0.205460	-2.070072
H	1.357521	-1.491045	1.600649
H	2.534881	-0.213153	1.184388
H	1.047976	0.205426	2.070078
H	2.443374	-1.033468	-1.122985
H	1.066724	-2.148285	-0.924171
H	0.986892	-0.822986	-2.121395
H	0.000003	3.132446	0.000005

**Table S13.** Coordinates for the optimized gas-phase geometry of <sup>t</sup>BuOBpin (total energy: -644.165421 a.u.).

Atoms	Coordinates		
	<i>X</i>	<i>Y</i>	<i>Z</i>
B	-0.278839	-0.489205	0.170852
O	0.154635	0.714983	-0.361149
O	0.761015	-1.301994	0.566906
O	-1.565673	-0.881150	0.310714
C	1.969209	-0.703430	0.061220
C	1.566711	0.802871	-0.072454
C	2.256347	1.550131	-1.200531
C	2.262414	-1.350533	-1.290363
C	3.100080	-0.973614	1.038961
C	-2.692151	-0.039079	-0.005153
C	-3.911893	-0.886328	0.335635
C	-2.654435	1.219180	0.859730
C	-2.675859	0.306091	-1.492543
C	1.707858	1.564200	1.243199
H	1.916218	2.595067	-1.212255
H	3.347196	1.544440	-1.055806
H	2.024779	1.102706	-2.174689
H	3.215673	-0.999102	-1.710164
H	2.315398	-2.439142	-1.153842
H	1.458050	-1.132474	-2.008121
H	3.316315	-2.050708	1.059459
H	4.013879	-0.443532	0.730427
H	2.830906	-0.660024	2.054849

H	-3.893533	-1.161607	1.399488
H	-4.837933	-0.332142	0.126576
H	-3.906743	-1.809610	-0.260503
H	-3.556136	1.824576	0.686424
H	-2.621288	0.940384	1.923325
H	-2.665931	-0.617427	-2.089898
H	-3.575014	0.881826	-1.756655
H	-1.787976	0.902067	-1.741585
H	-1.770509	1.825149	0.620763
H	2.762946	1.730402	1.502832
H	1.212868	2.540220	1.143034
H	1.225527	1.013313	2.064098

**Table S14.** Coordinates for the optimized gas-phase geometry of {PB}SnH{N(SiMe<sub>3</sub>)<sub>2</sub>} (total energy: -2392.475763 a.u.).

Atoms	Coordinates		
	X	Y	Z
Sn	0.420037	0.147727	-0.787356
P	-0.079318	-2.142836	0.608590
B	-1.785708	0.773564	0.008253
Si	3.713459	-0.378571	-1.368693
Si	2.920065	1.800158	0.633296
N	2.476184	0.413735	-0.379506
C	-1.392096	-1.410928	1.675328
C	1.221813	-2.792051	1.777182
C	-0.844163	-3.664185	-0.193552
C	1.785960	-1.648445	2.615626
C	2.343650	-3.491530	1.008616
C	-0.171750	-3.998850	-1.527354
C	-0.920468	-4.881553	0.727738
C	-1.751025	-2.105460	2.843845
C	-2.004588	-0.175198	1.329554
C	-3.002216	0.269264	2.225904
C	-3.372216	-0.426813	3.371874
C	-2.738672	-1.624994	3.693961
C	-1.877405	2.374634	0.283811
C	-1.692051	3.246332	-0.968356
C	-0.990955	2.922949	1.405921
C	-1.263594	4.397302	1.708670
C	-1.077940	5.250854	0.454218
C	-1.943994	4.731456	-0.693065

C	-2.694776	0.307641	-1.286882
C	-2.725981	-1.196001	-1.582284
C	-4.150506	0.792233	-1.117123
C	-3.590674	-1.559238	-2.790823
C	-5.021857	-1.059505	-2.604563
C	-5.031649	0.440839	-2.318822
C	5.085762	-1.113345	-0.280793
C	4.489620	0.830685	-2.596171
C	3.010417	-1.797969	-2.403636
C	4.767556	1.878948	1.023451
C	2.487692	3.405250	-0.266445
C	2.060683	1.715696	2.319256
H	0.505989	-0.515223	-2.405658
H	0.721205	-3.524175	2.431515
H	1.993177	-4.360922	0.436039
H	3.109929	-3.842709	1.716886
H	2.830120	-2.791728	0.312975
H	1.002997	-1.114968	3.173278
H	2.300333	-0.931492	1.958156
H	2.517509	-2.042590	3.338001
H	-1.869966	-3.332066	-0.399494
H	-1.465748	-4.662824	1.656009
H	0.076217	-5.267896	0.987304
H	-1.460851	-5.689104	0.210288
H	-0.123664	-3.125149	-2.194064
H	-0.741705	-4.789718	-2.038982
H	0.854369	-4.369870	-1.386253
H	-3.508298	1.213075	2.016075
H	-4.150574	-0.024465	4.022460
H	-3.003409	-2.175568	4.597188
H	-1.239432	-3.032828	3.108439
H	-2.924843	2.550495	0.607509
H	-1.100672	2.316978	2.320225
H	0.063346	2.827759	1.092929
H	-2.300176	4.508465	2.075018
H	-0.602250	4.753422	2.514909
H	-1.309305	6.306930	0.663510
H	-0.016466	5.212623	0.150381
H	-1.769929	5.325723	-1.603867
H	-3.008501	4.863970	-0.427581
H	-0.656367	3.119413	-1.345354
H	-2.353119	2.911108	-1.782294
H	-2.304101	0.802700	-2.198206

H	-1.705645	-1.580561	-1.751228
H	-3.125304	-1.714682	-0.690403
H	-3.157490	-1.095593	-3.694702
H	-3.580506	-2.649048	-2.956157
H	-5.632556	-1.290639	-3.491012
H	-5.480615	-1.591953	-1.752265
H	-6.061816	0.792237	-2.150871
H	-4.653474	0.978388	-3.206819
H	-4.576633	0.326916	-0.208121
H	-4.180024	1.880015	-0.954802
H	5.503009	-2.013010	-0.760353
H	5.910732	-0.402785	-0.129077
H	4.703499	-1.402930	0.710654
H	4.969538	1.684029	-2.093697
H	5.253638	0.325962	-3.208705
H	3.716368	1.226973	-3.273193
H	2.338094	-2.462676	-1.840125
H	2.456037	-1.428146	-3.277656
H	3.857805	-2.402020	-2.766857
H	5.097805	1.010828	1.612332
H	5.406203	1.962148	0.132135
H	4.929494	2.781784	1.635097
H	2.613474	4.283077	0.387575
H	3.149753	3.526872	-1.138628
H	1.449972	3.405618	-0.633698
H	1.920093	2.729168	2.727824
H	1.071865	1.234968	2.280006
H	2.687238	1.147594	3.024668

## 8. References

- (S1) A. A. Omaña, R. K. Green, R. Kobayashi, Y. He, E. R. Antoniuk, M. J. Ferguson, Y. Zhou, J. G. C. Veinot, T. Iwamoto, A. Brown and E. Rivard, *Angew. Chem. Int. Ed.*, 2021, **60**, 228.
- (S2) J. Sinclair, G. Dai, R. McDonald, M. J. Ferguson, A. Brown and E. Rivard, *Inorg. Chem.*, 2020, **59**, 10996.
- (S3) (a) M. Veith and F. Töllner, *J. Organomet. Chem.*, 1983, **246**, 219; (b) M. Veith and R. Rösler, *Z. Naturforsch.*, 1986, **41b**, 1071.
- (S4) Z. Huang, S. Wang, X. Zhu, Q. Yuan, Y. Wei, S. Zhou and X. Mu, *Inorg. Chem.*, 2018, **57**, 15069.

- (S5) T. Lui, J. He and Y. Zhang, *Org. Chem. Front.*, 2019, **6**, 2749.
- (S6) C. D. Schaeffer, L. K. Myers, S. M. Coley, J. C. Otter and C. H. Yoder. *J. Chem. Ed.*, 1990, **67**, 347.
- (S7) (a) G. Tintori, P. Nabokoff, R. Buhaibeh, D. Bergé-Lefranc, S. Redon, J. Broggi, and P. Vanelle. *Angew. Chem. Int. Ed.*, 2018, **57**, 3148; (b) T. Schaub, M. Backes and U. Radius, *Organometallics*, 2006, **25**, 4196.
- (S8) S. Bontemps, G. Bouhadir, K. Miqueu and D. Bourissou. *J. Am. Chem. Soc.*, 2006, **128**, 12056.
- (S9) (a) G. M. Sheldrick, *Acta Cryst.*, 2015, **A71**, 3; (b) G. M. Sheldrick, *Acta Cryst.*, 2015, **C71**, 3.
- (S10) M. J. Frisch, G. W. Trucks, H. B. Schlegel, G. E. Scuseria, M. A. Robb, J. R. Cheeseman, G. Scalmani, V. Barone, G. A. Petersson, H. Nakatsuji, X. Li, M. Caricato, A. V. Marenich, J. Bloino, B. G. Janesko, R. Gomperts, B. Mennucci, H. P. Hratchian, J.V. Ortiz, A. F. Izmaylov, J. L. Sonnenberg, D. Williams-Young, F. Ding, F. Lipparini, F. Egidi, J. Goings, B. Peng, A. Petrone, T. Henderson, D. Ranasinghe, V. G. Zakrzewski, J. Gao, N. Rega, G. Zheng, W. Liang, M. Hada, M. Ehara, K. Toyota, R. Fukuda, J. Hasegawa, M. Ishida, T. Nakajima, Y. Honda, O. Kitao, H. Nakai, T. Vreven, K. Throssell, J. A. J. Montgomery, J. E. Peralta, F. Ogliaro, M. J. Bearpark, J. J. Heyd, E. N. Brothers, K. N. Kudin, V. N. Staroverov, T. A. Keith, R. Kobayashi, J. Normand, K. Raghavachari, A. P. Rendell, J. C. Burant, S. S. Iyengar, J. Tomasi, M. Cossi, J. M. Millam, M. Klene, C. Adamo, R. Cammi, J. W. Ochterski, R. L. Martin, K. Morokuma, O. Farkas, J. B. Foresman and D. J. Fox, Gaussian 16, Revision B.01, Gaussian, Inc., Wallingford CT.
- (S11) Y. Zhao and D. G. Truhlar, *Theor. Chem. Acc.*, 2008, **120**, 215.
- (S12) (a) T. H. Dunning Jr., *J. Chem. Phys.*, 1989, **90**, 1007; (b) A. K. Wilson, D. E. Woon, K. A. Peterson and T. H. Dunning Jr., *J. Chem. Phys.*, 1999, **110**, 7667; (c) K.A. Peterson. *J. Chem. Phys.*, 2003, **119**, 11099.